T 179

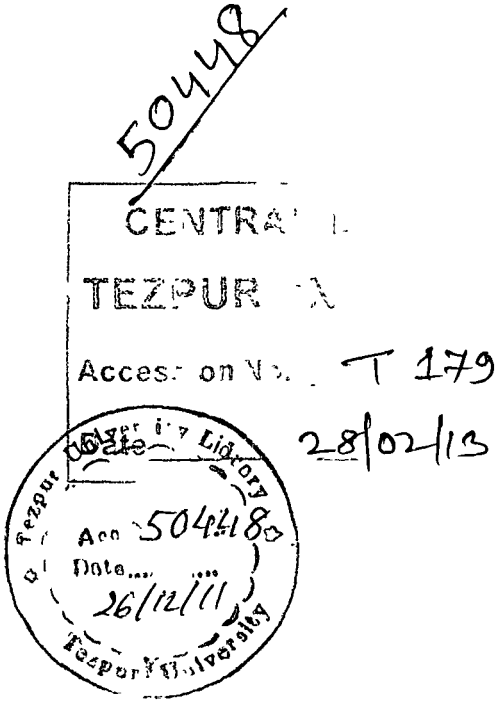
50448
CENTRAL
TEZPUR
Accession No. T 179
Date 28/02/13
Acc 50448
Date 26/12/11

DEVELOPMENT OF CORE-SHELL LATEX PARTICLES BY EMULSION POLYMERIZATION

A thesis submitted
in partial fulfillment of the requirements for the degree of

Doctor of Philosophy

By

Lakhya Jyoti Borthakur

Registration No. 019 of 2010

School of Science and Technology

Department of Chemical Sciences

Tezpur University

Napaam, Tezpur - 784028

Assam, India

May, 2011

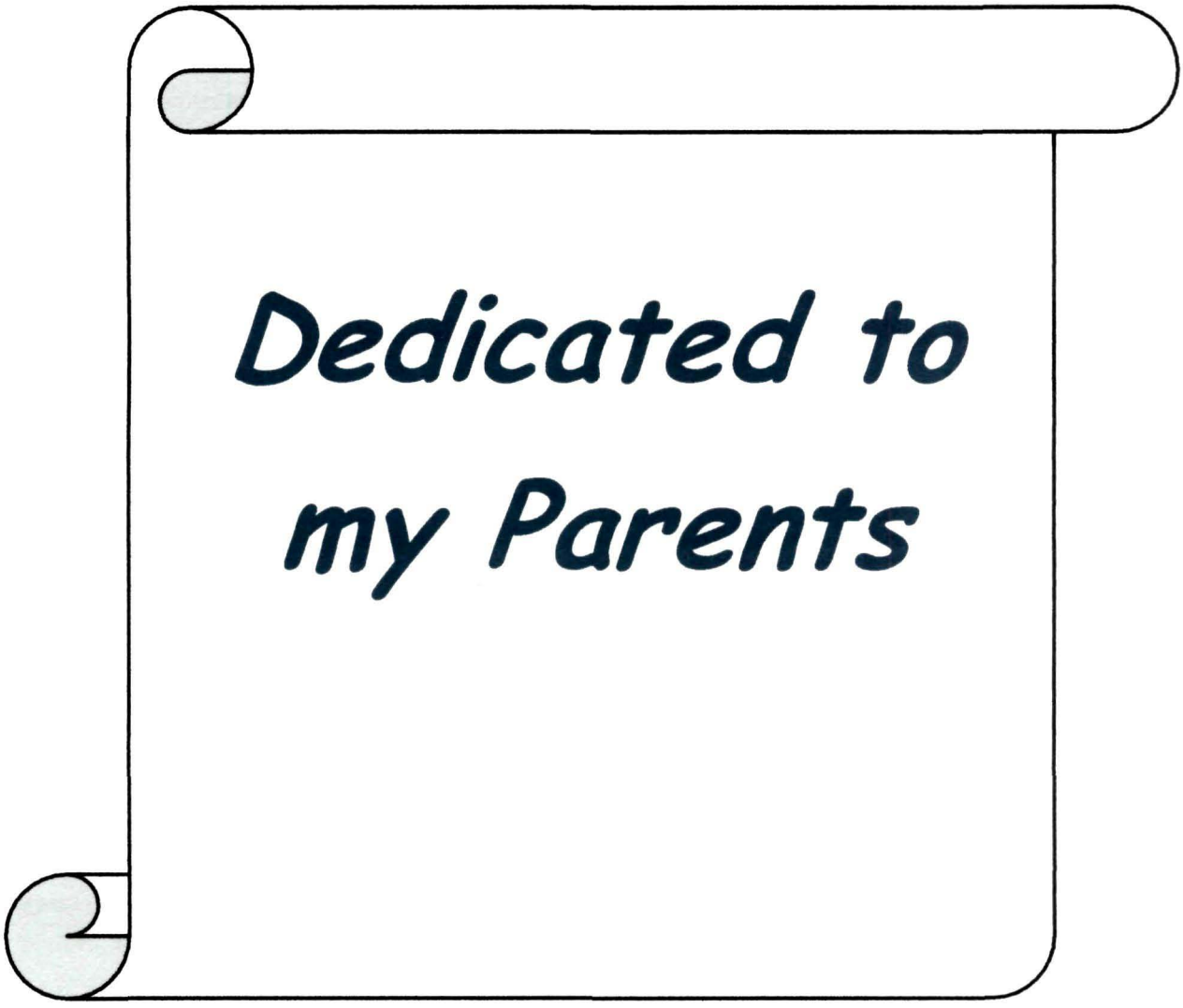
Dedicated to
my Parents

DEVELOPMENT OF CORE-SHELL LATEX PARTICLES BY EMULSION POLYMERIZATION

ABSTRACT

The present thesis deals with the development of three different types of core-shell particles by emulsion and miniemulsion polymerization technique. The core-shell morphology was fully characterized and their properties like thermal, electrical, electrochemical etc. were evaluated. Special emphasis was given to find potential applications of these newly designed core-shell particles. The contents of the thesis have been compiled into five chapters.

Chapter1 deals with the general introduction of core-shell particles. Various types of core-shell morphology, their potential applications, the thermodynamic and kinetic parameters that control the resulting morphology of the core-shell particles are discussed in detail. A brief review of synthetic procedures employed in developing core-shell particles of various types are presented in this chapter.

Chapter 2 deals with the synthesis of core-shell particle using poly (butyl acrylate-co-methacrylic acid-co-ethylene glycoldimethacrylate) as the core and poly (styrene-co-methylmethacrylate) as the shell by two stage seeded emulsion polymerization technique. The core-shell morphology is confirmed by SEM and TEM analysis. Physical properties like pH, viscosity, freeze thaw stability, solid content etc. of the core-shell particles are evaluated. These core-shell particles are used as an opaque pigment in emulsion paint and their performances are evaluated.

Chapter 3 deals with the synthesis of two sets of core-shell particles using poly (styrene-co-methylacrylate) (SMA) as the core and polypyrrole as the shell by miniemulsion polymerization technique. In the first set graphite is incorporated in the polypyrrole shell whereas in the second set silver nanoparticles are incorporated in the polypyrrole shell. The core-shell particles are characterized by FT-IR, UV-Visible, XRD, SEM and TEM analysis. The thermal, electrical and electro-chemical properties of the

particles are investigated. The graphite incorporated core-shell particles are used as ammonia gas sensor. The changes in resistivity of the core-shell particles on exposure to various concentration of ammonia vapour are discussed in this chapter.

Chapter 4 deals with the synthesis of core-shell nanocomposite particles of poly (styrene-co-methylacrylate) as the shell and organically modified bentonite as the core by miniemulsion polymerization under ultrasonic irradiation. The core-shell nanocomposite particles are characterized by FT-IR, XRD, SEM, TEM etc. A comparison of the thermal stability of the pristine copolymer to that of the nanocomposite particles are discussed in this chapter.

Chapter 5, the last chapter of the thesis deals with the conclusion and future scope of the thesis. The major findings of the thesis are reported in this chapter. The study reveals that core-shell particle using poly (butylacrylate-co- methacrylicacid-co-ethyleneglycol dimethacrylate) as the core and poly (styrene-co-methyl methacrylate) as the shell can replace up to 17% of TiO_2 as pigment in emulsion paints. The core-shell particles using poly (styrene-co-methylacrylate) (SMA) as the core and graphite incorporated polypyrrole as the shell can be potentially applied as ammonia gas sensor. Core-shell nanocomposite particles of poly (styrene-co-methylacrylate) as the shell and organically modified bentonite as the core show improved thermal stability than the pristine polymer and can find potential application as barrier coating materials in many industries.

DECLARATION BY THE CANDIDATE

The thesis entitled *"Development of core-shell latex particles by emulsion polymerization"* is being submitted to the Tezpur University in partial fulfillment for the award of the degree of Doctor of Philosophy in *Chemical Sciences* is a record of bonafide research work accomplished by me under the supervision of Prof. S. K. Dolui.

All helps received from various sources have been duly acknowledged.

No part of this thesis has been submitted elsewhere for award of any other degree.

Lakhya Jyoti Borthakur

Date: 2/5/11

Lakhya Jyoti Borthakur

Place: Tezpur

Department of Chemical Sciences

Tezpur University

TEZPUR UNIVERSITY

(A Central University by an Act of Parliament)

DISTRICT: SONITPUR:: ASSAM:: INDIA

Napaam, Tezpur-784028

Fax: 03712-267006 Ph: 03712-267004 ***Email : adm@agnigarh.tezu.ernet.in***

CERTIFICATE OF THE PRINCIPAL SUPERVISOR

This is to certify that the thesis entitled "*Development of core-shell latex particles by emulsion polymerization*" submitted to the School of *Science and Technology*, Tezpur University in partial fulfillment for the award of the degree of Doctor of Philosophy in *Chemical Sciences* is a record of research work carried out by *Mr. Lakhya Jyoti Borthakur* under my supervision and guidance.

All help received by him from various sources have been duly acknowledged.

No part of this thesis has been submitted elsewhere for award of any other degree.

Date: 2 May 2011

Place: Tezpur

S. K. Dolui

Professor

School of Science and Technology

Department of Chemical Sciences

TEZPUR UNIVERSITY

(A Central University by an Act of Parliament)

DISTRICT: SONITPUR:: ASSAM:: INDIA

Napaam, Tezpur-784028

Fax: 03712-267006 Ph: 03712-267004 ***Email : adm@agnigarh.tezu.ernet.in***

CERTIFICATE OF THE EXTERNAL EXAMINER AND ODEC

This is to certify that the thesis entitled "*Development of core-shell latex particles by emulsion polymerization*" submitted by ***Mr. Lakhya Jyoti Borthakur*** to Tezpur University in the **Department of Chemical Sciences** under the school of **Science and Technology** in partial fulfillment of the requirement for the award of the degree of Doctor of Philosophy in **Chemical Sciences** has been examined by us on _____ and found to be satisfactory.

Signature of:

Principal Supervisor

External Examiner

Date: _____

Preface

Core-shell particles are structured composite particles consisting of at least two different materials, one forms the core and the other forms the shell. These composite particles form a class of materials with unique colloidal and physical properties. Enhanced properties are often achieved in these specially designed particles which cannot be met by blending of two materials. The synthesis of such multiple phase composite particles provide an opportunity to tailor properties for a range of desired applications such as paints, coatings and additives, cosmetics, pharmaceuticals, paper industries, drug delivery, chromatographic columns etc. Core-shell particles may be of many types: inorganic-inorganic, organic-organic (polymer-polymer), hybrid organic-inorganic etc.

The present thesis deals with the development of three different types of core-shell particles by emulsion and mini-emulsion polymerization technique. Special emphasis was given to find potential application of these newly designed core-shell particles. The contents of the thesis have been compiled into five chapters.Chapter1 deals with the general introduction of core-shell particles. Chapter 2 deals with the synthesis of core-shell particle using poly (butyl acrylate-co- methacrylic acid -co- ethylene glycoldimethacrylate) as the core and poly (styrene -co- methylmethacrylate) as the shell by two stage seeded emulsion polymerization technique. These core-shell particles are used as an opaque pigment in emulsion paint and their performances are evaluated. Chapter 3 deals with the synthesis of two sets of core-shell particles using poly (styrene-co-methylacrylate) (SMA) as the core and polypyrrole as the shell by miniemulsion polymerization technique. In the first set graphite is incorporated in the polypyrrole shell whereas in the second set silver nanoparticles are incorporated in the polypyrrole shell. Chapter 4 deals with the synthesis of core-shell nanocomposite particles of poly (styrene-co-methylacrylate) as the shell and organically modified bentonite as the core by miniemulsion polymerization under ultrasonic irradiation. Chapter 5, the last chapter of the thesis deals with the conclusion and future scope of the thesis. The major findings of the thesis are reported in this chapter.

We hope that this study contributes a little knowledge to the rapidly advancing field of core-shell particles and also opens up the possibilities of further research on the subject.

This research was carried out in the Department of Chemical Sciences, Tezpur University with financial assistance from the Naval Material Research Board (NRB) and University Grants Commission (UGC) under sponsored research scheme.

Lakhya Jyoti Borthakur

Acknowledgement

I would like to express my deep sense of profound gratitude and indebtedness to my respected supervisor, Prof. S. K. Dolui for his inspiring guidance, endless patience, and work of freedom and the opportunity to work in his laboratory. It would have not been possible for me to bring out this thesis without his help, fatherly care, and constant encouragement throughout the research work.

I take the opportunity to thank Dr. Khargeswar Bhuyan, Prinicipal, Nowgong college for giving me necessary permission and leave to carry out my work. Without his help and support this work would have never been completed. Thanks to all my colleagues of the Deptt. Of Chemistry, Nowgong College for their help, support and co-operation.

I am grateful to all the faculty members of Department of Chemical Sciences for their help and suggestions.

I would like to acknowledge the sophisticated instrument facilities received from Dept. of Chemical Sciences and other Departments of Tezpur University.

I am thankful to Dr. T. Jana Shalimar Paints Ltd., Kolkata for his help in evaluating the pigment properties of the core-shell particles.

My special thanks go to Mr. B. Gohain, Dr. B. Saikia, Mr. N. Dutta, Mr. P. Nath, Mr. R. Borah, Mr S. Phukan, Mr. P. S. Barua, Mr. S. Das, Mr. R. Boruah, Mr. J. Borah, Mr. H. Gogoi, Miss B. Das, Mr. H. Das, Mr. G. B. Chhetry for their timely help in many situations.

I am thankful to all well wisher especially, , Tapasiba, Nandiniba, Digantada, Rabiulda, Sibdasda, Suvangshuda, Jyotishmoyda, Parashaba and Kausikda for their help.

I am truly thankful to my lab mates and friends Jatin, Binod, Anamika, Muhsina, Surajit, Isha, Amar, Monalisha, Chandramika, Dhaneswar, Pranab and Shyamalima who have taught and helped me in many aspect of life. It has been a great adventure. I will remember them forever for their friendship and help.

I am also thankful to all my friends especially Nirmala, Kalyan, Pubalee, Bulumani, Ajantaba, Lakhinath, Subrata, Suresh, Barnali, Shremayee, Harekrishna, Sivaprasad, Buddha, Uday, Goutam, Mridula, Jeenajyoti, Dhruba, Biplab, Ankur, Rashmi, Satya, Upamanyuda, Madhurjya, Subasit, Soumik, Smritimala, Nabanita, Jyotiprasad, Ranjan, sudhir, Nabanath, Prasenjitda, Narayan, Bimalendu, Kunal and Pinky for their support and help.

I am grateful to Mrs. Sutapa Dolui for her motherly care, kindness and encouragement and Swapnil for his brotherly affection and support. I thank the Naval material Research (NRB) and University Grants Commission (UGC) for funding the projects to complete this research. I would like to convey my respect and gratitude to my parents for their blessing, love and affection. I would like to express my heartiest love to all my family members for their constant encouragement, inspiration and support throughout my studies to fulfill my dream.

Finally, I thank the authorities of Tezpur University for granting me the permission to do this work.

Last but not least I would like to thank almighty for everything.

Lakhya Jyoti Borthakur

Contents

List of Tables

4

List of Figures

Abbreviations used in the thesis

AA	acrylic acid
ABCVA	4,4 - azobis – (4- cyanovaleric acid)
AIBN	2,2-azo-bis(isobutyronitrile)
ATRP	atom transfer radical polymerization
BA	butyl acrylate
BPO	benzoyl peroxide
CTA	Charge Transfer Agent
CTAB	cetyltrimethyl ammonium bromide
CTAT	cetyltrimethyl ammonium tartrate
CV	Cyclic voltammetry
DC	Direct Current
DMAEMA	2-(dimethylamino) ethyl methacrylate
DVB	divinylbenzene
EGDMA	ethylene glycol dimethylacrylate
eV	electron volt
FT-IR	Fourier transform infrared spectroscopy
G	Graphite
GPC	Gel permeation chromatography
HD	hexadecane
HOMO	Highest occupied molecular orbital
kHz	kilohertz
KPS	potassium persulfate
LBL	layer-by-layer
LMA	lauryl methacrylate
LUMO	Lowest unoccupied molecular orbital
M_n	Number average molecular weight
M_w	Weight average molecular weight
MA	methylacrylate

MAA	methaacrylic acid
MF	melamine-formaldehyde
MFFT	minimum film forming temperature
MHz	megahertz
MMA	methyl methacrylate
mPs	milipoise
MRI	magnetic resonance imaging
NIPA	N-isopropylacrylamide
NMP	N-methyl pyrrolidone
O/W	Oil/Water
PAN	polyacrylonitrile
PANI	polyaniline
PAPBA	Poly(3-aminophenylboronic acid)
PBMA	poly (butylmethylacrylate)
PDVB	poly divinylbenzene
PEDOT	poly (3,4 ethylenedioxythiophene)
PMA	polymethylacrylate
PMMA	Polymethylmethacrylate
P-NIPA	Poly(N-isopropylacrylamide)
PPy	polypyrrole
PPy/G	polypyrrole/graphite
PS	polystyrene
PSMA	poly (styrene-comaleic anhydride)
PSS	polystyrene sulfonate
PVAc	polyvinyl acetate
PVC	Polyvinyl chloride
PVOH	poly(vinyl alcohol)
SCK	shell cross linked knedel
SDBS	sodium dodecyl benzene sulphonate
SDS	sodium dodecyl sulphate

SEM	Scanning Electron Microscopy
SMA	poly(styrene-co-methyl acrylate)
Sty	Styrene
TEM	Transmission Electron Microscopy
TGA	Thermogravimetric analysis
T_g	Glass Transition temperature
THF	Tetrahydrofuran
UAc	uranyl acetate
UV	Ultra violet
VAc	vinyl acetate
VAE	vinyl acetate/ethylene
W/O	Water/Oil
XRD	X-ray diffraction
μm	micro meter

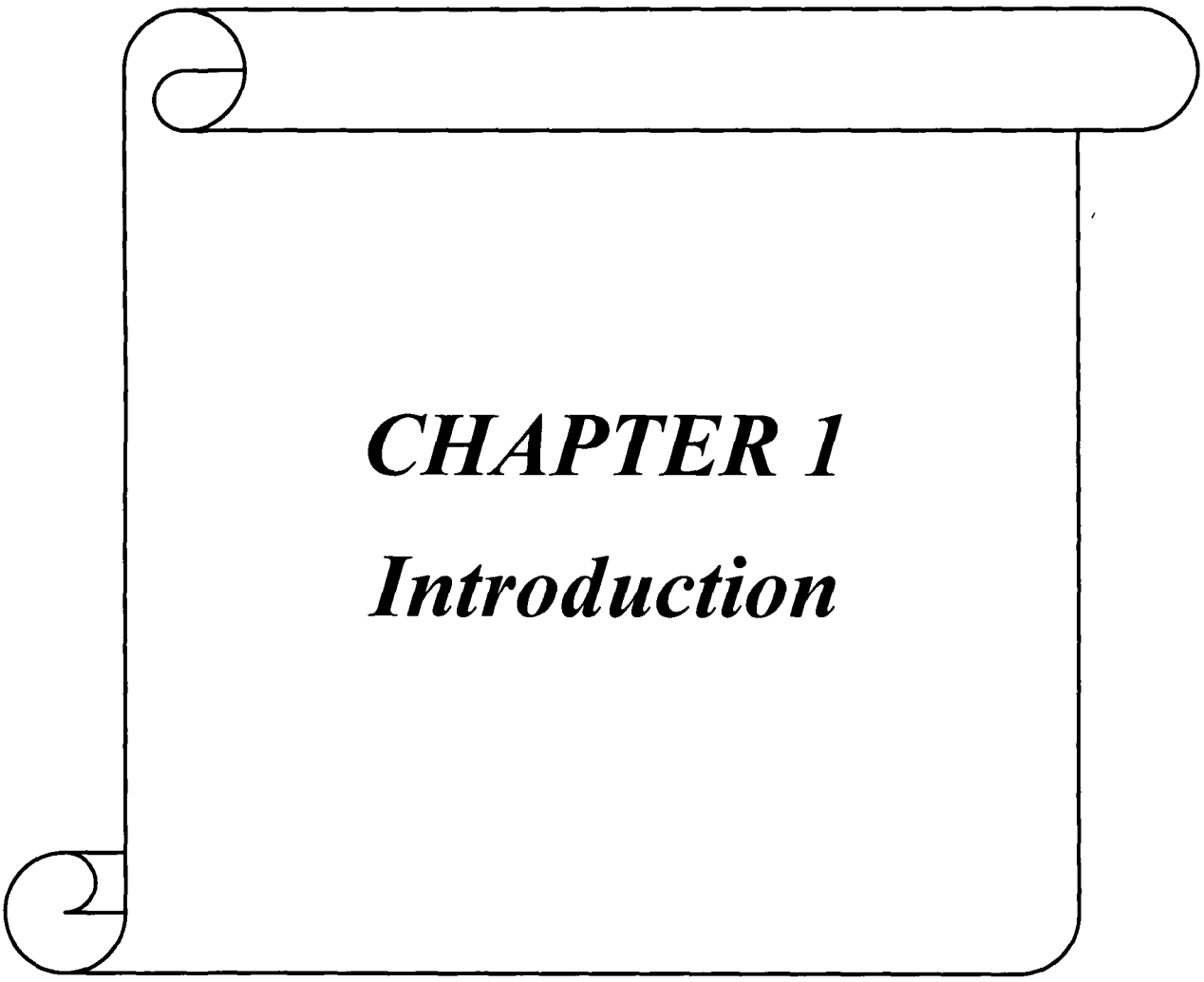

CHAPTER 1

Introduction

Chapter 1

1.1 Introduction

Advancement of polymer science is one of the most significant contributions of Chemistry for the welfare of humankind in the last century. From disposable wrappers to the artificial heart; polymer touches our lives as does no other class of material, with no end to new uses and improved products in sight. Now-a-days it is almost impossible to imagine a world without polymers.

Polymers or macromolecules or high polymers or giant molecules are high-molecular-weight materials composed of repeating subunits called monomers. These materials may be organic, inorganic or organometallic and synthetic or natural in origin. Polymers are essential materials for almost every industry as adhesives, building materials, paper, cloths, fibers, coatings, plastics, ceramics, concretes, liquid crystals, photo resists coatings etc. They are also major components in plant and animal body. They are important in nutrition, engineering, biology, medicine, computers, space exploration, healthcare and the environment. The first synthetic polymer was produced in 1909; called Bakelite which could be moulded at a high temperature and it would retain its shape once cooled. But it wasn't until the World War I that significant changes took place in the polymer industry. Synthetic polymers have found wide spread application because of their low density, low cost and better performance[1-8].

1.2 Surface coating/Paints

Surface coating materials are mixture of film-forming materials plus pigments, solvents and other additives. When applied to a surface and cured or dried, yields a thin film covering the substrate. Surface coatings include paints, drying oils and varnishes, synthetic clear coatings and other products whose primary function is to protect the surface of an object from the environment. These products can also enhance the aesthetic appeal of an object by accentuating its surface features or even by concealing them from view[9]. Most surface coatings employed in industry and by consumers are based on synthetic polymers such as polyacrylates, polystyrene, polyacrylamides etc[9]. The main components of a paint are[10-12]

- Binders
- Solvent
- Pigments
- Additives

1.2.1 Binders

Binders are the backbone of any paint. It is the only component that must be present; other components included optionally, depending on the desired properties of the cured film. The binder imparts adhesion, binds the pigments together and strongly influences properties such as gloss potential, exterior durability, flexibility and toughness. Binders include synthetic or natural resins such as acrylics, vinyl-acrylics, vinyl acetate/ethylene (VAE), polyurethanes, polyesters, melamine resins, epoxy or oils[11].

1.2.2 Solvent

The main purposes of the solvent are to adjust the curing properties and viscosity of the paint. It is volatile and does not become part of the paint film. It also controls flow and application properties and affects the stability of the paint while in liquid state. Its main function is as the carrier for the non volatile components. These volatile substances impart their properties temporarily; once the solvent has evaporated or disintegrated the remaining paint is fixed to the surface[12].

1.2.3 Pigment

Pigments are granular solids incorporated into the paint to contribute colour, toughness, texture or simply to reduce the cost of the paint. Pigments can be classified as either natural or synthetic types. Natural pigments include various clays, calcium carbonate, mica, silica, and talcs. Synthetics would include engineered molecules, calcined clays, precipitated calcium carbonate, and synthetic silica. Hiding pigments used in making paint opaque, also protect the substrate from the harmful effects of ultraviolet light. Hiding pigments include titanium dioxide, phthalo blue, red iron oxide, and many others[13].

1.2.4 Additives

Besides the three main categories of ingredients, paint can have a wide variety of miscellaneous additives, which are usually added in very small amounts and yet give a very significant effect on the product. Some examples include additives to modify surface tension, improve flow properties, improve the finished appearance, increase wet edge, improve pigment stability, impart antifreeze properties, control foaming, control skinning etc. Other types of additives include catalysts, thickeners, stabilizers, emulsifiers, texturizers, adhesion promoters, UV stabilizers, flatteners (de-glossing agents), biocides to Fight bacterial growth[11] etc.

Binders used in coating industries need to fulfil contradictory demands. They must show an excellent film formation and appearance as well as good blocking resistance and hardness[14]. A single polymer or a mere physical mixture of two or more polymers cannot fulfil these sorts of contradictory demands. To address these problems a new class of materials called core-shell polymer particles have emerged towards the end of the last century and is getting immense importance among the material scientists in recent time. The synthesis of such multiphase composite particles provides an opportunity to tailor properties for a range of applications such as paints, coatings, additives etc[15-16].

1.3 Core-shell particles

Core-shell particles are structured composite particles consisting of at least two different materials, one forms the core and the other forms the shell[17]. A typical core-shell particle is shown in the **Fig 1.1**.

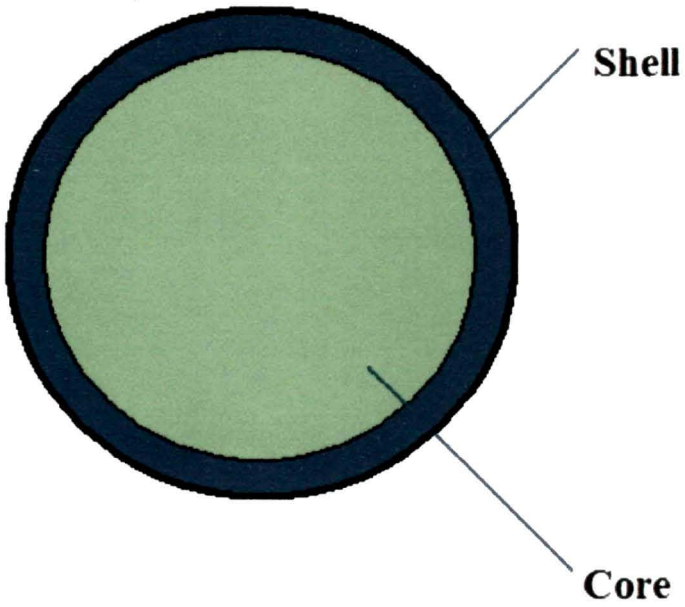

Fig 1.1: A typical core-shell particle

These composite particles form a class of materials with unique colloidal and physical properties[17]. Enhanced properties are often achieved in these specially designed particles than by blending the two materials. By using core-shell concept one can prepare lattices possessing two kinds of properties; one of the core and the other of the shell. For instance, now-a-days core-shell particles of an insulating polymer (core) and a conducting polymer (shell) are used to modify the mechanical properties of the conducting polymers[18-19]. Recently core-shell particles with different glass transition temperature were used to improve the mechanical properties of thermoplastics[20]. Core-shell particles are also used for many other applications such as coatings, adhesives, membrane separations, biotechnology and impact modifiers etc[15, 21].

In the paint industries, these core-shell particles can be of great importance due to their special structure. By using core-shell particles which have hard and soft domains formed from two different polymers having different T_gs it is possible to produce binders with a high blocking resistance due to the hard polymer and a low minimum film forming temperature due to the soft polymer[14]. Core-shell particles formed from polymers having difference in refractive index (between the core and shell phase) may potentially be applied as pigments in emulsion paints. This will

reduce the amount of TiO_2 used and will also increase the compatibility between the paint and the pigment. This can provide an economical and environmentally benign alternative. Depending on the types of core and shell materials used the resultant core-shell particles can have different properties and applications.

1.4 Classification of core-shell particles

The core-shell particles are diversely used for different industrial field including coating, biological, modern electronics etc. So, classification of these particles on the basis of their industrial application is a difficult task. However, they may be classified on the basis of their material property. Depending on the nature of the core and shell material used they may be classified as follows

- Organic core- inorganic shell
- Inorganic core - organic shell
- Inorganic core - inorganic shell
- Organic core - organic shell

1.4.1 Organic core - inorganic shell particles

In these type of particle core phase is made of organic or polymer materials while shell phase is made of inorganic materials. The shell materials mainly studied are either metal, metal oxide or silica. Due to the coating of such inorganic material these particles exhibit high abrasion resistance. Phadtare, et al.[22] synthesised gold coated polyurethane micro sized core-shell particles and studied the bio-catalytic activity of these particles in pepsin digestion. Polymer core with inorganic shell is also used for the synthesis of hollow particles[23-28]. After formation of the core-shell particle the core phase can be easily removed by either using suitable solvent or by calcination to form hollow particles. Inorganic coating on any organic or polymer material increases the colloidal stability of the core material.

1.4.2 Inorganic core - organic shell particles

In these type of particles core phase is made of inorganic core such as metal, metal oxide or silica and the shell phase is made of organic or polymer phase. The polymer coated inorganic material have a broad spectrum of applications ranging

from catalysis to additives and pigments, paints, cosmetics etc[29]. Magnetic nanoparticles coated with polymer are used for magnetic separation of biochemical products, cells and also used for control drug release within the body[30]. Different inorganic-organic composite particles find immense importance in biological field since their rich surface functional groups can be tailored easily to serve as conjugates for biological applications[31-32]. Some of the particles in this category are SiO_2/PAPBA (Poly(3-aminophenylboronic acid),[33] TiO_2/cellulose etc. The coat of PAPBA prevents agglomeration of particles and helps in controlling size. SiO_2/PAPBA is used in optical devices, sensors and electrical devices. The addition of cellulose improves the pigment properties of TiO_2.Some of these hybrids find application in dentistry as brace material and fillers[34-35].

1.4.3 Inorganic core –inorganic shell particles

In these types of particles both the core and the shell are made of inorganic materials. The inorganic materials widely used are metals, semiconductors or lanthanides. These particles are commercially used in fields like semiconductor, catalysis, quantum dots, optical bio-imaging etc.

Among different inorganic-inorganic composite particles metallic core-shell particles are getting much importance because of their wide range of applications. Metal coated with silica particles have wide application in optical sensing and the optical property may be tuned by varying the thickness of the silica shell. Ung et al.[36] modified the coating method to form uniform silica coating on nano silver core particles. Lu et al.[37] synthesised silica coated gold particles and Li et al.[38] synthesised silica coated silver particles by sol gel method and studied their properties. Silver/silica particles can be used in fluorescence imaging and the region of emission is dependent on the thickness of the silica shell.[38] Coating of Fe_2O_3 on MgO and CaO enhances their capacity of absorbing toxic materials (SO_2, H_2S etc.) from the environment[39-40]. Magnetic nanoparticles with different inorganic coating are used for magnetic resonance imaging (MRI) contrast agent, magnetic separation of oligonucleotides and other bio-components and magnetically guided site specific drug delivery system[41-42]. Gold coating on any particle increases the chemical stability by

protecting the core material from oxidation and corrosion. It also increases the bio-compatibility and affinity via amine/thiol terminal groups[42].

Among different inorganic composite particles semi conductor core-shell particles are of much importance. These types of core-shell particles have core made of semiconductor material, semiconductor alloy or metal oxide with shell made of semiconductor material, metal oxide or inorganic material like silica[43-45]. These structures can be binary with a core and shell or a tertiary structure with a core and two shells. The most common binary structure well known by the name quantum dots are CdSe/CdS, CdSe/ZnS, ZnSe/ZnS, CdTe/CdS. These are used for fluorescent bio-imaging.[46]

In another important type of inorganic core-shell particle the core is made of one or more lanthanide group element and shell is made of silica or any other lanthanide group elements. These particles show high luminescence and have potential application in the field of electronics and bio-imaging[47].

1.4.4 Organic core -organic shell particles

These are particles that have a polymeric core and a polymeric shell and are dispersed in a matrix which can be any material whose property is to be modified. One of the materials in this category is Polymethylmethacrylate (PMMA) coated Polyvinylchloride (PVC)/antimony trioxide composites[48]. The interaction between PMMA and the PVC along with antimony trioxide enhance toughness and strength of PVC. Some of these particles improve the thermal sensitivity of materials[49]. Polystyrene/Poly(N-isopropylacrylamide) (P-NIPA) core-shell nanoparticles with silver embedded in the NIPA coat are found to enhance the catalytic activity of silver by improving sensitivity[50].

The concept of polymeric core-shell composites has also been extensively used in the field of conducting polymers. Conducting polymers like polyaniline, polythiophene, polyacetylene, polypyrrole etc show good conductivity,[51] but they are often brittle in nature as well as insoluble and hence very difficult to make film from them. In order to improve the processing problem these conducting polymers are coated over seed particles of mechanically stable insulating polymers to give core-shell morphology. These composite particles have manifold applications such as

antistatic coating, dampers, clutches, electrodes, separation membranes, electro chromic devices, electro-chemomechanical actuators, and sensors[52-53]. Depending on the type of insulating polymer used as core these conducting polymer-coated latex particles can exhibit very good mechanical stability. Moreover, the amount of conducting polymer used can be greatly reduced in the shell phase without much loss of conductivity[54].

The core latex used in the preparation of conducting core-shell particles is usually prepared by surfactant free emulsion polymerization. A uniform layer of the conducting polymer is coated over the core particle by polymerizing the respective monomers in presence of these core particles. Polymerization of the conducting phase is normally carried out by oxidative chemical polymerization method. The conducting core-shell latexes show clear percolation behaviour. The conductivity strongly increases at a very distinct amount of the conducting polymer and reaches a value remarkably close to the conductivity of a pure conducting polymer that is polymerized using the same routine[55].

The reason for the formation of the core-shell structure in an in-situ polymerization is that the conducting polymer chains are insoluble in the medium (water) if their size exceeds a certain value. After this point, the polymer chains can either nucleate a new particle, aggregate with other polymer chains to form a conducting polymer-structure or adsorb onto an existing surface. If the polymerization of respective monomer is performed in the presence of core latex, a very large surface area will be present in the medium for the conducting polymer chains to absorb onto. If this happens, core-shell structures can be formed[55-56]. The process of the formation of conducting core-shell latexes is schematically depicted in **Fig1.2**.

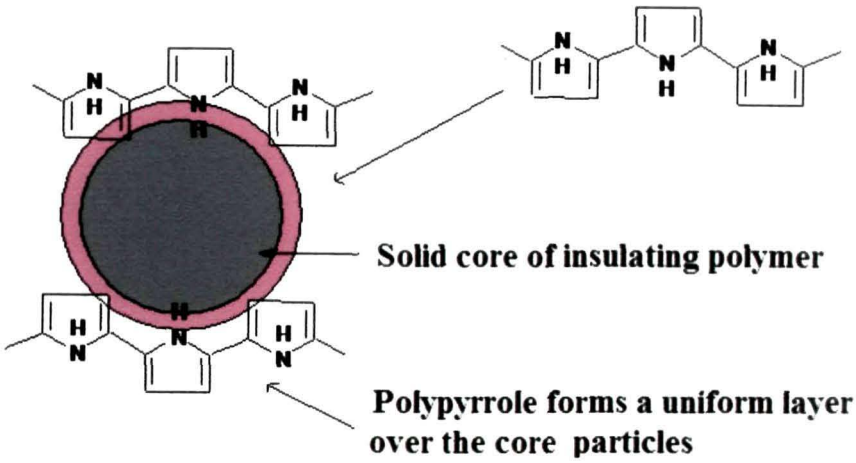

Fig 1.2: Schematic presentation of the formation of conducting core-shell latex via in-situ polymerization.

1.5 Synthesis of core-shell particles

Preparation of core-shell particles involves multi-step synthetic procedure. But the most important parameters needed to be considered are the uniformity in the coating of the shell phase and control on the thickness of the shell layer. There are various methods for the synthesis of core-shell particles used by different research groups viz. precipitation,[57-58] emulsion,[59-60] micro-emulsion,[61-62] sol-gel condensation,[63-64] layer by layer deposition[65-66] etc. Although many attempts have been made to control the thickness and uniformity of the shell, it is still a big challenge. The main difficulties associated are

- Agglomeration of the core phase in the medium.
- Preferable formation of separate shell particles rather than forming coating over the existing core phase.
- Incomplete coverage of the core surface

So preparation of core-shell particles with proper thickness and uniform coating is a challenging research topic in recent time. To achieve control over the coating the core phase is often modified so as to facilitate selective deposition of the shell phase on the core surface. Surfactants [29,67] and polymers [68, 69] are often used for the modification of the core surface. Surfactants and polymers can change the surface

charge and selectivity of the core particles so that shell phase is selectively deposited resulting completely coated core-shell particles with proper shell thickness.

Although many techniques are employed for the synthesis of polymeric core-shell particles the most extensively used technique is emulsion polymerization.

1.5.1 Emulsion Polymerization

Emulsions are heterogeneous mixtures of at least one immiscible liquid dispersed in another in the form of droplets[70]. In most cases, at least one of the liquids will be water or an aqueous solution. An emulsion is often described as either oil-in-water (O/W) or water-in-oil (W/O) where the first phase mentioned refers to the internal (or dispersed) phase. Generally, emulsions have average droplet sizes of at least several micrometres and the droplets have a rather broad size distribution unless special procedures are adopted (e.g., fractionation of the emulsion). In the context of polymer synthesis, emulsions can be used in three ways: as templates for the preparation of colloids, porous materials and composite materials respectively. (**Fig 1.3**) In order to produce colloids, polymerisation takes place in the dispersed monomer phase, although initiation tends to occur in monomer-swollen micelles rather than the larger monomer droplets[71-72]. In the case of an O/W emulsion polymerisation, this process leads to aqueous polymer latex. By contrast, polymerisation of the continuous phase of a concentrated emulsion followed by removal of the internal phase leads to the formation of emulsion templated porous materials[73]. Polymerisation of both the droplet phase and the continuous phase results in the production of composites [72, 74].

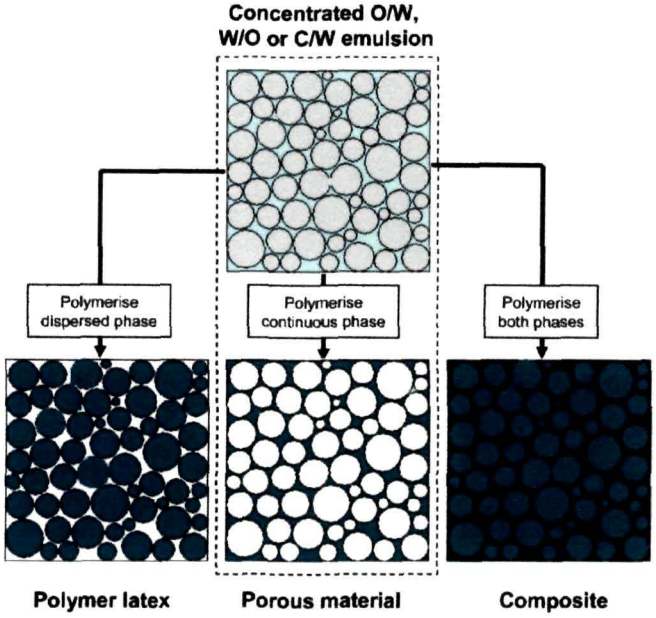

Fig 1.3: Schematic representation of polymerisation of an emulsion in the dispersed phase, continuous phase, and both phases for the preparation of colloids, porous materials, and composites respectively[70].

Emulsion polymerization normally consists of water insoluble monomer(s), a dispersing medium (usually water), a suitable surfactant(s) and a water soluble initiator[75]. The role of surfactant is to facilitate micelle formation. In addition surfactant plays an important role in stability, rheology and the particle size of the resulting latices. The locus of initiation in an emulsion polymerization is generally accepted to be in the aqueous phase. The polymerization process commences with radicals generated by the thermal decomposition (or otherwise) of the initiator, reacting with the monomer in the aqueous phase to form oligomeric radical species[76].

1.5.1.1 Mechanism of emulsion polymerization

The first successful theory to explain the distinct features of emulsion polymerization was largely developed by Smith, Ewart and Harkins[77](**Fig 1.4**). They divided the mechanism of emulsion polymerization into three stages or intervals[78-80].

Interval I: Particle nucleation occurs during this stage and is usually completed at low monomer conversion (2–10%) when most of the monomer is located in relatively large (1–10 nm) droplets. Particle nucleation takes place when radicals formed in the

aqueous phase grow via propagation and then enter into micelles or become large enough in the continuous phase to precipitate and form primary particles.

Interval II: It involves polymerization within the monomer swollen polymer particles, with the monomer supplied by diffusion from the droplets.

Interval III: It begins when the droplets disappear or at least reach a polymer fraction similar to that of the particles and continues to the end of the reaction

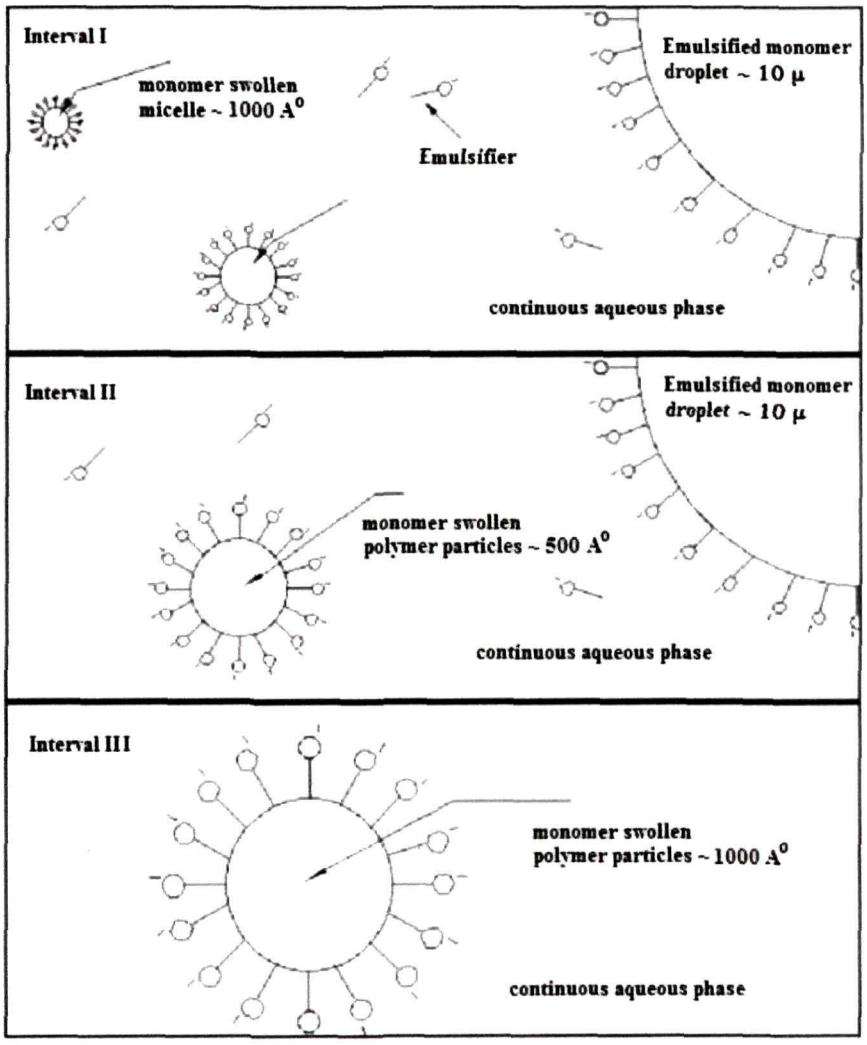

Fig 1.4: Various stages of emulsion polymerization[80]

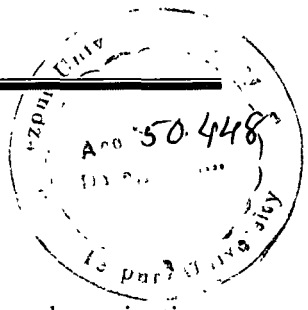

1.5.1.2 Emulsion Polymerization Components

1.5.1.2.1 Monomers

A wide variety of monomers can be polymerized by emulsion polymerization. Among them are butadiene, styrene, acrylonitrile, ethylene, vinyl chloride, vinyl acetate, vinylidene chloride, methacrylic acid and its alkyl esters (e.g., methyl, butyl, 2-ethyl hexyl) and others. The selection of monomers is governed by the intended latex end-use (e.g., paints, adhesives, sealants) and desired end-product properties (e.g., adhesive strength, minimum film forming temperature). Because end-products are usually specifically tailored formulations, compatibility with other latexes or common additives can also be tailored by appropriate monomer selection[81].

1.5.1.2.2 Stabilizers

There are two primary functions of a stabilizer in emulsion polymerization. One is to facilitate particle nucleation and the other is to stabilize the latex particles against flocculation as the polymerization proceeds. There are three basic types of stabilizers employed in emulsion polymerization[82-83].

i)Electrostatic stabilizers: Anionic or cationic surfactants which prevent coagulation by electrostatic repulsion arising from the charges located on the particle surfaces and their associated electric double layers. eg.sodium dodecyl sulphate (SDS) and stabilizers from the Aerosol series (sodium dialkyl sulfosuccinates).

ii)Polymeric (steric) stabilizers: Which stabilize the particles via entropic repulsion caused by the tendency of packing of two chains in the same space. eg. hydroxyethyl cellulose and poly(vinyl alcohol) (PVOH)

iii)Electrosteric stabilizers: Which display the characteristics of the previous two. These are rarely used in coating and adhesive applications and are often used in personal care products.

1.5.1.2.3 Initiators

In conventional emulsion polymerization, mostly water-soluble (e.g., potassium or ammonium peroxodisulfate) thermal and redox type initiators are used but oil-soluble initiators (e.g., benzoyl peroxide (BPO), 2,2-azo-bis(isobutyronitrile) (AIBN)) have also been employed[84]. Persulfate initiators are usually employed at temperatures above 50^0C where as redox initiators can be employed at lower temperatures and when high molecular masses with low degrees of branching are desirable.

1.5.1.2.4 Buffer

Due to possible hydrolysis reactions at acidic pH values, the presence of a buffer in an emulsion polymerization is desirable. Usually $NaHCO_3$, or Na_2CO_3 is employed[85]. If the pH is too low, the decomposition rate of the initiator may accelerate and thus, the number of radicals and subsequently, conversion increases[86].

1.5.1.2.5 Chain Transfer Agents (CTA)

The CTAs are added to regulate the molecular weight development in an emulsion polymerization. Although a large number of chemicals can act as a CTA (e.g., aldehydes, chlorinated aliphatics, disulfides, amines, and other carbonyl components), generally, the most employed are substances from the thiol family[87].

1.5.1.2.6 Dispersion Medium (Water)

Particle nucleation and stability in anionically stabilized emulsion polymerization can be affected by the presence of cations in natural water[88]. Thus, deionized and distilled water is used as a dispersing medium. In addition, while trace organic components in water may have little influence on the kinetics due to their low concentration, the presence of oxygen is of utmost concern even at low concentrations. Oxygen acts as a free-radical scavenger and its presence leads to a delay in the start of polymerization (induction period), which in some cases may be followed by a retardation period[89]. Thus, prior to polymerization, it is common to purge the reactor contents with nitrogen.

1.5.1.2.7 Additives

Additives are usually added to enhance the end product performance of emulsion polymers. For high performance formulations, it is necessary to have knowledge of polymer properties (e.g. composition, molecular weight, rheology), the properties of the additive and the compatibility of the two. Different additives can be added to latex depending on its end use. Some commonly used additives are cellulose derivatives, polyvinyl alcohol, starch, silicones, sulfosuccinates, disulfosuccinates etc[90].

1.5.2 Seeded emulsion polymerization

For the preparation of core shell particles, where both the core as well as the shell is made up of polymers, a series of consecutive emulsion polymerization sequences seems to be the most convenient method. Here the second stage monomer is polymerized in the presence of first stage seed particles. A large number of emulsion polymerization techniques are available for designing this type of core-shell particles. However the most commonly used methods were developed by Kowalski et al.[91], Vogels[92] and Blakenship[93] and subsequently modified by Vanderhoff[94]. The process developed by Kowalski and colleagues[91] is essentially the following: First of all, a core latex comprised of particles containing carboxylated comonomers (or other ionisable monomers), usually in the range from 25 to 40 wt% is prepared. Next, a hard polymeric shell, typically based on styrene or methyl methacrylate is prepared on to the previously obtained carboxylated core particles. In the final step carboxyl groups of the core are neutralised with bases at temperature close to the glass transition temperature (T_g) of the shell polymer. Venderhoff et al.[94] have prepared hollow particles (core) with definite morphology using this technique.

1.5.3 Acid/alkali Swelling Method

In the acid/alkali swelling method[95] first of all, seed latex with carboxylic acid groups is prepared; secondly, a hard permeable polymer shell is formed on the outer surfaces of the carboxylic core polymer particles; thirdly, at around the glass transition temperature (Tg) of the shell, particles containing water and polyelectrolyte

are prepared by neutralizing the carboxylic acid groups of the core polymer particles using volatile alkali. The latex particles with a great number of carboxylic acid groups are first synthesized by several steps and then neutralized by alkali and swelling. When the latex particles have swollen enough, they are acidified to make the outer layer shrinkage cavity close. Then the aggregated polymers, with an inner layer of polycarboxylate containing water and outer layer of carboxylic acid groups, are obtained. At last, the aggregated polymers are acidified to make the outer of latex particles case-hardened to form the hollow microspheres[96-97]. Hollow polymer particles can be made by etching away the core of a core-shell particle. For example, after the synthesis of core-shell particles with a cross-linked polystyrene shell, the poly(methyl methacrylate) core was dissolved with methylene chloride[98]. The diameter of the resulting hollow capsules could be adjusted between 15 and 30 nm by variation of the surfactant to monomer ratio. The shell thickness was approximately 2–5 nm.

1.5.4 Dynamic swelling method

Okubo et al.[99] synthesized hollow core shell particles with polydivinylbenzene shell and polystyrene core using dynamic swelling method. Here PS latex particles are first synthesized by seed polymerization. Then the latex particles are swelled in toluene and divinylbenzene (DVB) was mixed with solvent. Then DVB is induced to polymerize. After the polymerization, PS is removed and hollow microspheres with a polydivinylbenzene (PDVB) shell are formed. In order to prove the above experiment, further studies were carried by Okubo and his co-workers [100] using the method of suspension polymerization to polymerize the PS/ DVB/toluene mixture solution in different proportions. They found that the hollow structure was affected by molecular weight and the concentration of PS indicating that PS plays an important role in the dynamic swelling method.

1.5.5 Template method

In the template method, a polymer shell is formed on the surface of template particles and then the template particle is removed and hollow polymer shells are obtained[101].The template method is often used to prepare hollow polymer

microspheres of different materials and has been proven as a very successful method[102-103]. The processes of the template method for preparing hollow polymer micro spheres include two steps. First, the polymer shell is formed on the interface between the template and the surrounding continuous phase due to the deposition or reaction of the solute on the surface of the dispersed templates. Second, the hollow structure can be obtained by removing the template materials[104]. However, despite of its simple process, the template method is limited because it requires a large amount of template, resulting in high cost. The schematic illustration of preparing hollow structure with the template method is shown in **Fig 1.5**.

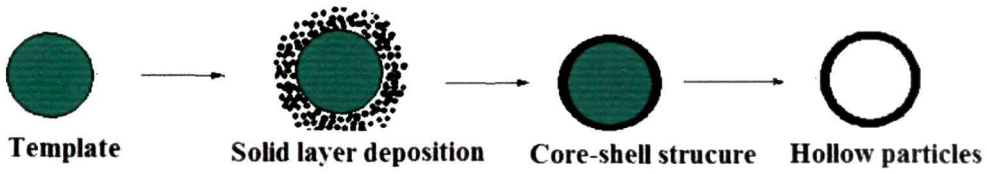

Fig1.5: Schematic illustration of formation process of hollow micro spheres structure for template method[105]

1.5.6 Layer-by-Layer method (LBL)

Core-shell as well as hollow particles can also be prepared by layer-by-layer (LBL) assembly technique. LBL method is suitable for preparing micro spheres with controllable wall thickness. With the LBL technique many template materials such as latex particles of melamine-formaldehyde (MF) resin, erythrocytes, some inorganic salts, PS and poly (styrene-co-maleic anhydride) (PSMA) microspheres could be prepared[106]. The hollow microspheres prepared by LBL method possess uniform shell thickness and good spherical morphology, but this method is relatively complex, so its application is limited[107].

1.5.7 Miniemulsion method

Miniemulsion polymerization is another most extensively used technique for the development of core-shell latex particles[108-109]. A schematic representation of the

miniemulsion polymerization process and the formation of different morphologies including core-shell are given in **Fig 1.6**.

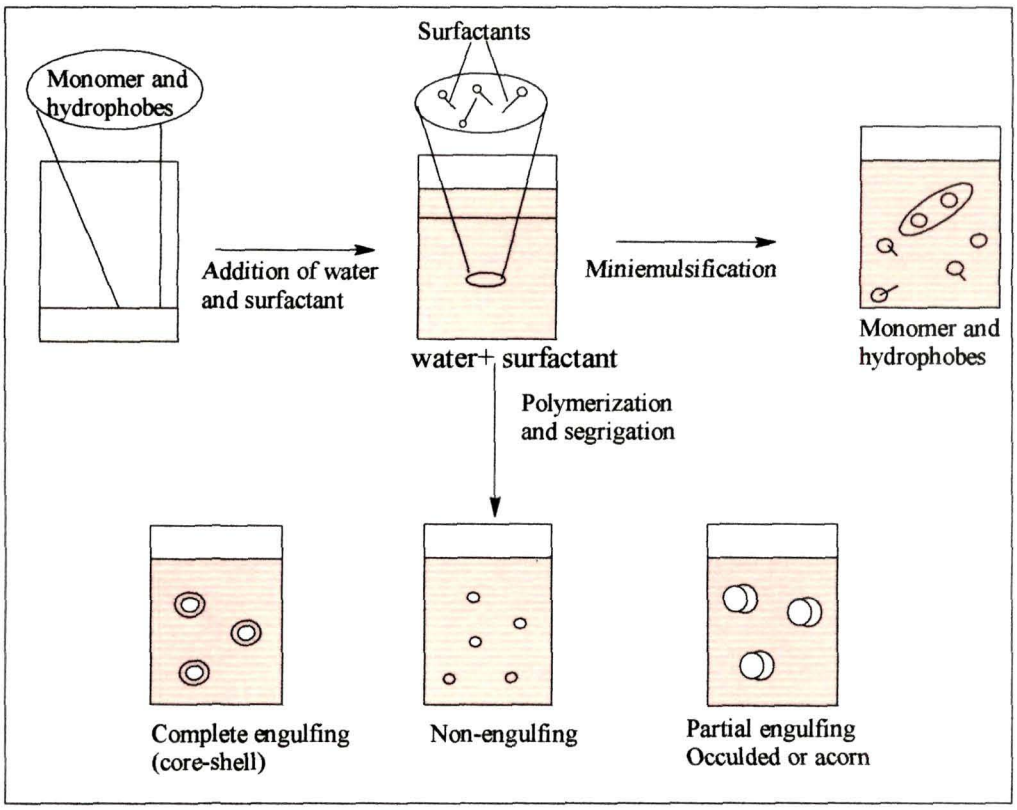

Fig 1.6: The principle of miniemulsion polymerization and the formation of different particle morphology[108]

Number of literatures deal with the difference between conventional emulsion and miniemulsion polymerization[110-111].The basic difference lies in the size of the monomer droplets. The size of the dispersed droplets in miniemulsion is quite small (between 50 and 500 nm) relative to the size of the monomer droplets in an emulsion system (ranging from 1 to 100 μm)[112]. This difference in droplet size is responsible for the different mechanisms of particle nucleation operating in the two systems.

Miniemulsion polymerization involves the use of an effective surfactant/ co-stabilizer system to produce very small monomer droplets. The droplet surface area in these systems is very large and most of the surfactant is adsorbed at the droplet surface. Particle nucleation is primarily via radical (primary or oligomeric) entry into monomer droplets, since little surfactant is present in the form of micelles or as free surfactant available to stabilize particles formed in the continuous phase. Both oil-

and water-soluble initiators may be used; the important feature is that the reaction proceeds by polymerization of the monomer in this small droplets[110, 113].

1.5.7.1 Preparative methods of miniemulsions

In principle, miniemulsion polymerization is carried out by dissolving a suitable surfactant system in water and dissolving the co surfactant in monomer(s), followed by premixing under vigorous stirring[110]. The mixture is then subjected to a highly efficient homogenization process called miniemulsification. Following are the most commonly used devices to achieve homogenization: rotor-stator devices, sonifiers and high pressure homogenizer. Today ultrasound, first reported in 1927,[114] is used especially for the homogenization of small latex quantities whereas rotor-stator devices are used to prepare large quantity of latex[115].

Different monomers, with a wide range of water solubilities have been polymerized by this technique. This includes vinyl acetate (VAc),[116] methyl methacrylate (MMA),[117,] butyl acrylate (BA)[118] and styrene (Sty)[119]. System containing more than one monomer has also been prepared including miniemulsions in which very water-soluble monomers such as acrylic acid (AA) [120] and methaacrylic acid (MAA) [121] have been used.

The vast majority of miniemulsion polymerizations reported in the literature have been stabilized with anionic surfactants. This is probably because of the widespread application of anionic surfactants in macroemulsion polymerization and due to their compatibility with neutral or anionic (acid) monomers and anionic initiators. However, Landfester and coworkers[122] have used the cationic surfactants cetyltrimethyl ammonium bromide (CTAB) and cetyltrimethyl ammonium tartrate (CTAT) for the production of styrene miniemulsions. They reported that these surfactants produce similar particle sizes to anionic surfactants used at the same levels. Bradley and Grieser[123] reported the use of dodecyltrimethyl ammonium chloride for the miniemulsion polymerization of MMA and BA.

In miniemulsion polymerization either water-soluble or oil-soluble initiators may be used. Bechthold and Landfester[124] studied the miniemulsion polymerization of styrene using the water soluble initiator potassium persulfate (KPS). They found that the reaction rate slightly increases with increase of the initiator concentration.

However, increasing the initiator concentration caused a significant reduction of the average degree of polymerization. An oil soluble initiator can be mixed with the oil phase before premixing with the surfactant/water solution. Oil-soluble initiators are preferred for the polymerization of water soluble monomers such as methyl methacrylate, vinyl chloride etc[125]. Oil-soluble initiators are also used for polymerization of extremely low water soluble monomers such as lauryl methacrylate (LMA). Alducin and Asua[126] have studied the molecular weight distribution of polystyrene miniemulsion polymerized with oil-soluble initiators. Ghazaly et al.[127] have used AIBN for the miniemulsion copolymerization of a hydrophobic bifunctional macromer. The polymerization progressed much faster when KPS was used than when AIBN was used. This may be due to the tendency of oil-soluble initiator radicals to recombine before initiating polymerization, as discussed by Luo[128].

A very important factor for formulation of a stable miniemulsion is the choice of an appropriate co-surfactant. Landfester et al.[122] found that the predominant requirement for an efficient co surfactant is an extremely low water solubility (less than 10^{-7} mL mL^{-1}) independent of its chemical nature. The water insoluble compound is usually a fatty acid or long chain alkene. The addition of co-surfactant such as hexadecane[129] or cetyl alcohol[119] can efficiently retard the destabilization of the nanodroplets by Ostwalds ripening. Monomer soluble polymers have also been used as co-surfactant in miniemulsion polymerization. Miller et al.[130] used 1 wt% of polystyrene with cetyl alcohol as a co-surfactant for miniemulsion of styrene. They found that the reaction proceeds at faster rate and resulted lattices with smaller particle size in comparison with conventional mini emulsion containing no polystyrene. They attributed this result to involve the entry of radicals to the preformed polymer particles. Wang and Schork[131] used PS, PMMA and PVAc as the co-stabilizers in miniemulsion polymerizations of VAc with PVOH as the surfactant. They found that PMMA and PS were effective kinetic costabilizers (at 2- 4% wt on total monomer) for this system. While the polymeric co-stabilizers did not give true miniemulsions, ostwald ripening was retarded long enough for predominant droplet nucleation to take place.

1.5.7.2 Properties of miniemulsion

One of the main advantages of miniemulsion polymerization is the ability to produce high solid content, low viscosity latices can be successfully synthesised and results with latex particles having almost same size as the initial droplets. Ouzineb et al.[132] carried out miniemulsion of styrene and butyl acrylate to produce high solid content low viscosity lattices. Products with solid contents greater than 70 wt% and viscosities as low as 350 mPs at a shear rate of 20 s^{-1}were obtained. Other advantages that miniemulsion can provide over other polymerization techniques are

- Allows copolymerization of monomers with different solubilities.
- Allows the incorporation of hydrophobic materials, which can be polymerized in emulsion polymerization with difficulty [133].
- Polymer lattices with better colloidal stability can be prepared [134].
- High solid content lattices with no coagulation can be obtained [135].

1.5.8 Microemulsion Method

In microemulsion method particle size and morphology can be controlled precisely. Microemulsion is a mixture of oil and water with suitable surfactant and co-surfactant. Surfactants form reverse micelles and the co-surfactants reduce the electrostatic repulsive force between the charged head group of the surfactants. For particle formation reagents are added in the aqueous phase; micelles act as a centre for nucleation and epitaxial growth of the particles. Changing the molar ratio of water to surfactant, particle size and morphology can be controlled. By this method mainly inorganic core-shell particles such as metal, metal oxide or semi conductor particles are synthesised. Hota et al.[136,137] synthesised CdS-Ag_2S core-shell nanoparticles by this technique. Using this technique Carpenter et al.[138] coated gold over iron particles. Lambert[139], Decker[140] and Carnes[141] synthesised different nanoparticles with core-shell morphology by microemulsion technique. Different research group[142-145] predicted that the particle formation in microemulsion is due to the intermiceller exchange of reactants and new born particles by both single and multiple microemulsion system.

1.5.9 Sol-gel method

The sol-gel is a wet chemical technique (chemical solution deposition) widely used in the material science and ceramic engineering mainly for synthesis of metal oxide nanoparticles. The sol-gel process is two step process; hydrolysis of the metal salt followed by condensation process. This method is mainly applied for the synthesis of metal or metal oxide/polymer core-shell particles. Using this method semi- conductor core-shell nanoparticles have also been synthesised[146-147]

1.5.10 Mechanochemical Synthesis

In this process both mechanical and chemical forces are applied for the synthesis of core-shell particles. There are many kinds of mechanical forces applied for particle synthesis but amongst them most extensively used are ultrasound and electrical potential.

1.5.10.1 Sonochemical Synthesis

In this technique particles are synthesised by chemical process with constant ultrsonication to improve reaction rate, breaking agglomeration and enhance the dispersion in the solvent. Ultrasonic irradiation of the frequency range of 20 kHz to 1 MHz has been used in most of the sonication methods. Ultrasonic cavitations generate local high temperature and high pressure and a very rigorous environment for chemical reaction. Thus these cavities act as micro reactor for reaction to occur and mechanical force too enhance the reaction rate. The chemical reaction that occur depends on the shell material used as the core is synthesised separately and added to the reaction mixture[126]. Composites such as iron oxide with gold shell and iron/cobalt alloy nanoparticles are synthesised by this technique[148,149]. Pol et al.[147] synthesised Ag coated silica particles in presence of inert argon gas by sonochemical technique.

1.5.10.2 Electrodeposition

Formation of shell over the core with charged polymer and inorganic material can be carried out by this method in presence of electrical potential. In general electric field is varied like a wave with positive and negative cycles. It is found that the metal deposits over core surface during negative cycle where as charged polymer

deposits during the positive cycle. Therefore by controlling the cycle time span the thickness of the shell material can be controlled. Material deposition occurs in one of the electrodes. The matrix material for the core-shell particle formation can be the electrode or the electrolytic medium. Banerjee et al.[150] studied the synthesis of iron oxide shell over iron in silica nanoparticles by electrodeposition method and Chipra et al.[151] describes the synthesis of ppy-iron nanoparticles by this technique. Both the procedure are almost similar but in the former case the electrolytic medium and silica gel is used as the matrix for the nanocomposite while in the later case no material is used as matrix and hence they belongs to class of nanoparticles. CuI-Au and CuS-Au core-shell nanoparticles were synthesised by Gu et al.[152] using electrochemical atomic layer deposition.

1.6 Morphology of the core-shell particles

Many literature have focused on understanding the mechanism of formation of polymer-polymer core-shell particles[108.153]. Depending on the synthetic conditions, there can have core-shell particles with various structures. Both thermodynamic and kinetics of polymerization affect the type of structure that may be achieved[154.155]. These include normal core-shell structures, heterogeneous structure with occlusion of one polymer embedded in the other, inverted core-shell structures, where the core and shell materials are exchanged or formation of raspberry-like and confetti-like etc[109,156-160]. Some possible morphologies are depicted in **Fig 1.7**

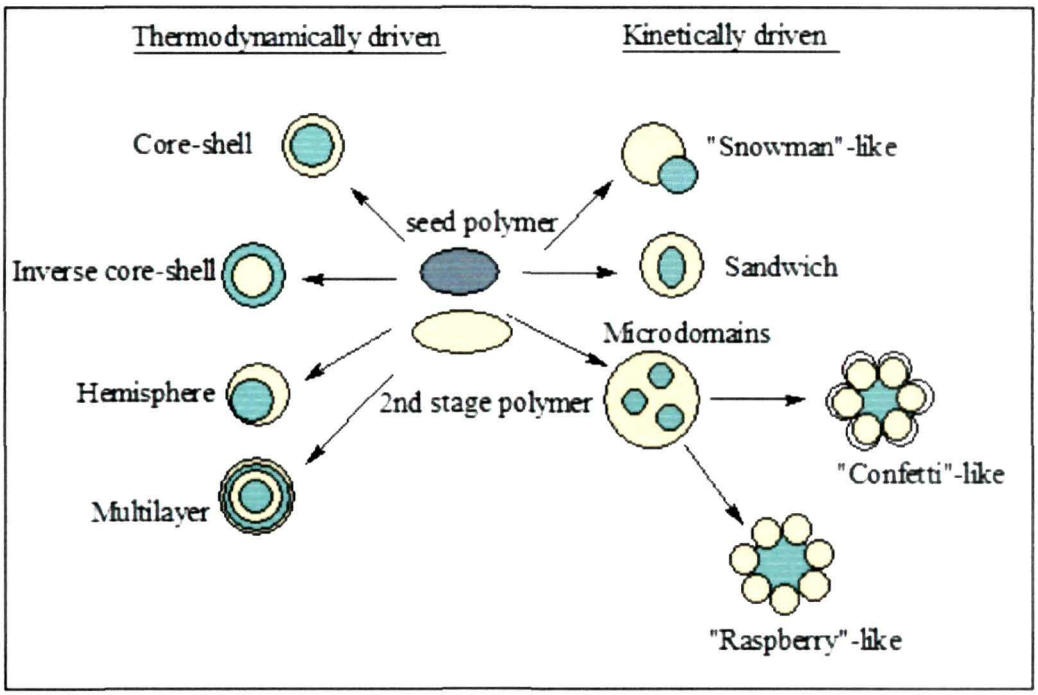

Fig 1.7: Some possible core-shell morphology

1.6.1 Prediction of particle morphology

The final morphology of the synthesised core-shell particle is of vital importance. The properties and hence the end on application largely depends on this morphology, i.e. the arrangement of the polymers within these particles. Many publications deal with the factors on which the morphology of the core-shell composite particles depends. In the preparation of poly(methyl methaacrylate) (PMMA)/polyacrylonitrile (PAN) core-shell particles, Chen et al.[157] observed that the morphology of the particles depends on the thermodynamic and kinetics of the polymerization. These were predicted using a mathematical model presented by Winzor and Sunberg[161] and Chen et al.[156-158]. In another publication Sundberg and Durrant[162] focused on the fundamental factors that determine the final morphology of the core-shell particles. They applied equilibrium thermodynamics to the phase separated particles to understand the basic controlling factors on which the final morphology depend. They found that the interfacial tension at the polymer-water and polymer-polymer interface along with the cross linking density play dominant role in determining the particle morphology. The thermodynamic factors rely mainly on the interfacial energy between the core and the shell surface. The system favours morphology where the

overall surface free energy and the energy of molecular interaction is minimum. Thermodynamic factors are usually used to determine the equilibrium morphology whereas kinetic factors such as mobility of the polymer chain determine the ease with which the equilibrium morphology can be achieved.

1.6.2 Thermodynamic theory of particle formation

The prime factor that needs to be considered is the equilibrium morphology, which determines the final structure provided that the kinetic factors favour the desired morphology. The most important parameter here is the contribution of the surface free energy which is influenced by the type of monomer used, the type and amount of surfactant and initiator used for polymerization, the reaction temperature and the difference in the hydrophobicity of the monomers used and polymers prepared[15,136]. It was found that for minimum interfacial free energy of the system the more hydrophilic polymer should preferably form the outer layer of the particle so that it is in contact with the water phase.

A thermodynamic theory which was first studied by Torza and Mason in 1970 is used to predict the morphology of the particles[163]. According to this theory the preferred morphology is the one which has the lowest interfacial energy. They studied a system containing two immiscible liquids, phase 1 and 3, suspended in a third immiscible liquid phase 2. They used the following equation to predict the morphology of the resultant latex

$$S_i = \sigma_{jk} - (\sigma_{ij} + \sigma_{jk}) \qquad 1.1$$

Where S_i is the spreading coefficient, σ_{jk} is the interfacial tension between phase j and phase k and σ_{ij} is the interfacial tension between phase i and phase j ($i \neq j \neq k = 1, 2, 3$)

It was found that if σ_{12} is greater than σ_{23}, then there are three possible sets of values for S_i These are

$$S_1 < 0;\ S_2 < 0;\ S_3 > 0$$

$$S_1 < 0;\ S_2 < 0;\ S_3 < 0$$

$$S_1 < 0;\ S_2 > 0;\ S_3 < 0$$

These three sets of value correspond to three possible equilibrium morphologies which may be formed in this model: complete engulfment, partial engulfment and non-engulfment of the core phase. Thus by adjusting the required parameters one can achieve the desired core-shell morphology. A schematic view of the possible morphologies predicted by this theory is given in **Fig1.8**

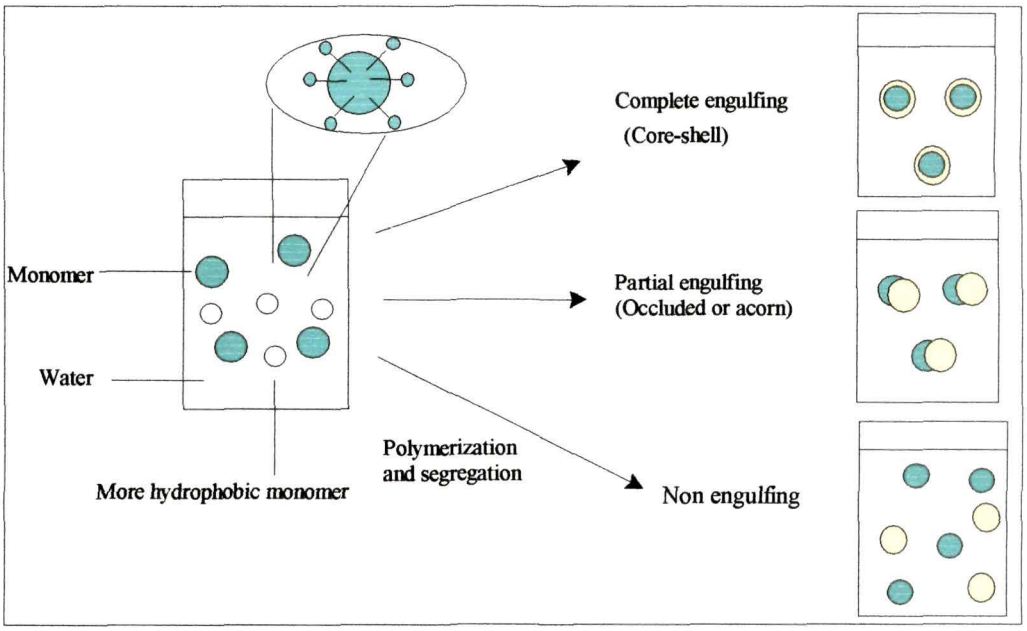

Fig 1.8: A schematic view of the possible morphologies predicted by the Torza and Mason thermodynamic theory[79]

1.6.3 Kinetics of Particle formation

According to the kinetic theory the morphology of the final particles largely depends on diffusion, relative rate of initiation, monomer consumption and phase rearrangement within the particles themselves[158]. Here the factors that need to be considered are the degree of cross linking, the viscosity at the polymerization locus, the monomer concentration, glass transition temperature of the polymers and the reaction temperature. It is assumed that the equilibrium morphology of the final latex particles are predominantly determined by the thermodynamic criteria while the kinetic criteria determines the ease with which the thermodynamically favoured morphology is achieved. However, mobility of the polymer chains plays an imperative role in shaping the final morphology. When the mobility of the polymer chain is restricted the rate of phase separation and rearrangement of the polymer chains becomes slower than the polymerization rate. In such circumstances a non

equilibrium condition occurs and kinetics become the predominant factor in controlling the particle morphology.

Another important factor is ease with which the oligomeric radicals enter the polymerization loci. The non equilibrium particle morphology is profoundly dependent on the mobility of these oligomeric radicals. These radicals enter the polymer particles from the water phase and if their mobility or diffusion rate is limited then the second stage polymer preferably forms the outer layer of the particles. In such case core-shell is the most likely morphology. The work of Torza and Mason[163] can be taken as an example, where the key factor in governing the equilibrium morphology is the high mobility of the liquid phase. Kinetic factors include the followings-

1.6.3.1 Influence of anchoring effect induced by initiators

Cho and Lee [164] used electron microscopy to study the effect of different polymerization parameters on which the final morphology of the particles depends. MMA and Sty were used for polymerization in the model study. Factors that were investigated in their study were the anchoring effect of the ionic terminal groups that are introduced into a sample through the use of an ionic initiators, pH and viscosity of the polymerization locus. They found that the change in particle morphology was very much related to the type and concentration of the initiator used and the temperature at which polymerization was carried out. Three initiators KPS, AIBN, and 4, 4□-azobis-(4-cyanovaleric acid) (ABCVA), were used in this study. The anchoring effect due to the ionic terminal groups of the ionic initiators was found to be the vital factor in controlling the particle morphology. They found that when the water-soluble initiator KPS was used, particles with core-shell morphologies were obtained. This was attributed to the anchoring effect of the terminal SO_4^{2-} end group. This leads to a surface- active oligomer, which anchors itself at the water/oil interface on entering the monomer droplet. Thus it may be inferred that anchoring effect plays a pivotal role in determining the final morphology of the particles.

1.6.3.2 Influence of Viscosity

The viscosity in the polymerization locus is one of the key factor in determining the particle morphology. A low viscosity in the polymerization locus enhances the mobility of the polymer chain in the polymerization locus[165]. This facilitates the migration of the two immiscible phases into two different domains, which leads to the thermodynamically favoured morphology. A high viscosity will decrease the degree of phase separation by creating a kinetic barrier towards polymer chain diffusion. This is most likely to occur when the T_g of at least one of the polymer is close or above the reaction temperature. Another case is when the monomer is fed slowly throughout the second stage polymerization; an extremely high viscosity is generated in the polymerization locus. It then becomes difficult for the two polymer phases to rearrange themselves into their thermodynamically favoured or equilibrium morphology.

According to Cho and Lee[164] the controlling factor in the generation of non-equilibrium morphologies is the competition between the phase separation and polymer kinetics. Viscosity in the polymerization loci controls the mobility of the polymer molecules and hence the particle morphology. With a high viscosity in the polymerization locus the morphology was uneven, in which the PS rich domains were present in the PMMA rich region. On the other hand at low viscosity, clear phase separation between the PS rich and PMMA rich region occurs leading to a well-defined core-shell particle.

1.6.3.3 Influence of polymer cross-linking

Sheu et al.[166] studied the effect of cross linking on the phase separation of interpenetrating polymer networks. They studied the effect of divinylbenzene on the phase separation of polystyrene/polystyrene latex interpenetrating polymer networks. They observed that phase separation of the resulting particles largely depends on the extent of cross linking of the latex particles. When polymer phase is cross-linked, their chain mobility is restricted which lead to the formation of composite particles with morphology not favoured by thermodynamic criteria. They investigated the kinetics of phase separation by examining the changes in particle morphology using optical microscopy, which revealed that the phase separation was induced by the

relaxation of the polymer chains before polymerization began and it increases with increased monomer conversion. They inferred that the phase separation was indeed caused by the formation of a cross linked network inside the particles. In addition, the degree of phase separation and the number of separated domains increases with increased cross linker concentration in the seed particles.

1.7 Application of core-shell particles

Core-shell particles in the combined form have significant industrial applications specially coating, biomedical and electronics field. But separately, core and shell have different use in presence of the other. Here we discuss some industrial application of core-shell particles and also use of core and shell in presence of the other.

1.7.1 Core material property

For the synthesis of hollow particles from core-shell particles, the property of core material is an important factor. It is easy to synthesize hollow particle if the degradation temperature of the core phase is relatively low or the core material have a high solubility in a suitable solvent[23-28]. To achieve these criteria polymeric core are the most suitable. Magnetic nanoparticles such as iron oxide or cobalt core particles are used to enhance the MRI image by improving the contrast.

1.7.2 Shell material property

Shell material coating on the core surface increases the colloidal stability of the core particles. Amongst the different inorganic material silica is the most extensively used shell material .Since silica is an inert material it does not effect the redox stability of the core material; it just block the core particle so that the colloidal stability of the particle increases. Moreover, since silica is optically transparent the chemical properties of the core particle can be studied spectroscopically. Silica reduces the bulk conductivity of the metal particle; prevent the photo catalytic degradation of the polymeric material. Silica shell is also used to modulate the position and intensity of the colloidal metal surface plasmon absorption band[36].

Core-shell particles with polymeric shell and hollow particles are used for control drug delivery,[167,168] enzyme transplantation,[168] contaminated waste removal, gene therapy etc.

1.7.3 Core and shell material properties

Carbon coated TiO_2[169] and carbon coated with $Li_3V_2(PO_4)_3$ core-shell particles[170] are used to increase the efficiency of lithium ion batteries. The core-shell particles are biocompatible and used for control drug delivery purpose and encapsulated drug without affecting the core material. Au/Ag core-shell nanocomposite particles are used for labelling cancer and tumour cells[171].

Depending on the type and nature of material used in core and shell phase core-shell particles have been extensively used in various fields. **Table 1.1** shows a few applications of core-shell particles depending on the types of material used.

Table 1.1: Various core-shell particles and their potential applications

Sl. No	Core-shell particle		Field of Application	Purpose of Application
	Core Phase	Shell Phase		
1	Polystyrene	Polybutylacrylate, Polymethylacrylate	Surface Coating	Binder/pigment to improve hiding power of coating
2	Polybutyl acrylate	Polypyrrole, Polyaniline	Impact Modifier, Chemical Sensor	To improve the mechanical strength of the conducting polymers
3	Nanoclays	Polystyrene, Polybutylacrylate	Nanocomposite	To improve the thermal stability of the polymer
4	Gold	Silica	Optoelectronics	Optical sensing materials
5	Silver	Silica	Optoelectronics	As fluorescent bioimaging
6	Particles of $CuInS_2$	Acetonitrile	Organoelectronics	In photovoltaics

1.8 Objectives and plan of the work

Core-shell particles are now-a-days getting much importance among the material researchers because of their unique morphology, improved properties and versatility in applications. In the core-shell morphology two or many materials are entangled together and hence these particles show properties of all its components. The synthesis of such multiple phase composite particles provides an opportunity to tailor properties for a range of desired applications such as paints, coatings and additives, cosmetics, pharmaceuticals, paper industries, drug delivery,

chromatographic columns etc. Core-shell particles may be many types: inorganic-inoganic, organic-organic(polymer-polymer), hybrid organic-inorganic etc.

Polymer-polymer core-shell particles are of much importance in the paint and coating industries. In paint industries TiO_2 is used as pigment in emulsion paints. Since TiO_2 has comparatively high refractive index than the polymer phase, so it imparts hiding power in coatings. However, TiO_2 is purchased by weight whereas paint is sold by volume. So use of TiO_2 as hiding pigment is not cost effective. Moreover, the compatibility between polymers and TiO_2 is poor. Core-shell particles which have hard domains (formed from a high T_g polymer) and soft domains (formed from a low T_g polymer) can be potentially used in the paint industries as an opaque pigment.

Another type of core-shell particles having an insulating thermosetting plastic as core and an intrinsically conducting polymer as shell is gaining immense interest in present time. Although PANI, ppy etc. show good conductivity they have very poor mechanical strength and film forming ability. So, to improve their mechanical strength and to achieve better processibility they are often combined with insulating polymers to give core-shell morphology. These sort of core-shell particles are effectively used in many optoelectronic devices such as sensors, rechargeable betteries etc.

Polymer-inorganic nanocomposites with core-shell morphology are another class of material with good potential application. Nanocomposites exhibit unique and great enhancement of properties over traditional composites. Core-shell nanocomposites are often used to improve various properties of polymers such as thermal stability, optical properties, mechanical properties etc.

In the present thesis an effort have been made to prepare a set of polymer-polymer core-shell particles and to find some applications of these particles in emulsion based paints and optoelectronic devices. Following objectives are set to carry out the above mentioned research work:

Objectives of the present investigation

- Preparation of core-shell particles by seeded emulsion polymerization and their characterization by SEM, TEM, GPC technique.
- Application of the core-shell particles in emulsion satin paint and evaluation of their opaque properties.
- Preparation of core-shell particles with insulating core and conducting shell and their characterization by UV-Visible, FT-IR, XRD, SEM and TEM analysis.
- Investigation of electrical, electrochemical and thermal properties of the core-shell particles.
- Application of the core-shell particles as toxic gas sensor.
- Development of nanocomposite particles with core-shell morphology and their characterization by SEM, TEM, TGA etc.

To fulfil the above objectives the following plans of work have been adopted.

- Preparation of core-shell particles with poly (n-butyl acrylate- co-methacrylic acid-co- ethylene glycol dimethylacrylate) as core and poly(styrene-co- methylmethacrylate) as shell by seeded emulsion polymerization.
- Characterization of the core-shell particles by SEM, TEM and GPC.
- Application of the core-shell particles in emulsion satin paints and evaluation of its pigment properties.
- Preparation of core-shell particles with poly(styrene-co-methyla acrylate) as core and ppy as the shell by surfactant free mini emulsion polymerization.
- Characterization of the particles by FT-IR, SEM, TEM and TGA; evaluation of electrical and electrochemical properties.
- Application of the core-shell particle as ammonia sensor.
- Development of core-shell nanocomposite of poly(styrene-co-methyl acrylate) and bentonite clay by ultra sonic assisted mini-emulsion polymerization.
- Characterization of the nanocomposite by FT-IR, SEM, TEM and TGA analysis.

References

1. Bahadur, P., Sastry, N.V. *Principles of Polymer Science* (Narosa Publishing House, New delhi, 2003)
2. Maiti, S. *Polymer materials- Science, Technology, Development* (Anusandhan Prakashan, 2009)
3. Billmeyer, F.W. *A textbook of polymer science* (A Wiley Interscience Publication, John Wiley and Sons, New York, 1994)
4. Stevens, M.P. *Polymer Chemistry-An Introduction* (Addison Wesley Publ. Co. Inc. New York, 1973)
5. Brandrup, J.E.H. *Immergut (Ed) Polymer Handbook* (John Wiley and sons, New York, 1989)
6. Ghosh, P. *Polymer Science & Technology- Plastics, Rubbers, Blends and Composites* (Tata Mcgraw Hill, London, 2006)
7. Turner, A. (Jr.), Edward, F.W. *Organic Polymers* (Prentice-Hall, Englewood Cliffs. New Jersey, 1967)
8. Odian, G. *Principle of polymerization* (John Wiley and Sons, New York, 2004)
9. www. Wikipedia.org (11/2/2011)
10. Rodger, T. *Paint Technology Handbook* (Grand Rapids, USA, 2007)
11. Berendsen A. M. *Marine painting manual* (London: Graham & Trotman,1989)
12. Bently, J. Turner, G.P.A. *Introduction to Paint Chemistry and Principles of Paint Technology* (Unk. Publishers, London, 1997)
13. Patton, T.C. *Paint Flow and Pigment Dispersion* (Wiley-Interscience, NewYork, 1979)
14. Schuler, B., Baumstark, R., Krisch, S., Pfau, A., Sanor, M., Zosel, A. Structure and Properties of Multiphase Particles and Their Impact on the Performance of Architectural Coatings. *Prog. Org. Coat.* **40,** 139–150 (2000)
15. Stubbs, J., Sundberg, D. Fundamental Studies on Morphology Control for Latex Systems with Application to Waterborne Coatings: The Effect of Polymer Radical Mobility in Latex Particles During Polymerization. *J. Coat. Technol.* **75,** 59–67 (2003)
16. Basset, D. Hydrophobic Coatings from Emulsion Polymers. *J. Coat. Technol.* **73,** 42–55 (2001)

17. Dimonie, V., Daniels, E., Shaffer, O., El-Aasser, M. Control of Particle Morphology, In Emulsion Polymerization and Emulsion Polymer (John Wiley & Sons Ltd. NewYork, 1997)
18. Skotheim T.A., Elsenbaumer, J.R. *Reynolds Handbook of conducting polymers* (Marcel Dekker, New York, 1998)
19. Pickup, N.L., Sharpio, J.S., Wong, D.K.Y. Extraction of mercury and silver into base-acid treated polypyrrole films: A possible pollution control technology. *J Polym. Res.* **8,** 151-157 (2001)
20. Nellipan, V., El-Aasser, M., Klein, A., Daniels, E. Effect of the core/shell latex particle interphase on the mechanical behavior of rubber-toughened poly (methyl methacrylate). *J Appl. Poly. Sci.* **65**, 581-593 (1997)
21. Lu, M., Keskkula, H., Paul, D. Thermodynamics of solubilization of functional copolymers in the grafted shell of core-shell impact modifiers: 2. Experimental *Polymer* **37**, 125-135 (1996)
22. Phadtare, S. et al. Direct assembly of gold nanoparticle "shell" on polyurethane microsphere "cores" and their application as enzyme immobilization templates. *Chem. Mater.* **15**, 1944-1949 (2003)
23. Caruso, F. Hollow capsule possessing through colloidal templating and self assembly. *Chem. Eur. J.* **6,** 413-419 (2000)
24. Caruso, R.A., Susha, A., Caruso, F. Multilayered titania, silica and laponite nanoparticle coating on polystyrene colloidal templates and resulting inorganic hollow spheres. *Chem. Mater.* **13,** 400-409 (2001)
25. Caruso, R.A., Caruso, F., Mohwald, H. Nanoengineering of inorganic and hybrid hollow spheres by colloidal templating. *Science* **282,** 1111-1114 (1998)
26. Sgraja, M., Bertling, J., Kummel, R., Jansens, P.J. Inorganic and hybrid hollow spheres by coating of microcapsules as template. *J. Mater. Sci.* **41**, 5490-5494 (2006)
27. Song, C., Wang, D., Gu, G., Lin, Y., Yang, J., Chen, L., Fu, X., Hu, Z. Preparation and characterization of silver/TiO_2 composite hollow spheres. *J. Colloid Inter. Sc.* **272,** 340-344 (2004)
28. Yang, J., Lind, J.U., Trogler, W.C. Synthesis of hollow silica and titania nanospheres. *Chem. Mater.* **20**, 2875-2877 (2008)

29. Hoffman-Caris, C.H.M. Polymer at the surface of oxide nanoparticles. *New J. Chem.* **18,** 1087-1096 (1994)

30. Dresco, P.A., Zaitsev, V.A. Gambino, R.J., Chu, B. Preparation and properties of magnetite and polymer magnetite nanoparticles. *Langmuir* **15,** 1945-1951 (1999)

31. Gittins D.I., Caruso, F. Tailoring the polyelectrolyte coating of metal nanoparticles. *J. Phys. Chem. B.* **105**, 6846-6852 (2001)

32. Watson, K.J., Zhu, J., Nguyen, S.T., Markin, C.A. Hybrid nanoparticles with block copolymer shell structure. *J. Am. Chem. Soc.* **121**, 462-463 (1999)

33. Zhang, Y.P., Lee, S.H., Reddy, K.R., Gopalan, A.I., Lee, K.P. Synthesis and characterization of core-shell SiO_2 nanoparticles/ poly(3-aminoboronic acid) composites. *J. Appl. Poly. Sci.* **104**, 2743-2750 (2007)

34. Debrujin, J.D., Brink, I.V.D., Mendes, S., Dekker, R., Bovell, Y.P., Blitterswijk, C.A.V. Bone induction by implants coated with cultured osteogenic bone marrow cells. *Adv. dent. Res.* **13**, 74-81 (1999)

35. Olea, N. et al. Estrogenicity of resin-based composites and sealants used in dentistry. Environ. *Health Perspective* **104**, 298-305 (1996)

36. Ung, T., Liz-Marzn, L.M., Mulvaney, P. Controlled method for silica coating of silver colloids, influence of coating on the rate of chemical reactions. *Langmuir* **14**, 3740-3748 (1998)

37. Lu, Y., Yin, Y., Li, Z.Y., Xia, Y. Synthesis and self-assembly of Au@SiO_2 core-shell colloids. *Nano letters* **2**, 785-788 (2002)

38. Li, T., Moon, J., Morrone, A.A., Mecholsky, J.J., Talham, D.R., Adair, J.H. Preparation of Ag/SiO nanosize composites by a reverse micelle and sol-gel techniques. *Langmuir* **15**, 4328-4334 (1999)

39. Decker, S., Klabunde, K.J. Enhancing effect of Fe_2O_3 on the ability of nanocrystalline calcium oxide to absorb SO_2. *J. Am. Chem. Soc.* **118,** 12465-12466 (1996)

40. Carnes C.L., Klabunde, K.J. Unique chemical reactivities of nanocrystalline metal oxides towards hydrogen sulphide. *Chem. Mater.* **14,** 1806-1811 (2002)

41. Santra, S., Tapec, R., Theodoropoulou, N., Dobson, J., Hebard, A., Tan, W. Synthesis and characterization of silica-coated iron oxide nanoparticles in

microemulsion: the effect of non-ionic surfactants. *Langmuir* **17,** 2900-2906 (2001)

42. Wang, L. et al. Monodispersed core-shell Fe_3O_4 @ Au nanoparticles. *J. Phys. Chem. B.* **109**, 21593-21601 (2005)
43. Lambert, K., Geyter, B.D., Moreels, I., Hens, Z. PbTe/CdTe core/shell particles by cation exchange, a HR-TEM study. *Chem. Mater.* **21**, 778-780 (2009)
44. Hota, G., Idage, S.B., Khilar, K.C. Characterization of nano-sized Cds-Ag_2S core-shell nanoparticles using XPS techniques. *Colloids Surf. A: Physicochemical and Engineering Aspects* **293**, 5-12 (2007)
45. Mews, A., Echymuller, A., Giersig, M., Schooss, D., Weller, H. Preparation, characterization and photophysics of the quantum dot quantum well system CdS/HgS/CdS. *J. Phys. Chem.* **98**, 934-941 (1994)
46. Schreder, B. et al. Raman characterization of CdTe/CdS core-shell clusters in colloids and films. *J. Crys. Growth.* **214**, 782-786 (2000)
47. Yi, S.S., Bae, J.S., Moon, B.K., Jeong, J.H., Kim, J.H. Highly enhanced luminescence of nanocrystalline TiO_2:Eu^{3+} phosphors. *Optic. Mater.* **28**, 610-614 (2006)
48. Xie, X.L., Li, R.K.Y., Liu, Q.X., Mai, Y.W. Structure property relationship of in-situ PMMA modified nano-sized antimoni trioxide filled poly (vinyl chloride) nanocomposites. *Polymer* **45**, 2793-2802 (2004)
49. Lu, Y., Mei, Y., Ballauff, M. Thermosensitive core-shell particles as carrier system for metallic nanoparticles. *J. Phys. Chem. B.* **110,** 3930-3937 (2006)
50. Garito, F.A., Hsaio, Y.L., Gao, R. Thermal polymer nanocomposite. (US Patent, **S20030174994**, 2003)
51. Gangopadhyay, R., De, A. Conducting polymer nanocomposites: a brief overview. *Chem Mater.* **12,** 608-622 (2000)
52. Skotheim TA, Elsenbaumer JR, *Reynolds (Eds.). Handbook of Conducting Polymers* (Marcel Dekker, New York, 1998)
53. Pickup, N.L., Shapiro, J. S., Wong, D. K. Y. Extraction of mercury and silver into base-acid treated polypyrrole films: A possible pollution control technology. *J. Poly. Res.* **8,** 151-157 (2001)

54. Huijs, F.M., Lang, J. Kalicharan, D. Formation of transparent conducting films based on core-shell latices: Influence of the polypyrrole shell thickness. *J. Appl. Polym. Sci.* **79,** 900-909 (2001)

55. Fitch, R.M. *Polymer Colloids, A comprehensive introduction* (Academic Press, San Diego, USA, 1997)

56. Roncali, J., Garreau, R., Yassar, A., Marque, P., Garnier, F., Lemaire M. Effects of steric factors on the electrosynthesis and properties of conducting poly(3-alkylthiophenes) *J. Phys. Chem.* **91**, 6706–6714 (1987)

57. Imhof, A. Preparation and characterization titania- coated polystyrene spheres and titania shells. *Langmiur* **16,** 1602-1611 (2001)

58. Ocana, M., Hsu, W.P., Matijevic, E. Preparation and properties of uniform-coated colloidal particles. 6. Titania on zinc oxide. *Langmuir* **7**, 2911–2916 (1991)

59. Zou, H., Wu, S., Shen, J. Polymer/Silica Nanocomposites: Preparation, Characterization, Properties, and Applications. *Chem. Review.* **108**, 3893-3957(2008)

60. Okaniwa, M. Synthesis of poly (tetrafluoroethylene)/poly(butadiene) core-shell particles and their graft copolymerization. *J. App. Poly. Sci.* **68,** 185-190 (1998)

61. Hota, G., Jain, S., Khilar, K. C. Synthesis of CdS–Ag_2S core-shell/composite nanoparticles using AOT/*n*-heptane/water microemulsions . *Colloid Surf. A: Physicochemical and Engineering Aspects* **232,** 119-127 (2004)

62. Han, M. Y., Huang, W., Chew, C.H., Gan, L. M. Large Nonlinear Absorption in Coated Ag_2S/CdS Nanoparticles by Inverse Microemulsion. *J. Phys. Chem. B.* **102**,1884-1887 (1998)

63. Song, C., et al. Preparation and characterization of silver/TiO_2 composite hollow spheres. *J. Colloid Interface Sci.* **272**, 340-344 (2004)

64. Li, T., Moon, J., Morrone, A. A., Mecholsky, J. J., Talham, D. R., Adair J. H. Preparation of Ag/SiO_2 Nanosize Composites by a Reverse Micelle and Sol−Gel Technique. *Langmiur* **15**, 4328-4334 (1999)

65. Srivastava, S., Kotov, N. A. Composite layer-by-layer (LBL) assembly with inorganic nanoparticles and nanowires. *Acc. Chem. Res.* **41,** 1831-1841 (2008)

66. Shenoy D.B., Antipov, A.A., Sukhorukov G.B., Mhwald, H. Layer-by-layer engineering biocompatible, decomposable core-shell structure. *Biomacromolecules* **4**, 265-272 (2003)

67. Wu, T.M., Chu, M. Preparation and characterization of thermoplastic vulcanization/silica nanoparticles. *J. App. Poly. Sci.* **98**, 133-144 (2005)

68. Liz-Marzan, L.M., Giersig, M., Mulvaney, P. Synthesis of nanosized gold-silica core-shell particles. *Langmuir* **12,** 4329-4335 (1996)

69. Perro, A., Reculusa, S., Bourget-Lami E.,Duguet, E, Ravaineom S. Synthesis of hybrid colloidal particles, from snowman-like and raspberry-like morphologies. *Colloid surf. A: Physicochemical and Engineering Aspects* **284,** 78-83 (2006)

70. Myers, D. *Surfaces, Interfaces, and Colloids: Principles and Applications* (Wiley-VCH,1999)

71. Lovell, P. A., El-Aasser, M. S. *Emulsion Polymerisation and Emulsion Polymers* (John Wiley & Sons, New York, 1997)

72. Zhang, H., Cooper, A.I. Synthesis and applications of emulsion-templated porous materials. *Soft. Matter.* **1**, 107-113 (2005)

73. Zhang, H., Cooper, A. I. Synthesis of Monodisperse Emulsion-Templated Polymer Beads by Oil-in-Water-in-Oil (O/W/O) Sedimentation Polymerization. *Chemistry of Materials* **14**, 4017-4020 (2002)

74. Ruckenstein, E., Li, H. The concentrated emulsion approach to toughened polymer composites: A review. *Polym. Compos* **18**, 320–331 (1997)

75. Helmiyati, Budianto, E., Priyono, W., Yulizar, Y. The Kinetics and Mechanism of the Core-shell Styrene-butyl Acrylate Polymerisation. *J. Phy. Sci.* **21**, 39–52 (2010)

76. Tauer , K., Hernandez, H., Kozempel, S.,Lazareva, O., Nazaran, P. Towards a consistent mechanism of emulsion polymerization-new experimental details. *Colloid Polym Sci.* **286,** 499–515 (2008)

77. Okubo, M.(edt.) *Advances in Polymer Science: Polymer Particles* (Spingerlink, 2005)

78. Amaral, M.D., Asua J.M. Synthesis of large, high-solid-content latexes by miniemulsion polymerization Issue. *J Poly. Sci. Part A: Polymer Chemistry* **42,** 4222–4227 (2004)

79. Antonietti, M., Landfester, K. Polyreactions in miniemulsions. *Progress in Polymer Science* **27,** 689-757 (2002)

80. Asua, J.M. Miniemulsion polymerization. *Progress in Polymer Science* **27,** 1283-1346 (2002)

81. Gilbert, R.G. *Emulsion Polymerization- A Mechanistic Approach* (Academia Press, London, 1995)

82. Hellgren, A.C., Weissenborn, P., Holmberg K. Surfactants in water-borne paints. *Progress in Organic Coatings* **35**, 79-87 (1999)

83. Warson, H. *The Application of Synthetic Resin Emulsion* (Ernest Benn, London, 1972)

84. BurguiNre, C. et al. Block Copolymers of Poly(styrene) and Poly(acrylic acid) of Various Molar Masses, Topologies, and Compositions Prepared via Controlled/Living Radical Polymerization. Application as Stabilizers in Emulsion Polymerization. *Macromolecules* **34,** 4439- 4450. (2001)

85. Du, Y.Z., Ma, G.H., Nagai M., Omi, S. Synthesis of high solid lattices by thermally initiated emulsion polymerization *J. Appl. Polym. Sci.* ***85,*** 2478-2483 (2002)

86. Young, Z.D., Fu,Q.H., Yuan, H., Shinzo, O.M.I. Thermal Emulsion Polymerization without any Conventional Initiators and Emulsifiers. *Chinese Chemical Letters* **17,** 553-556 (2006)

87. Flory, P. J. *Principles of Polymer Chemistry* (Cornell University Press, Ithaca, NewYork, 1953)

88. Garidel, P., Hildebrand, A. Thermodynamic Properties of Association Colloids. *Journal of Thermal Analysis and Calorimetry* **82,** 483–489 (2005)

89. Song, J.S., Winnik, M.A. Cross-linked monodisperse micron-sized polystyrene particles by two-stage dispersion polymerization. *Macromolecules* **38,** 8300-8307 (2005)

90. Rodger, T., *Paint Technology Handbook* (Grand Rapids, Michigan, USA, 2007)

91. Kawalski, A., Vogel, M. Hollow-particle latexes: Preparation and properties *U.S. Patent* **4970241** (1990)

92. Vogel, M. Method for improving erasability or erasable marking compositions. *U.S. Patent* **5447560** (1995)

93. Blakenship, R.M. Encapsulated hydrophilic polymers and their preparation *U.S. Patent* **5494971** (1996)

94. Vanderhoff, J.W., Park, J.M., El-Aasser, M.S. Preparation of Particles for Microvoid Coatings by Seeded Emulsion Polymerization. *ACS Symposium Series* **492,** 272- 281 (1992).

95. Kowalski, A., Vogel, M., Blankenship, R M. Sequential hetero polymer dispersion and a particulate material obtainable therefrom, useful in coating compositions as a thickening and/or opacifying agent. *U.S. Patent* **4427836** (1984)

96. Okubo, M., Ito, A., Kanenobu, T. Production of submicron-sized multi hollow polymer particles by alkali/cooling method. *Colloid and Polymer Science* **274**, 801-804 (1996)

97. Okubo, M., Mori, H. Production of multi-hollow polymer particles by the stepwise acid/alkali method. *Colloid and Polymer Science* **275**, 634-639 (1997)

98. Kobayashi, H., Suzuki, T., Moritaka, M., Miyanaga, E., Okubo, M. Preparation of multihollow polystyrene particles by seeded emulsion polymerization using seed particles with incorporated nonionic emulsifier: effect of temperature. *Colloid and Polymer Science* **287**, 251-257 (2009)

99. Okubo, M., Minami, H. Formation mechanism of micron-sized monodispersed polymer particles having a hollow structure. *Colloid and Polymer Science* **275**, 992-997 (1997)

100. Okubo, M., Konishi, Y., Minami, H. Production of hollow polymer particles by suspension polymerization. *Colloid and Polymer Science* **276,** 638-642 (1998)

101. Bai, F.Y., Fang, S. J. Progress in research on hollow polymer particles by vesicles templating. *Chinese Journal of Colloid & Polymer* **23,** 26-30 (2004)

102. Li, G.C., Zhang, Z. K. Synthesis of submicrometer-sized hollow titania spheres with controllable shells. *Materials Letters* **58,** 2768-2771 (2004)

103. Li, W.Z., Qin, C.G., Xiao, W.M. Preparation of hollow layered MoO_3 microspheres through a resin template approach. *Journal of Solid State Chemistry* **178,** 390-394 (2005)

104. Yang, Y., Chu, Y., Yang, F.Y. Uniform hollow conductive polymer microspheres synthesized with the sulfonated polystyrene template. *Materials Chemistry and Physics* **92**, 164-171 (2005)

105. Wang A.J., Lu, Y.P., Sun, R.X. Recent progress on the fabrication of hollow microspheres. *Materials Science and Engineering: A* **460**, 1-6 (2007)

106. Ding, S.J., Zhang, C.L., Yang, M. Template synthesis of composite hollow spheres using sulfonated polystyrene hollow spheres. *Polymer* **47**, 836-840 (2006)

107. Bin, W., Shujun, W., Hongguang, S., Hongyan, L., Jie, L., Ning, L. A review of recent progress in preparation of hollow polymer microspheres. *Pet. Sci.* **6,** 306-312 (2009)

108. Van Zyl, A.J.P., Sanderson, R.D., Wet-Roos, D., Klumperman, B. Core/Shell Particles Containing Liquid Cores: Morphology Prediction, Synthesis, and Characterization. *Macromolucules* **36,** 8621-8629 (2003)

109. Chen, Y.C., Dimonie, V., El-Aasser, M.S. Interfacial phenomena controlling particle morphology of composite latexes. *J. Appl. Polym. Sci.* **42,** 1049-1063 (1991)

110. Kim, N., Sudol, E.D., Dimonie, V.L., El-Aasser, M.S. Comparison of Conventional and Miniemulsion Copolymerizations of Acrylic Monomers Using Poly (vinyl alcohol) as the Sole Stabilizer. *Macromolucules* **37**, 2427-2433 (2004)

111. Aizpurua, I., Barandiaran, M.J. Comparison between conventional emulsion and miniemulsion polymerization of vinyl acetate in a continuous stirred tank reactor. *Polymer* **40**, 4105-4115 (1999)

112. Sudol, E.D., El-Aasser, M.S. *Miniemulsion Polymerization, In Emulsion Polymerization and Emulsion Polymers, Lovell, P., El-Aasser, M.S. Eds.* (John Wiley & Sons Ltd., New York, 1997)

113. Soma, J., Papadopoulos, K.D. Ostwald Ripening in Sodium Dodecyl Sulfate-Stabilized Decane-in-Water Emulsions. *Journal of Colloid and Interface Science* **181**, 225-231 (1996)

114. Wood, R., Loomis, A. The Physical and Biological Effects of High Frequency Sound Waves of Great Intensity. *Philosopical Magazine* **4**, 417-436 (1927)

115. Asua, J.M. Miniemulsion polymerization. *Progress in polymer Science* **27**, 1283-1346 (2002)

116. Wang, S., Schork, F.J. Miniemulsion polymerization of vinyl acetate with nonionic surfactant. *J. Appl. Polym. Sci.* **54**, 2157-2164 (1994)

117. Reimers, J., Schork, F.J. Robust nucleation in polymer-stabilized miniemulsion polymerization. *J. Appl. Polym. Sci.* **59**, 1833-1841 (1996)

118. Tang, P.L., Sudol, E.D., Adams, M., El-Aasser, M. S., Asua, J. M.Seeded emulsion polymerization of *n*-butyl acrylate utilizing miniemulsions. *J. Appl. Polym. Sci.* **42**, 2019-2028 (1991)

119. Choi, Y.T., El-Aasser, M.S., Sudol, E.D., Vanderhoff, J.W. Polymerization of styrene miniemulsions. *Journal of polymer science: Part A: Polymer Chemistry* **23**, 2973-2987 (1985)

120. Unzué, M.J., Asua, J.M. Semicontinuous miniemulsion terpolymerization: Effect of the operation conditions. *J. Appl. Polym. Sci.* **49**, 81-90 (1993)

121. Masa, J.A., De Arbina, L.L., Asua, J.M. A comparison between miniemulsion and conventional emulsion terpolymerization of styrene, 2-ethylhexyl acrylate and methacrylic acid. *J. Appl. Polym. Sci.* **48**, 205- 213 (1993)

122. Landfester, K., Bechthold, N., Tiarks, F., Antonietti, M. Miniemulsion Polymerization with Cationic and Nonionic Surfactants: A Very Efficient Use of Surfactants for Heterophase Polymerization. *Macromolecules* **32**, 2679-2683 (1999)

123. Bradley, M., Grieser, F. Emulsion polymerization synthesis of cationic polymer latex in an ultrasonic field. *J. Colloid Interf Sci.* **251**, 78-84 (2002)

124. Bechthold, N., Landfester, K. Kinetics of Miniemulsion Polymerization As Revealed by Calorimetry. *Macromolecules* **33**, 4682–4689 (2000)

125. Saethre, B., Mørk, P.C., Ugelstad, J. Preparation of poly(vinyl chloride) latexes by polymerization of stabilized monomer droplets. *Journal of polymer science: Part A: Polymer Chemistry* **33**, 2951-2959 (1995)

126. Asua, J., Alduncin, J., Forcada, J. Miniemulsion Polymerization Using Oil-Soluble Initiators. *Macromolecules* **27**, 2256- 2261 (1994)

127. Ghazaly, H.M., Daniels, E.S., Dimonie, V.L., Klein, A., El-Aasser, M.S. Miniemulsion copolymerization of *n*-butyl methacrylate with crosslinking monomers. *J. Appl. Polym. Sci.* **81**, 1721-1730 (2001)

128. Luo, Y, Schork, F.J. Emulsion and miniemulsion polymerizations with an oil-soluble initiator in the presence and absence of an aqueous-phase radical scavenger. *Journal of polymer science: Part A: Polymer Chemistry* **40**, 3200-3211(2002)

129. Delgado, J., El-Aasser, M.S., Vanderhoff, J.W. Miniemulsion copolymerization of vinyl acetate and butyl acrylate. I. Differences between the miniemulsion copolymerization and the emulsion copolymerization processes. *Journal of polymer science: Part A: Polymer Chemistry* **24**, 861-874 (1986)

130. Miller, C.M., Sudol, E.D., Silebi, C.A., El-Aasser, M.S. Polymerization of Miniemulsions Prepared from Polystyrene in Styrene Solutions. 1. Benchmarks and Limits. *Macromolecules* **28**, 2754–2764 (1995)

131. Wang, S., Schork, F.J. Miniemulsion polymerization of vinyl acetate with nonionic surfactant. *J Appl Polym Sci.* **54**, 2157-2164 (1994)

132. Ouzineb, K., Graillat, C., McKenna, T. F.High-solid-content emulsions. V. Applications of miniemulsions to high solids and viscosity control. *J Appl. Polym. Sci.* **97**, 745-752 (2005)

133. Wu, X.Q., Schork, F.J. Batch and Semibatch Mini/Macroemulsion Copolymerization of Vinyl Acetate and Comonomers. *Ind. Eng. Chem. Res.* **39,** 2855–2865 (2000)

134. Schork, F.J., Luo, Y., Smulders, W., Russum, J.P., Butté, A. Fontenot, K. Miniemulsion Polymerization. *Advances in Polymer Science* **175**, 129-255 (2005)

135. Tauer, K., Müller, H., Schellenberg, C., Rosengarten, L. Evaluation of heterophase polymerizations by means of reaction calorimetry. *Colloids and Surfaces A: Physicochemical and Engineering Aspects* **153**, 143-152 (1999)

136. Hota, G., Jain, S., Khilar, K.C. Synthesis of CdS - Ag_2S/ core-shell / composites nanoparticles using AOT / n-heptane / water microemulsion. *Colloids Surf. A: Physicochemical and Engineering Aspects* **232**, 119 – 127 (2004)

137. Hota, G., Idage, S.B., Khilar, K.C. Characterization of nano-sized CdS - Ag_2S core-shell nanoparticles using XPS techniques. *Colloids Surf. A: Physicochemical and Engineering Aspects* **293,** 5-12 (2007)

138. Carpenter, E.E., Sangegerio, C., O'Connor, C.J. Effect of shell thickness on blocking temperature of nanocomposites of metal particles with gold shell. *Mag. IEEE. Trans.* **35**, 3496-3498 (1999)

139. Lambert, K., Geyter, B.D., Moreels, I., Hens, Z. PbTe / CdTe core/shell particles by cation exchange, a HR-TEM study. *Chem. Mater.* **21,** 778-780 (2009)

140. Decker, S., Klabunde, K.J. Enhancing effect of Fe_2O_3 on the ability of nanocrystalline calcium oxide to adsorb SO_2. *J. Am. Chem. Soc.* **118**, 12465-12466 (1996)

141. Carnes, C.L., Klabunde, K.J. Unique chemical reactivities of nanocrystalline metal oxide towards hydrogen sulfide. *Chem. Mater.* **14**, 1806 - 1811(2002)

142. Viswanadh, B., Tikku, S., Khilar, K.C. Modeling core-shell nanoparticle formation using three reactive microemulsion. *Colloids Surf. A: Physicochemical and Engineering Aspects* **298**, 149-157 (2007)

143. Ethayaraja, M., Bondyopadhyaya, R. Model for core-shell nanoparticle formation by ion-exchange mechanism. *Ind. Eng. Chem. Res.* **47**, 5982-5985 (2008)

144. Shukla, D., Mehra, A. Modeling shell formation in core-shell nanocrystals in reverse micelle system. *Langmuir* **22**, 9500-9506 (2006)

145. Tojo, C., Blanco, M.C., Rivadulla, F., Lopez- Quintela, M.A. Kinetics of the formation of particles in microemulsions. *Langmuir* **13**, 1970-1977 (1997)

146. Boissière, M., Meadows, P.J., Brayner, R., Hélary, C., Livage, J. Coradin, T. Turning biopolymer particles into hybrid capsules: the example of silica/alginate nanocomposites. *J. Mater. Chem.* **16,** 1178-1182 (2006)

147. Caruso, F. Nanoengineering of particle surface. *Adv. Mater.* **13,** 11-21 (2001)

148. Pol, V. G., Srivastava, D. N., Palchik, O., Palchik, V., Slifkin, M. A., Weiss, A.M., Gedanken, A. Sonochemical Deposition of Silver Nanoparticles on Silica Spheres. *Langmuir* **18,** 3352-3357 (2002)

149. Wu, W., He, Q., Chen, H., Tang, J., Nie, L. Sonochemical synthesis, structure and magnetic properties of air-stable Fe_3O_4/Au nanoparticles. *Nanotechnology* **18,** art. No. 145609 (2007)

150. Li, Q., Li, H., Pol, V.G., Bruckental, I., Koltypin, Y., Moreno, J. C., Nowik, I., Gedanken, A. Sonochemical synthesis, structural and magnetic properties of air-stable Fe/Co alloy nanoparticles. *New J. Chem.* **27,** 1194-1199 (2003)

151. Banerjee, S., Roy, S., Chen, J.W., Chakravorty, D. Magnetic properties of oxide- coated iron nanoparticles synthesised by electrodeposition. *J. Magnetism Magnetic materials* **219,** 45-52 (2000)

152. Chipara, M., Skomski, R., Sellmyer, D.J. Electrodeposition and magnetic properties of poypyrrole- Fe nanocomposites. *Mater. Lett.* **61,** 2412-2415 (2007)

153. Gu, C., Shannon, C., Xu, H., Park, M. Formation of metal-semiconductor core-shell nanoparticles using electrochemical atomic layer deposition. *ECS Transactions* **16,** 181-190 (2008)

154. Meng, F., Hiemstra, C., Engbers, G. H. M., Feijen, J. Biodegradable Polymersomes. *Macromolecules* **36,** 3004-3006 (2003)

155. Chen, W., Zhu, M., Song, S., Sun, B., Chen, Y., Adler, H.J.P. Morphological Characterization of PMMA/PAN Composite Particles in Nano to Submicro Size. *Macromolecular Materials and Engineering* **290,** 669–674 (2005)

156. Kirsch, S., Doerk, A., Bartsch, E., Sillescu, H., Landfester, K., Spiess, H.W. Synthesis and Characterization of Highly Cross-Linked, Monodisperse Core–Shell and Inverted Core–Shell Colloidal Particles.

Polystyrene/Poly(*tert*-butyl Acrylate) Core–Shell and Inverse Core–Shell Particles. *Macromolecules* **32,** 4508-4518 (1999)

157. Chen, Y. C., Dimonie, V., El-Aasser, M. S. Effect of interfacial phenomena on the development of particle morphology in a polymer latex system. *Macromolecule,* **24,** 3779-3787 (1991)

158. Chen, Y.C., Dimonie, V. L., Shaffer, O. L. Development of morphology in latex particles: The interplay between thermodynamic and kinetic parameters. *Polymer International* **30,** 185-194 (1993)

159. Chen, Y.C., Dimonie, V. L., El-Aasser, M. S. Role of surfactant in composite latex particle morphology. *J. Appl. Polym. Sci.* **45,** 487-499 (1992)

160. Loxley, A., Vincent, B. Preparation of Poly (methylmethacrylate) Microcapsules with Liquid Cores. *Journal of Colloid and Interface Science* **208,** 49-62 (1998)

161. C.L., Winzor, Sundberg, D.C. Conversion dependent morphology predictions for composite emulsion polymers: 1. Synthetic latices. *Polymer* **33,** 3797-3810 (1992)

162. Sundberg, D.C., Durant, Y.G. Latex Particle Morphology, Fundamental Aspects: A Review. *Polymer Reaction Engineering* **11,** 379-432 (2003)

163. Torza, S., Mason, S. G. Three-phase interactions in shear and electrical fields. *Journal of Colloid and Interface Science* **33,** 67-83 (1970)

164. Cho, I., Lee, K.W. Morphology of latex particles formed by poly (methyl methacrylate)-seeded emulsion polymerization of styrene. *J. Appl. Polym. Sci.* **30**, 1903-1926 (1985)

165. Wang, H. H., Li, X. R., Fei, G. Q., Mou, J. Synthesis, morphology and rheology of core-shell silicone acrylic emulsion stabilized with polymerizable surfactant. *eXPRESS Polymer Letters* **4,** 670-680 (2010)

166. Sheu, H.R., El-Aasser, M.S., Vanderhoff, J. W. Phase separation in polystyrene latex interpenetrating polymer networks. *Journal of polymer science: Part A: Polymer Chemistry* **28**, 629-651 (1990)

167. Crotts, G., Park, T.G. Preparation of porous and nonporous biodegradable polymeric hollow microspheres. *Journal of Controlled Release* **35,** 91-105 (1995)

168. Pathak, C.P., Sawhney, A.S., Hubbell, J.A. Rapid photopolymerization of immunoprotective gels in contact with cells and tissue. *J. Am. Chem. Soc.* **114,** 8311–8312 (1992)

169. Zhang, H.P., Yang, L. C., Fu, L.J., Cao, Q., Sun, D. L., Wu, Y. P., Holze, R. Core-shell structured electrode materials for lithium ion batteries. *J Solid State Electrochem.* **13**, 1521-1527 (2009)

170. Ren, M.M., Zhou, Z., Gao, X.P., Peng, W.X., Wei, J.P. Core–Shell $Li_3V_2(PO_4)_3$@C Composites as Cathode Materials for Lithium-Ion Batteries. *J. Phys. Chem. C.* **112**, 5689–5693 (2008)

171. Lee, S. et al. Biological imaging of HEK293 cells expressing PLC_{Y1} using surface enhanced Raman Spectroscopy. *Anal. Chem.* **79**, 916-922 (2007)

CHAPTER 2

Preparation of core-shell latex particles by emulsion co-polymerization of styrene and butyl acrylate and evaluation of their pigment properties in emulsion paints

Chapter 2

2.1 Introduction

Designing of new functional materials has gained a lot of importance amongst material scientists in recent time. To cope up with the ever increasing demand these materials many times need to fulfil contradictory properties in terms of their application. To fulfil these sorts of contradictory demands, core-shell particles are most extensively used in recent time[1-8]. For example binders used in coatings need to show excellent film formation and appearance as well as good blocking resistance and hardness[9-10]. In the paint industries, these core-shell particles can be of great importance due to their special structure. A core-shell particle consisting of a hard domain [formed from a high glass transition temperature (Tg) polymer] and soft domains (formed from a low Tg polymer) can meet the above mentioned demands effectively. These particles possess high block resistance and low minimum film forming temperature (MFFT). The low Tg polymer (soft phase) is responsible for good film elasticity, a sufficient film formation without solvent and a high film gloss whereas the high Tg polymer (hard phase) provides a good blocking resistance and surface hardness to the films. This is in agreement with the old formulators rule that higher the pigment volume concentration of a paint, the lower the tackiness of the paint film will be. The hard phase while acting as transparent filler providing block resistance should not detract from gloss or flexibility as it is well distributed and oriented in the polymer film having been grafted onto the soft phase during polymerization. Core-shell particles formed from polymers having difference in refractive index (between the core and shell phase) may potentially be applied as pigments in emulsion paints. This will reduce the amount of TiO_2 used and will also increase the compatibility between the paint and the pigment. This can provide an economical and environmentally benign alternative.

A part of this chapter is published in

* **L. J. Borthakur**, T. Jana, S.K. Dolui. *J. Coat. Technol. Res.*, **7**, 765–772 (2010)

The concept of polymeric core-shell composites has also been extensively used in the field of conducting polymers. Conducting polymers like PANI, polythiophene, polyacetylene, ppy etc show good conductivity but they are often brittle in nature[11-14] as well as insoluble and hence very difficult to make film from them. In order to improve the process difficulty these conducting polymers are coated over seed particles of mechanically stable insulating polymers to give core-shell morphology. These composite particles have manifold applications such as antistatic coating, dampers, clutches, electrodes, separation membranes, electro chromic devices, electro-chemomechanical actuators and sensors[15-18]. Depending on the type of insulating polymer used as core these conducting polymer-coated latex particles can exhibit very good mechanical stability. Moreover, the amount of conducting polymer used can be greatly reduced in the shell phase without much loss of conductivity[19].

Preparation of core-shell particles involves multi-step synthetic procedure. But the most important parameters need to be considered are the uniformity in the coating of the shell phase and control on the thickness of the shell layer. There are various methods for the synthesis of core-shell particles used by different research groups viz. precipitation,[20-21] emulsion,[22-23] micro-emulsion,[24-25] sol-gel condensation,[26-27] layer by layer deposition [28-29] etc. So preparation of core-shell particles with proper thickness and uniform coating is a challenging research topic in recent time. To achieve control over the coating the core phase is often modified so as to facilitate selective deposition of the shell phase on the core surface. Surfactants[30-31] and polymers[32-33] are often used for the modification of the core surface. Surfactants and polymers can change the surface charge and selectivity of the core particles so that shell phase is selectively deposited resulting completely coated core-shell particles with proper shell thickness.

Although many techniques are employed, two staged seeded emulsion polymerization is the most extensively used technique for the preparation of core-shell particles[34-36]. Depending on the reaction conditions this process not only allows the formation of core-shell morphology but also results other morphologies like acorn, half-moon, inverse core-shell, raspberry, inclusion etc. Using this method, Okubo et al.[37] prepared different kinds of core-shell polymer particles. Moreover,

they developed a dynamic swelling method for the preparation of many multiform core–shell particles[38]. Wooley et al.[39] first reported the synthesis of shell cross linked knedel (SCK) micelles with a hydrophilic shell[40-42]. Using a polymer micro sphere as a core, Zheng and Stover synthesized new core-shell polymer particles. The shells were prepared by atom transfer radical polymerization (ATRP). Min et al.[43] synthesized a PMMA shell directly on the surface of a crosslinking PS core via ATRP, but the complete removal of the contamination of the catalyst from the system was very difficult. Hawker et al.[44] synthesized hollow polymeric microcapsules by surface-initiated living free-radical polymerization. In 2004, Wang et al. [45] reported the preparation of hydrophilic core-shell particles by initiating the graft polymerization of 2-(dimethylamino) ethyl methacrylate (DMAEMA) from the surfaces of polymer particles by oxyanionic polymerization.

This chapter includes the synthesis of core-shell particle using poly (butyl acrylate-co- methacrylic acid -co- ethylene glycol dimethacrylate) as the core and poly (styrene-co-methyl methacrylate) as the shell by two stage seeded emulsion polymerization technique. All the physical properties of the core as well as the core-shell particles are evaluated. These newly synthesised core-shell particles along with TiO_2 were used as binders in emulsion satin paints. Different formulations were made with different core-shell particles and the respective paint properties of all the formulations are evaluated.

2.2 Experimental

2.2.1 Materials

The monomers methyl methacrylate (MMA), *n*-butyl acrylate (BA), styrene (Sty), and methacrylic acid (MAA) were received from Aldrich and washed with 5% sodium hydroxide solution followed by washing with distilled water to remove the inhibitors. The cross linker ethylene glycol dimethyl acrylate (EGDMA) was purchased from Aldrich and used as received. The initiator potassium per sulphate ($K_2S_2O_8$) obtained from Merck was recrystallized before use. The anionic surfactant sodium dodecyl benzene sulphonate (SDBS), non-ionic surfactant Triton X-100, ammonia solution and $NaHCO_3$ were of analytical grade and used as received

without further purification. Double distilled water was used for all purposes. All reactions were carried out in a 1 litre resin kettle equipped with a mechanical stirrer, a condenser, a nitrogen inlet, a thermometer and a pressure equaliser funnel.

2.2.2 Instrumentations

2.2.2.1 Scanning Electron Microscopy (SEM)

The scanning electron microscope (SEM) is a type of electron microscope that images the sample surface by scanning it with a high-energy beam of electrons in a raster scan pattern. The electrons interact with the atoms that make up the sample producing signals that contain information about the sample's surface topography, composition and other properties such as electrical conductivity.

The surface topography of the particles was studied with a Jeol-JSM-6390L V Scanning Electron Microscope. For the analysis latex samples were sputter coated with platinum of thickness of $200A^0$.

2.2.2.2 Transmission Electron Microscopy (TEM)

Transmission electron microscopy (TEM) is a microscopy technique whereby a beam of electrons is transmitted through an ultra thin specimen, interacting with the specimen as it passes through. An image is formed from the interaction of the electrons transmitted through the specimen; the image is magnified and focused onto an imaging device. TEM is capable of imaging at a significantly higher resolution than light microscopes, owing to the small de Broglie wavelength of electrons. This enables to examine fine detail of even as small as a single column of atoms, which is tens of thousands times smaller than the smallest resolvable object in a light microscope.

For the TEM analysis a Philips EM 400 at an acceleration voltage of 100 kV was used. All images were taken at a magnification of 60000 or 120000. Latex samples were cleaned by using a filtration unit (Advantec MFS Inc. type UPH-76) to remove all water soluble oligomers from the emulsion. All latex samples were diluted to 3% solids and washed with distilled water in the filtration cell using a polycarbonate nuclepore membrane with a pore size of 0.1 micron.

The diluted latex was treated with 2wt% aqueous solution of uranyl acetate (UAc). One drop of diluted sample was placed onto copper (Cu) grid and allowed to dry. For potential staining of the shell phase by RuO_4, the sample was exposed to RuO_4 vapour. The RuO_4 vapour was generated by the reaction of Ruthenium (III) chloride hydrate and sodium hyperchloride solution. All the samples were dried at 30^0 C for 24 h before TEM measurements.

2.2.2.3 Gel Permeation Chromatography

The molecular weight of the particles were determined using a modular Waters 600 gel permeation chromatography (GPC) with three ultra styrgel columns of linear, 10^3 and 10^4 A^0 porosities and a 410 differential refractometer was used for determination of molecular weight distributions. Tetrahydrofuran (THF) was used as a mobile phase with a flow rate of 1.0ml/min. and the instrument was standardized with polystyrene standards.

2.2.2.4 Viscosity

The viscosity of the core-shell emulsion was determined by Brookfield Viscometer (RVT Model) at 30^0C.

2.2.2.5 pH Determination

A standard digital pH meter was used with a saturated calomel electrode and a glass electrode to determine the pH of the core-shell emulsions.

2.2.2.6 Solid Content or Non-volatile Content

The non volatile content of the core-shell particles were determined by gravimetric analysis 2 g of the core-shell particles were heated for 1 hour at 120^0 C for weighing the left residue. From the residue percentage of solid content is reported.

2.2.2.7 Freeze Thaw Stability

The samples were taken in air-tight plastic bottles and kept at -5^{0}C for 16 h and then at 30^{0}C for 8 h. Then it was checked whether the emulsion was gelled or not.

2.2.2.8 Optical property

This was studied by evaluating contrast ratio (*K/S*) value[6]. The instrument used was X-rite spectrophotometer (model no SP-60).

2.2.2.9 Gloss

Paint films were drawdown on glass plate (wet film thickness- 150 micron) and dried for 12 hrs and checked the gloss by using digital sheen Multiheaded Gloss meter.

2.2.2.10 Rock Hardness

Paint film drawn on a glass plate (wet film thickness 150 micron) and dried for 7 days at 30^{0}C at relative humidity of 80%. Then the hardness was checked using Sword Rocker Hardness Tester (Sheen Instrument) and results are given as % glass where reference is glass plate (100%).

2.2.2.11 Washability

Dry paint film on glass plate was dipped into de-ionized water and checked adhesion failure with time.

2.3 Synthesis of the core-shell particle by seeded emulsion polymerization

2.3.1 Synthesis of the core (Step I)

The recipe for the synthesis of the core latex is given in **Table 2.1**. In a typical synthesis, to a 1litre resin kettle equipped with a reflux condenser, a nitrogen inlet, a mechanical stirrer, a thermometer and a pressure equaliser funnel 40 g of distilled water, 0.05g of $NaHCO_3$ and 0.05g of SDBS was added and then heated to 80^{0}C under nitrogen atmosphere. When temperature reached 80^{0}C, 0.50g of $K_2S_2O_8$

(in 20 mL of water) was added. Then a pre-emulsion of 15g of BA, 2.15g MAA, 0.01g SDBS, 0.225g of EGDMA and 15g of water was added to the resin kettle in 2h. The temperature was maintained at 80^0C and polymerization was carried out for another 3 h. Then it is cooled to room temperature to get the core particle. The core particles were then treated with ammonia solution to ionize the MAA carboxylic group.

Table 2.1: Recipe for the core latex

Sl. No.	Ingredients	Quantity (in g)
1	Distilled Water	55
2	$NaHCO_3$	0.05
3	SDBS	0.06
4	$K_2S_2O_8$	0.05
5	BA	15
6	MAA	2.15
7	EGDMA	0.225

2.3.2 Synthesis of the core-shell particle (Step II)

The recipe for the synthesis of the core-shell latex is given in **Table 2.2**. In a typical synthesis 63g of water, 36g of the core latex (synthesized in step I) and 0.087g of $K_2S_2O_8$ were taken in an another resin kettle under nitrogen and temperature is raised to 80^0C . When temperature reaches 80^0C, a pre-emulsion of 22g of water, 11g of styrene, 17.5g of MMA, 0.35g of SDBS and 0.22g of Triton X-100 were added drop wise in 2 h. The temperature was maintained at 80^0C and polymerization was carried out for another 3h.Then the reaction mixture was cooled to room temperature and neutralised by ammonia (20%) to get the core-shell particle.

Table 2.2: Recipe for core-shell latex

Sl. no	Ingredients (in grams)	Core shell latex		
		CS IA	CS IB	CS IC
1	Core-particles	36	36	36
2	Distilled water	85	105	85
3	$K_2S_2O_8$	0.087	0.087	0.087
4	Styrene	11	13.8	11.3
5	MMA	17.5	22	18
6	SDBS	0.35	0.35	0.35
7	Triton X-100	0.22	0.22	0.22

CS IA, CS IB, and CS IC are core-shell particles at different core:shell ratios. For CS IA (core:shell) = 55:45, CS IB (core:shell) = 50:50, and CS IC (core:shell) = 45:55

By changing the composition of feeding monomer a series of core-shell latex particle were synthesized (**Table 2.3**)

Table 2.3: The monomer composition in core-shell latex

Sl. No	Core Composition BA:MAA:EGDMA	Shell Composition Styrene:MMA	Resulted Morphology
1	100:15:1.5	2:1	No core-shell
2	100:15:1.5	3:2	No core-shell
3	100:15:1.5	5:8	Spherical core-shell
4	100:15:1.5	6:8	Distorted core-shell
5	100:15:1.5	7:8	No core-shell

2.3.3 Synthesis of the random copolymer

The recipe for the random copolymerization of styrene, butylacrylate, methacrylic acid and methyl methacrylate is given in **Table 2.4**. In a typical synthesis

to a 1litre resin kettle equipped with a reflux condenser, a nitrogen inlet, a mechanical stirrer, a thermometer and a pressure equaliser funnel 105 g of water, 0.1g of $NaHCO_3$ and 0.05g of SDBS was added and then heated to 80^0C under nitrogen atmosphere. When temperature reaches 80^0C, 0.15g of $K_2S_2O_8$ (in 20 mL of water) was added. Then a pre-emulsion of 11g of BA, 2.2g of MAA, 9g of Styrene, 5.5g of MMA, 50g of water, 0.2g of Triton X-100 and 0.25g of SDBS was added in 2 h. Then polymerization was continued for another 5 h.

Table 2.4: Recipe of the random copolymer

Sl. No.	Ingredients	Quantity (g)
1	Distilled water	120
2	$NaHCO_3$	0.1
3	SDBS	0.3
4	Triton X-100	0.2
5	$K_2S_2O_8$	0.15
6	Styrene	18
7	BA	22
8	MAA	4.5
9	MMA	11

2.4 Application of the core-shell particles as pigment in emulsion satin paints

The core-shell particles thus prepared were applied as a pigment in emulsion paint. Several emulsion paints were formulated using these core-shell particles as pigment along with TiO_2. A typical recipe of an emulsion satin paint is given in **Table 2.5**. In order to evaluate the performance of different formulated paints, different panels were made on Lineta paper using bar coater (No. 100).

To verify whether the enhancement of the properties are really due to core-shell morphology or not, we prepared a random copolymer of the monomers used in the core-shell particles and formulated paint with this copolymer and its properties

were evaluated. The property of this paint is compared with the standard paint (with 100% TiO_2).

Table 2.5: Recipe for the emulsion satin paints

Sl. No	Ingredients(in grams)	Standard Paint	CS - Piant
1	Water	21	21
2	Sodium hexameta phosphate	0.20	0.20
3	Biocide	0.4	0.4
4	Anionic dispersing agent (lutron 850)	0.7	0.7
5	Non ionic emulsifier (hydroxide AAO)	0.4	0.4
6	Defoamer	0.2	0.2
7	Hydroxy Ethyl Cellulose	0.5	0.5
8	Dry film preservative (actiside EP paste)	0.9	0.9
9	Ammonia (22%)	0.2	0.2
10	Di ethylene glycol	2.2	2.2
11	TiO_2 (Rutile, RC-822)	18.00	14.94
12	Core-shell latex	---	3.06
13	China clay	5.00	5.00
14	Talc (5μm)	9.00	9.00
15	Calcite (5μm)	5.00	5.00
16	Pure acrylic emulsion (30% solid content)	35.00	35.00
17	Pine oil	1.3	1.3

Standard: 100% TiO_2, no core-shell, **CS-Paint** 83% TiO_2, 17% core-shell particle

2.4.1 Evaluation of Emulsion paints

To verify the pigment property of the synthesized core-shell particles in emulsion satin paints following properties were evaluated

a) Optical Properties

b) Gloss

c) Rock Hardness

d) Washability

2.5 Results and Discussions

2.5.1 Physical properties of the core-shell particles

The physical properties of the core-shell latex are listed in **Table 2.6**. For the core particles maximum solid content was found to be 25% which increases up to 42% in case of the core-shell particles. It is very obvious that with the increase of polymeric component the percentage of non-volatile components increases. Similarly, the viscosities of the core-shell particles are almost doubled than the core latex. The pH of the core particles is in the acidic range (3.2). However as the core-shell particles were neutralised with ammonia their pH was recorded within the alkaline range (8-9). It was observed that both the core and core-shell latex pass the freeze thaw test. This implies that the emulsions of both core and core-shell particles are sufficiently stable to find various ends on applicability.

Table 2.6: Physical properties of the core latex, core-shell particles and random copolymer

Sl. No	Properties	Core latex	Core-shell particle			Random Copolymer
			CS IA	CS IB	CS IC	
1	Solid Content(%)	25	40	42	40	40
2	Viscosity(cPs)	28	60	58	55	60
3	pH (at 30^0C)	3.2	8.7	8.5	8.4	8.3
4	Freeze thaw stability	Pass	Pass	Pass	Pass	Pass
5	Particle Size	0.5μm	0. 75μm	0.75μm	0.75μm	0.5μm

2.5.2 Gel Permeation Chromatography (GPC)

In the newly designed core-shell particles the core phase was partially cross linked with EGDMA. The Gel permeation Chromatogram of the core-shell particles shows a bi-modal mode. The first peak have M_w=3,82,700 and M_n=2,45,200 with

polydispersity index of 1.6. The first peak corresponds to the molecular weight of the core phase. The second peak have M_w=21,200 and M_n=14,800 with polydispersity index of 1.4. The second peak corresponds to the molecular weight of the shell phase. It is observed that the second peak has a relatively low molecular weight in comparison to the normal emulsion polymer products. Since the shell phase was formed over the surface of the core particles, it may be assumed that normal emulsion polymerization kinetics was not followed and hence the polymers thus obtained have relatively low molecular weight (the second peak) than in the case of normal emulsion polymerization. The bi-modal nature of polymerization gives an evidence of formation of core-shell morphology.

2.5.3 Morphology of the core-shell structure

The core was prepared using mixture of BA, MAA and EGDMA in the ratio of 10:1.5:0.15. The incorporation of MAA offers carboxyl content in the polymer. The carboxyl content of the core was neutralized with ammonia to make the polymer hydrophilic. This core polymer was used for the core-shell latex preparation. The shell composition was changed with different monomer mixtures (ref. **Table 2.3**). The pre-emulsion of the shell components were added drop wise by means of a pressure equaliser funnel. The monomers of the shell phase get absorbed on the core polymer particles and they subsequently undergo polymerization thereby forming the shell. EGDMA was used as a cross linker. The use of cross linking agent helps in holding both the core and the shell phase together. However, the amount of cross linker used is very small so that viscosity of the medium does not increase abruptly. The core polymer contains carboxyl group (copolymer of MAA) and on neutralization with alkali core-shell particle forms carboxylated group in the core which is hygroscopic in nature. A schematic representation of the preparation of the core-shell particles are given in **Fig 2.1**.

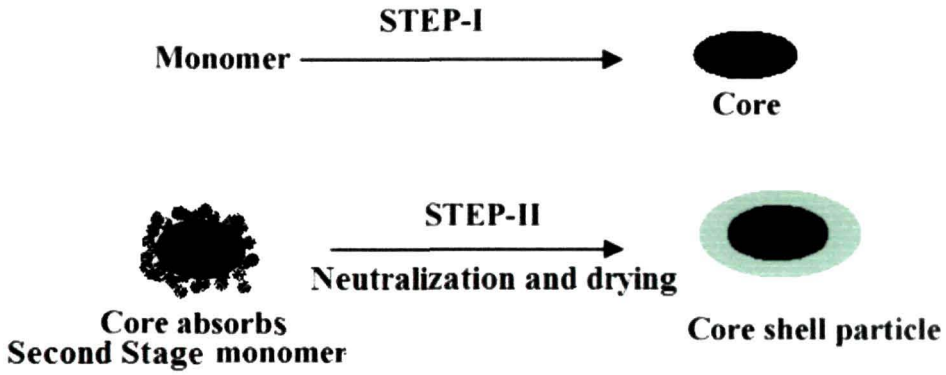

Fig 2.1: Schematic representation of formation of core-shell particles.

2.5.3.1 SEM Analysis

From the SEM analysis (**Fig 2.2-2.5**) it is found that both the cores as well as the core-shell particles are spherical and have smooth surface. This implies that shell phase is quite uniform. From the SEM micrographs it is seen that the approximate diameter of the core particles are ~ 0.5μm whereas the diameter of the core-shell particles are of ~ 0.75 μm. It is seen that the random copolymer particles have a diameter of ~ 0.5 μm. It is seen that the core-shell particles have a larger diameter than the corresponding core particles. However it may be observed that in case of the random copolymer particles there is no significant increase of particle diameter. So, the increase of particle size gives strong evidence that an extra layer is formed over the core particles, resulting formation of core-shell structure. It was observed that with the increasing concentration of the styrene in the shell composition, the core-shell morphology gets distorted from their typical spherical structure. The spherical core-shell morphology is observed when the styrene to MMA ratio is 60:40 by percentage. For further confirmation of the core-shell morphology TEM images of the core-shell particles were taken.

2.5.3.2 TEM Analysis

TEM micrographs (**Fig 2.6-2.9**) show a slight difference in contrast between the outer and inner portion of the particle. From the TEM analysis it is found that the core particles are ~ 0.5μm whereas the diameters of the core-shell particles are of ~ 0.75 μm. Fig 2.8 shows the TEM images of the core-shell particles with higher styrene concentration in the shell. As the concentration of styrene is increased the spherical morphology of the core-shell latex gets distorted. The determining factor in the generation of non-equilibrium morphologies is the competition between phase separation and polymerization kinetics. Viscosity in the polymerization locus controls the mobility of the polymer molecules and hence the particle morphology. With a high viscosity in the polymerization locus the core and shell phase cannot undergo facile phase separation and the resultant morphology seems to be uneven. However at relatively low viscosity, clear phase separation between the core and shell phases occurs and leads to a well defined core-shell morphology[46]. With increase in styrene concentration the viscosity of the medium increases and it becomes difficult for the two polymer phases to rearrange themselves to the thermodynamically stable morphology. When the concentration of styrene in the shell composition is relatively low, no core-shell morphology is resulted. This may be due to the reason that in such a situation there is no sufficient amount of shell monomer present to be absorbed by the core particles and hence no core-shell morphology is obtained.

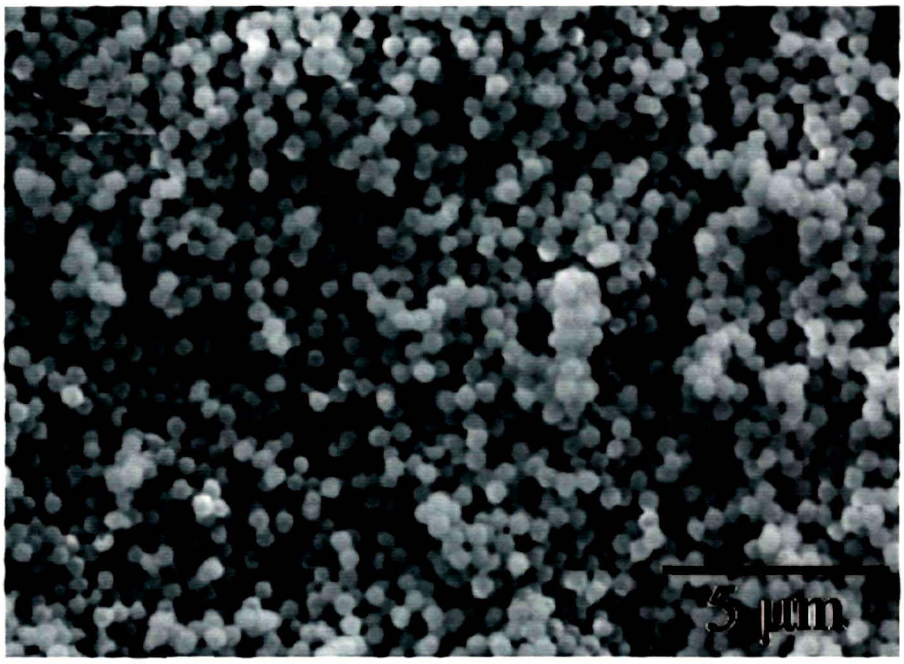

Fig 2.2: SEM micrograph of the core particles

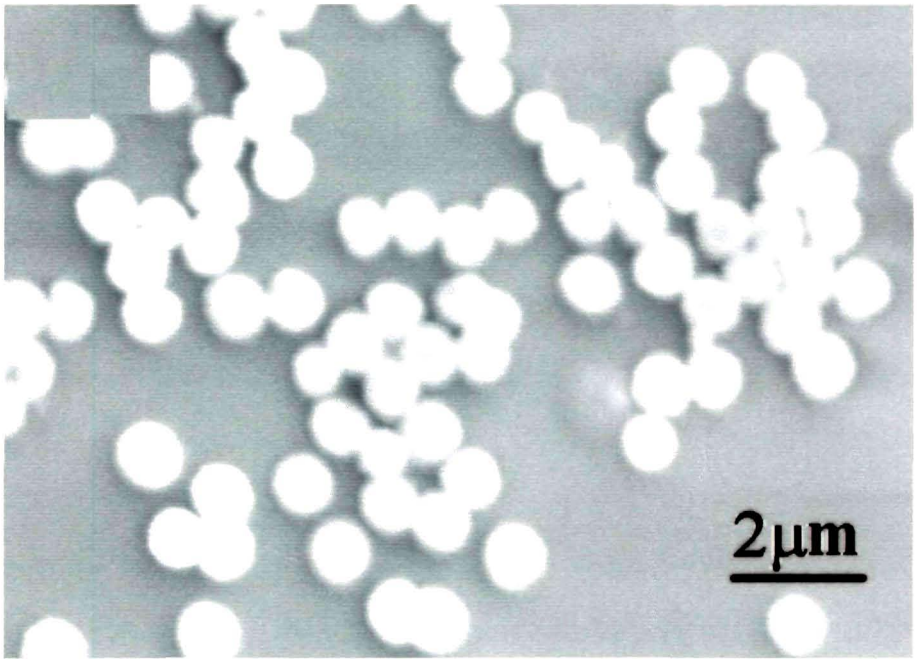

Fig 2.3: SEM micrograph of the core-shell particles

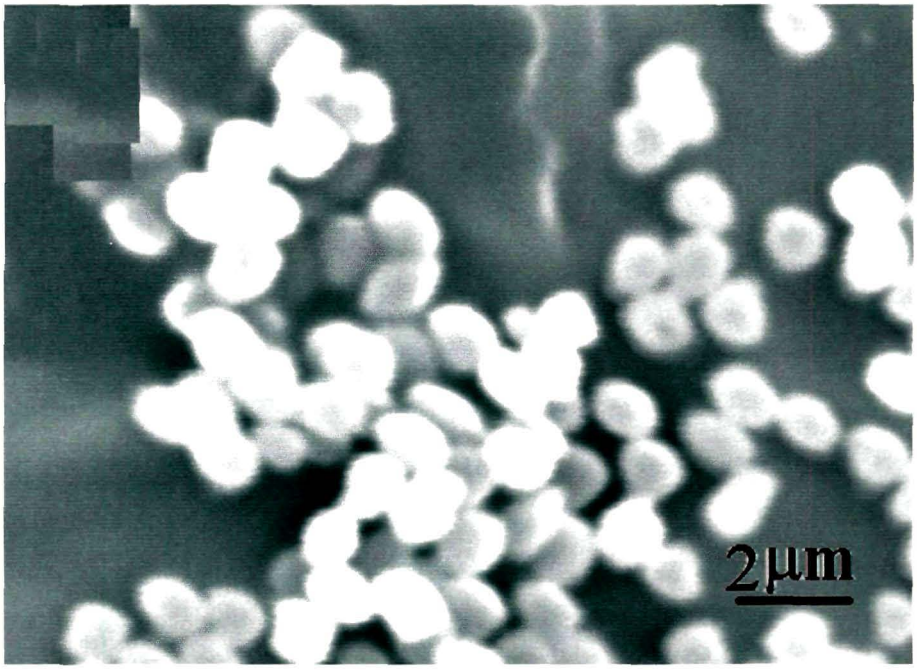

Fig 2.4: SEM micrograph of the core-shell particles with distorted morphology at higher concentration of styrene

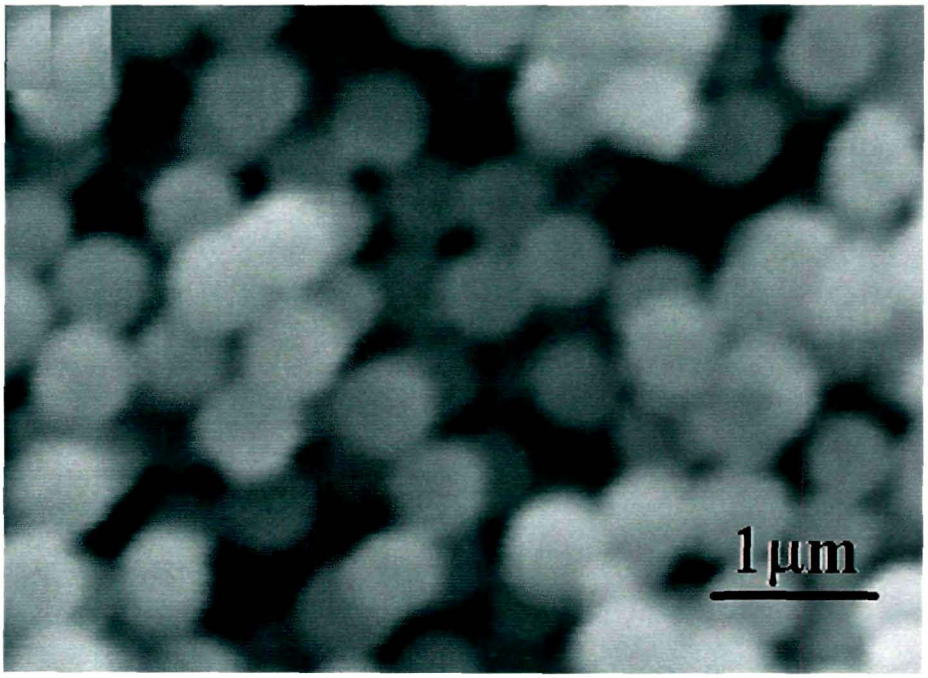

Fig 2.5: SEM micrograph of the random copolymer particles

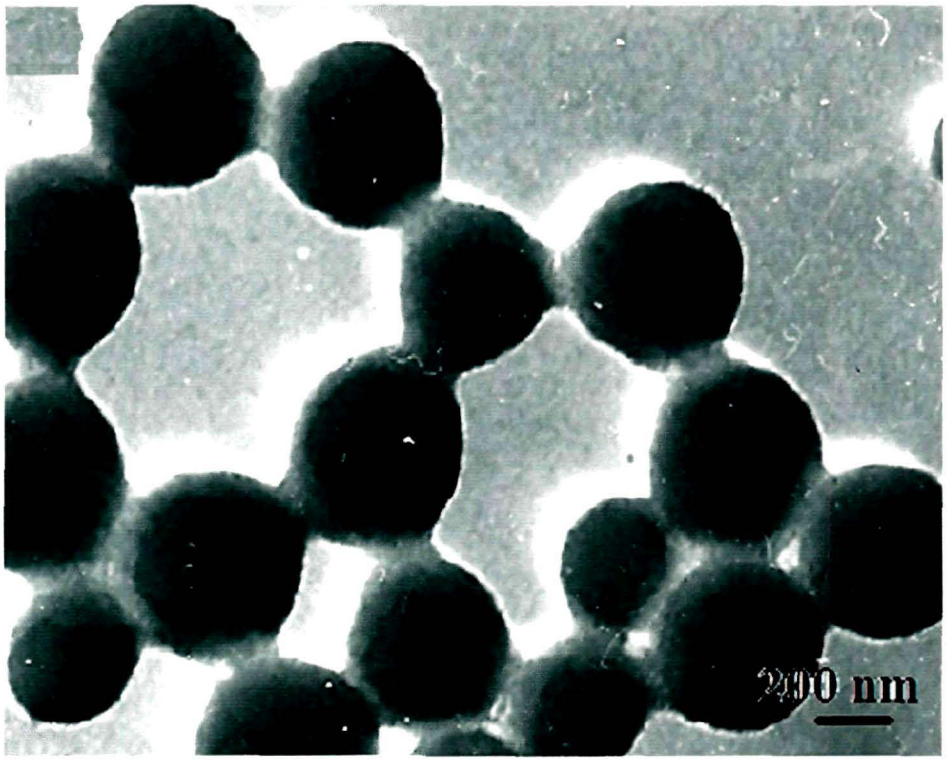

Fig 2.6: TEM image of the core particles

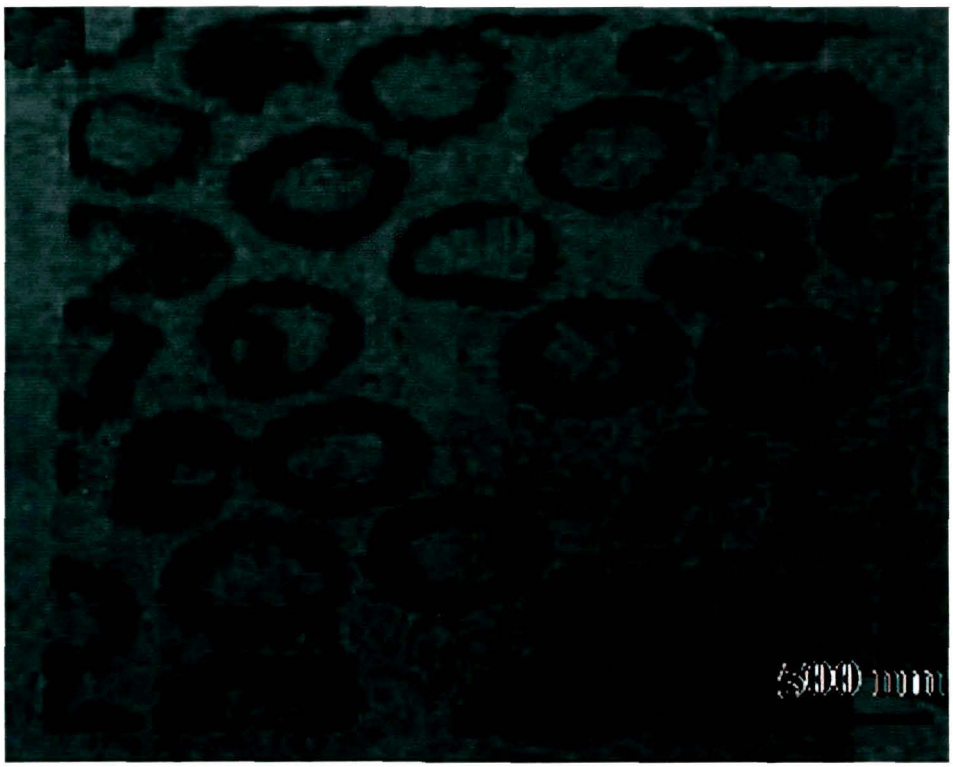

Fig 2.7: TEM image of the core-shell particles

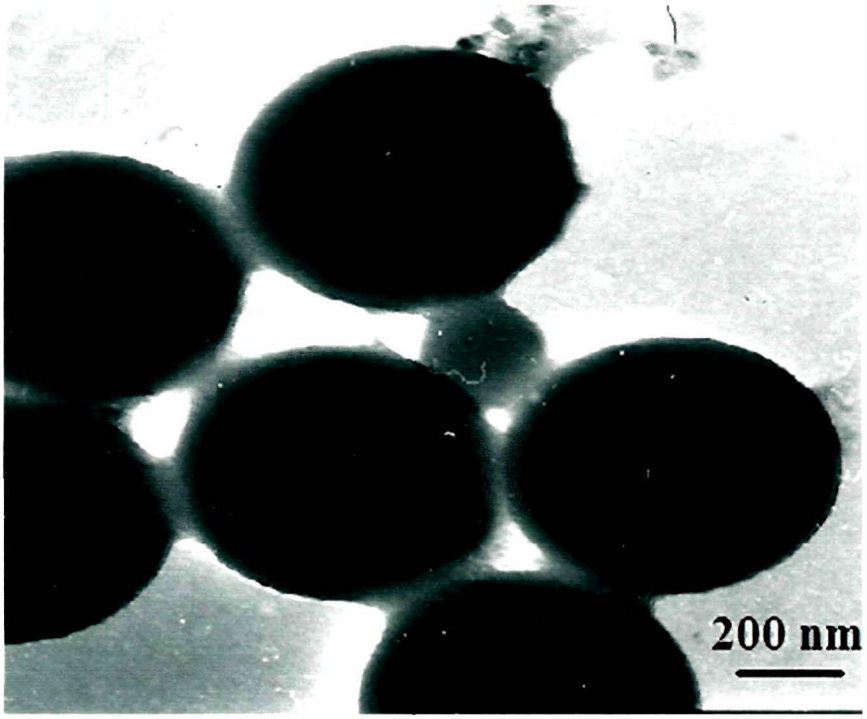

Fig 2.8: TEM image of the distorted core-shell particles at higher concentration of styrene in the shell monomer

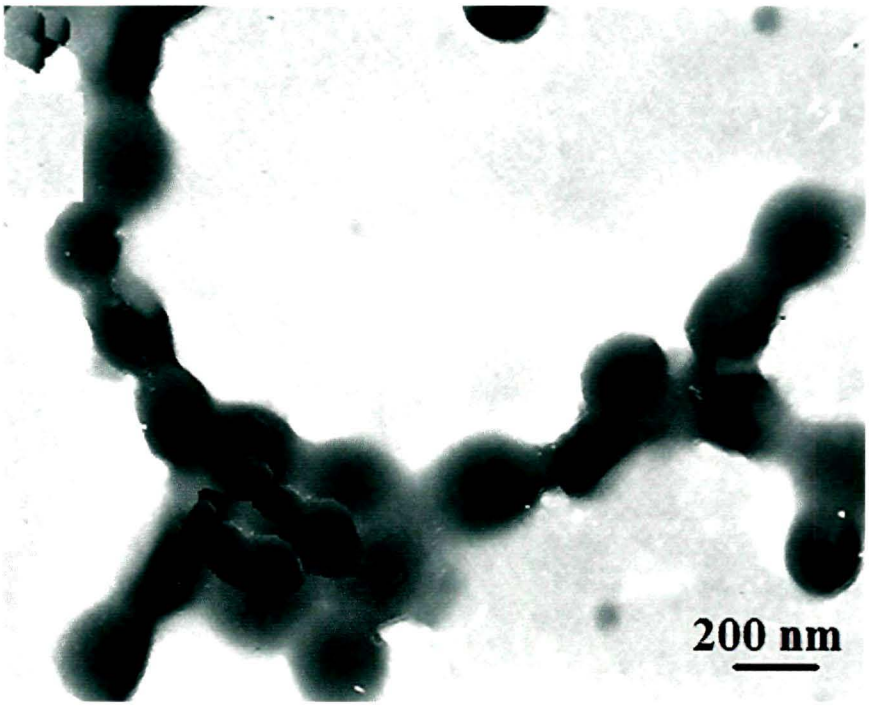

Figure 2.9: TEM image of the random copolymer particles

2.6 Properties of the emulsion paint

TiO_2 is used as a pigment in emulsion paint to provide hiding power. The hiding power of paint is evaluated by measuring the opacity of the emulsion paint. In this work the newly synthesized core-shell were used as pigment in emulsion paint along with TiO_2. The results show (**Table 2.7**) that the contrast ratio of the emulsion paint does not decreases even up to 17% reduction of TiO_2 content. Particles with Sty:MMA ratio of 60:40 by percentage shows the best result in this regard. In fact, these core-shell particles shows slight enhancement in hiding power. This enhancement may be attributed to the hollow structure of the core particles as well as the uneven surface of the core-shell latex particles (Table 2.7). It is also observed that the replacement of TiO_2 by the core-shell particles does not affect the other properties like gloss, rock hardness, washability etc. Thus these newly synthesized core-shell particles can be potentially applied as an alternative pigment in emulsion paints.

The paint formulated with the random copolymer shows a lower opacity (contrast ratio 80.22) in comparison to the core-shell latex of the same composition. This shows that the potentiality of the core-shell particles as pigment is related to their special type morphology. In core-shell morphology the core contains air void which causes the opacity by itself by scattering light effectively. These air voids and non-pigmented emulsions are both transparent to light, but they have difference in refractive indices causing opacity in the dried film of the emulsion paint. Incorporation of such core-shell polymer in the water based paints together with well dispersed TiO_2 will enhance the opacity of the paint. This will effectively reduce the amount of TiO_2 used and hence is cost effective.

Table2.7: Application properties of the emulsion paint

		Gloss @85 BYK	Opacity (Contrast ratio)	Washability	Rock Hardness (%on glass)
Formulation1	Standard	33.36	88.26	Pass	20
	. CS IA	35.72	95.65	Pass	22
Formulation2	Standard	33.84	88.26	Pass	20
	CS IB	35.44	94.27	Pass	18
Formulation3	Standard	33.62	88.26	Pass	20
	CS IC	35.08	93.99	Pass	18
Formulation4	Standard	33.62	88.26	Pass	20
	CS RCP	28.42	80.22	Pass	17

Standard 100% TiO_2

CS IA, CS IB, CS IC Standard with 83% TiO_2 and 17% respective core-shell particles

CS RCP Standard with 83% TiO_2 and 17% random copolymer particles

2.7 Conclusion

- A series of core-shell particles were prepared by seeded emulsion polymerization. The core contains poly (n-butyl acrylate- co- methacrylic acid- co- ethylene glycol dimethylacrylate) and the shell contains poly (styrene-co-methyl methacrylate) as shell.

- SEM analysis shows the spherical nature of the core as well as core-shell particles; TEM analysis confirms the core-shell morphology of the newly synthesised particles. The core-shell particles have a distinct difference in contrast between the core and shell phase. The core particles are ~ 0.5μm whereas the diameters of the core-shell particles are of ~ 0.75 μm.

- However it is observed that the spherical nature of these core-shell particles gets distorted as we increase the styrene concentration in the core. The distortion of the morphology may be attributed to the increase in viscosity of the polymerization loci.

- These newly designed core-shell particles were applied as pigment in emulsion paint. It is found that the optical properties of the paint do not change up to 17% reduction of TiO_2 in the pigment volume.

- The gloss, rock hardness and washability of the emulsion paint remains unchanged due to the use of this core-shell particles in the pigment. Thus these core-shell particles can be potentially applied as a pigment in emulsion paint which will reduce the amount of TiO_2 used and hence is very much cost effective.

References

1. Marinakos, S.M., Brousseau III, L.C., Jones, A., Feldheim, D. L. Template Synthesis of One-Dimensional Au, Au–Poly (pyrrole) and Poly(pyrrole) Nanoparticle Arrays. *Chem. Mater.* **10**, 1214-1219 (1998)
2. Quaroni, L., Chumanov, G. Preparation of Polymer-Coated Functionalized Silver Nanoparticles. *J. Am. Chem. Soc.* **121**, 10642-10643 (1999)
3. Xiong, Y., Chen, G.S., Guo, S.Y. The preparation of core-shell $CaCO_3$ particles and its effect on mechanical property of PVC composites. *J. Appl. Polym. Sci.* **102**, 1084-1091 (2006)
4. Chen, J.P., Su, D.R. Latex Particles with Thermo-Flocculation and Magnetic Properties for Immobilization of α-Chymotrypsin. *Biotechnol. Prog.* **17**, 369-375 (2001)
5. Sparnacci, K., Laus, M., Tondelli, L., Magnani, L., Bernardi, C. Core–shell microspheres by dispersion polymerization as drug delivery systems. *Macromol. Chem. Phy.* **203**, 1364-1369 (2002)
6. Liu, G., Zhang, H.,Yang, X.,Wang, Y. Facile synthesis of functional silica/polymer composite materials and hydrophilic hollow polymer microspheres. *Journal of Applied Polymer Science* **111**, 1964–1975 (2009)
7. Pimpha, N., Rattanonchai, U., Surassmo, S., Opanasopit, P., Rattanarungchai, C. Preparation of PMMA/acid-modified chitosan core-shell nanoparticles and their potential as gene carriers. *Colloid & Polymer Science* **286**, 907-916 (2008)
8. Tsuji, M., Hikino, S., Tanabe, R., Matsunaga, M. Syntheses of Ag/Cu alloy and Ag/Cu alloy core Cu shell nanoparticles using a polyol method. *Cryst. Eng. Comm.* **12**, 3900-3908 (2010)
9. Khan, A.K., Roy, B.C., Dolui, S.K. Preparation of core-shell emulsion polymer and optimization of shell composition with respect to opacity of paint film. *Progress in Organic Coatings* **62**, 65-70 (2008)
10. Khan, A.K., Roy, B.C., Maiti, J., Dolui, S.K. *Preparation of core-shell latex from co-polymer of styrene-butyl acrylate-methyl methacrylate and their paint properties. Pigment & Resin Technology* **38**, 159-164 (2009)
11. Gangopadhyay, R., De, A. Conducting polymer nanocomposites: a brief overview. *Chem. Mater.* **12**, 608-622 (2000)

12. Stubbs, J., Sundberg, D. Fundamental studies on morphology control for latex systems with application to waterborne coatings: The effect of polymer radical mobility in latex particles during polymerization. *Journal of Coating Technology* **75**, 59-67 (2003)

13. Basset, D. Hydrophobic coatings from emulsion polymers. *Journal of Coating Technology* **73**, 42-55 (2001)

14. Schuler, B., Baumstark, R., Krisch, S., Pfau, A., Sanor, M., Zosel, A. Structure and properties of multiphase particles and their impact on the performance of architectural coatings. *Progress in Organic Coatings* **40**, 139-150 (2000)

15. Skotheim T.A., Elsenbaumer *J.R. Reynolds (Eds.). Handbook of Conducting Polymers* (Marcel Dekker, New York, 1998)

16. Pickup, N.L., Shapiro, J. S., Wong, D. K. Y. Extraction of mercury and silver into base-acid treated polypyrrole films: A possible pollution control technology. *J. Poly. Res.*, **8,** 151-157 (2001)

17. Huijs, F.M., Lang, J. Kalicharan, D. Formation of transparent conducting films based on core-shell latices: Influence of the polypyrrole shell thickness. *J. Appl. Polym. Sci.* **79,** 900-909 (2001)

18. Imhof, A. Preparation and characterization titania- coated polystyrene spheres and titania shells. *Langmiur* **16,** 1602-1611 (2001)

19. Ocana, M., Hsu, W.P., Matijevic, E. Preparation and properties of uniform-coated colloidal particles. 6. Titania on zinc oxide. *Langmuir* **7,** 2911–2916 (1991)

20. Zou, H., Wu, S., Shen, J. Polymer/Silica Nanocomposites: Preparation, Characterization, Properties and Applications. *Chem. Review.* **108**, 3893-3957 (2008)

21. Okaniwa, M. Synthesis of poly (tetrafluoroethylene)/poly(butadiene) core-shell particles and their graft copolymerization. *J. App. Poly. Sci.* **68,** 185-190 (1998)

22. Hota, G., Jain, S., Khilar, K. C. Synthesis of CdS–Ag_2S core-shell/composite nanoparticles using AOT/*n*-heptane/water microemulsions. *Colloid Surf. A: Physicochemical and Engineering Aspects,* **232,** 119-127 (2004)

23. Han, M. Y., Huang, W., Chew, C.H., Gan, L. M. Large Nonlinear Absorption in Coated Ag_2S/CdS Nanoparticles by Inverse Microemulsion. *J. Phys. Chem. B.* **102**, 1884-1887 (1998)

24. Song, C., et al. Preparation and characterization of silver/TiO_2-composite hollow spheres. *J. Colloid Interface Sci.* **272**, 340-344 (2004)

25. Li, T., Moon, J., Morrone, A. A., Mecholsky, J. J., Talham, D. R., Adair J. H. Preparation of Ag/SiO_2 Nanosize Composites by a Reverse Micelle and Sol−Gel Technique. *Langmiur* **15**, 4328-4334 (1999)

26. Srivastava, S., Kotov, N. A. Composite layer-by-layer (LBL) assembly with inorganic nanoparticles and nanowires. *Acc. Chem. Res.* **41,** 1831-1841 (2008)

27. Shenoy D.B., Antipov, A.A., Sukhorukov G.B., Mhwald, H. Layer-by-layer engineering biocompatible, decomposable core-shell structure. *Biomacromolecules* **4**, 265-272 (2003)

28. Hoffman-Caris, C.H.M. Polymer at the surface of oxide nanoparticles. *New J. Chem.* **18,** 1087-1096 (1994)

29. Wu, T.M., Chu, M. Preparation and characterization of thermoplastic vulcanization/silica nanoparticles. *J. App. Poly. Sci.* **98**, 133-144 (2005)

30. Liz-Marzan, L.M., Giersig, M., Mulvaney, P. Synthesis of nanosized gold-silica core-shell particles. *Langmuir* **12,** 4329-4335 (1996)

31. Perro, A., Reculusa, S., Bourget-Lami E., Duguet, E, Ravaineom S. Synthesis of hybrid colloidal particles, from snowman-like and raspberry-like morphologies. *Colloid surf. A: Physicochemical and Engineering Aspects* **284,** 78-83 (2006)

32. Winnik, M., Zhao, C., Shaffer, O., Shivers, R. Electron microscopy studies of polystyrene-poly(methyl methacrylate) core-shell latex particles *Langmuir* **9**, 2053-2066 (1993)

33. Stutman, D., Klein, A., El-Aasser, M., Vanderhoff, J. Mechanism of core/shell emulsion polymerization. *Industrial & Engineering Chemistry Product Research and Development* **24**, 404-412 (1985)

34. Grancio, M., William, D. The morphology of the monomer–polymer particle in styrene emulsion polymerization. *Journal of Polymer Science PartA-1: Polymer Chemistry* **8**, 2617-2629 (1970)

35. Hughes, L., Brown, G. Heterogeneous polymer systems. I. Torsional modulus studies. *Journal of Applied Polymer Science* **5**, 580-588 (1961)

36. Okubo, M., Mori, H. Production of multi-hollow polymer particles by the stepwise acid/alkali method. *Colloid Polym. Sci.* **275**, 634-639 (1997)

37. Okubo, M., Ito, A., Nakamura, T. Effect of molecular weight on the production of multi-hollow polymer particles by the alkali/cooling method. *Colloid Polym. Sci.* **275**, 82-85 (1997)

38. Thurmond II, K.B., Kowalewski, T., Wooley, K.L. Water-Soluble Knedel-like Structures: The Preparation of Shell-Cross-Linked Small Particles. *Journal of American Chemical Society* **118**, 7239-7240 (1996)

39. Zheng, G.D., Stover, H.D.H. Grafting of Polystyrene from Narrow Disperse Polymer Particles by Surface-Initiated Atom Transfer Radical Polymerization. *Macromolecules* **35**, 6828-6834 (2002)

40. Zheng, G.D., Stover, H.D.H. Grafting of Poly (alkyl (methacrylates) from Swellable Poly(DVB80-*co*-HEMA) Microspheres by Atom Transfer Radical Polymerization. *Macromolecules* **35**, 7612-7619 (2002)

41. Zheng, G.D. Stover, H.D.H. Grafting of Poly(alkyl (methacrylates) from Swellable Poly(DVB80-co-HEMA) Microspheres by Atom Transfer Radical Polymerization. Macromolecules **35,** 7612-7619 (2002)

42. Zheng, G.D., Stover, H.D.H. Formation and Morphology of Methacrylic Polymers and Block Copolymers Tethered on Polymer Microspheres. *Macromolecules* **36**, 1808-1814 (2003)

43. Min, K., Hu, J.H., Wang, C.C., Elassir, A. Surface modification of polystyrene latex particles via atom transfer radical polymerization. *J. Polym Sci Part A: Polym. Chem.* **40**, 892-900 (2002)

44. Blomberg, S., Ostberg, S., Harth, E., Bosman, A.W., Van Horn, B., Hawker, C.J. Production of crosslinked, hollow nanoparticles by surface-initiated living free-radical polymerization. *J. Polym Sci Part A: Polym. Chem.* **40**, 1309-1320 (2002)

45. Jin, L., Deng, Y., Hu, T., Wang, C. Preparation and Characterization of core–shell polymer particles with protonizable shells prepared by oxyanionic polymerization. *J. Polym Sci Part A: Polym. Chem.* **42**, 6081-6088 (2004)

46. Cho, I., Lee, K. Morphology of latex particles formed by poly (methyl methacrylate)-seeded emulsion polymerization of styrene. *Journal of Applied Polymer Science* **30**, 1903-1926 (1985)

CHAPTER 3

Preparation of conducting composite particles of poly (styrene-co-methyl acrylate) as the core and polypyrrole as the shell by mini emulsion polymerization

Chapter 3

3.1 Introduction

Conducting polymers have been a subject of intensive research since their discovery in 1977 due to many potential applications in organic electronics. Conducting polymers like polyaniline, polythiophene, polyacetylene, polypyrrole etc[1-16] have been extensively studied in recent time because of their good conductivity and their potential applications in various fields like sensors, actuators, catalysis, field effect transistors, light emitting diodes, capacitors etc[17-34]. However, there is a serious processing and stability problems associated with these pristine conducting polymers as they are often brittle in nature and it is very difficult to make film from them. In order to improve the process difficulty much attention has been made in combining these conducting polymers with mechanically stable insulating polymers to give core-shell morphology. These composite particles have manifold applications such as antistatic coating, dampers, clutches, electrodes, separation membranes, electro chromic devices, electro-chemomechanical actuators, and sensors[3,4,16]. These core-shell conducting composites have two advantages. Firstly, depending on the type of insulating polymer used as core these conducting polymer-coated latex particles can exhibit very good mechanical stability and secondly the amount of conducting polymer used can be greatly reduced in the shell phase without much loss of conductivity[5].

Conducting polymer coated latex particles were first reported in 1987[35] and subsequently this approach has found widespread attention[36-39]. Since 1995, Armes et al. have published a series of papers describing the coating of various conducting polymers, such as polypyrrole (PPy), polyaniline (PANI)[40] and poly (3,4 ethylenedioxythiophene) (PEDOT)[41] on micrometer-sized polystyrene (PS)[42] latexes.

A part of this chapter is published in

* **L.J.Borthakur**, S.Sharma, S.K.Dolui. *J Mater Sci: Mater Electron* (article in press).

* **L. J. Borthakur** , S. Konwer , R. Das , S. K. Dolui. *J. Polym Res* (article in press)

They described a detailed study of the surface composition and morphology of these micrometer-sized, PPy-coated PS latexes. Yamamoto and co-workers[43] reported the styrene-butadiene latexes coated with PPy using the H_2O_2–HBr–Fe^{3+} oxidant system. Jianjun Wang et al.[44]developed a core of a thermoplastic non-conducting polymer surrounded by a corona of a polyelectrolyte [e.g., polystyrene sulfonate, (PSS)] and into this corona (i.e. matrix) domains of a conducting polymer PPy was embedded via oxidative polymerization of the suitable monomer (pyrrole) such that an electrical percolating shell is formed. Huijs et al.[45]described the preparation of PBMA latex particles coated with PPy and focussed on the influence of the amount of PPy on the morphology and the conductivity of the core-shell latex particles. They also studied the effects of the thickness of PPy shell, the annealing temperature and the nature of the counter-anion on the film forming ability of the latex. Han Chen et al.[46] reported the voltammetric conversion of conducting PANI coated PS latex particles dispersed in aqueous acid solution in order to find not only a relationship between the partial reaction and particle size, but also the irreversibility of the conversion. Ma[47] had prepared PANI/SBS composite materials using emulsion polymerization techniques. Ruckenstein and Yang[48] obtained PANI/PS conducting materials using oxidative polymerization method in which SDS aqueous solution was used as continuous phase and the benzene solution containing aniline and PS was used as the dispersed phase. Huang Liyan et al.[49] developed a series of mono dispersed styrene-butyl acrylate (SBA) copolymer latex particles with different BA contents, coated with PPy and studied the effects of the concentration of PPy, the BA content in SBA copolymer and the nature of the counter-anion on the electrical conductivity of compression moulded samples. Ying Wang et al.[50] synthesized electrically conducting core-shell nanoparticles (PANI/PS-PSS) by coating poly (styrene-co-styrene sulfonate) (PS-PSS) nanoparticles with PANI and studied the stability of the coated latexes and the conductivity of PANI/PS-PSS pellets. The role of the aniline content was also investigated in this literature. Jang[51] reported the selective fabrication of amorphous PPy nanoparticles with diameter of 2 nm, using micro emulsion polymerization at low temperature. Wang et al[52] reported the preparation of PANI coated PS-PSS nanoparticles with diameters of 25–30nm by in situ micro emulsion polymerization method. Jang and Oh[53] have successfully synthesized conducting polymer

nanoparticles with diameter of several nanometres by low temperature micro emulsion polymerization. Jang reported the selective fabrication of amorphous PPy nanoparticles with diameter of 2 nm, using micro emulsion polymerization at low temperature.

In this chapter we describe the synthesis of two sets of core-shell particles with poly (styrene-co-methyl acrylate) (SMA) as the core and PPy as the shell by mini emulsion polymerization. In the first set graphite was incorporated in the PPy shell and in the second set silver nanoparticles were incorporated in the PPy shell. The effect of the concentration of graphite and silver nanoparticles in the shell phase on conductivity of the core-shell particles was investigated. The effect of copolymer composition of the core on the overall conductivity of the final core-shell particles has also been studied. The graphite incorporated core-shell particle was used as ammonia gas sensor. The changes in resistivity of the core-shell particles on exposure to various concentration of ammonia vapour were investigated. The graphite incorporated core-shell particles show good sensitivity even in very low concentration of ammonia.

3.2 Experimental

3.2.1Materials

The monomers styrene (Sty) and methyl acrylate (MA) were received from Aldrich and washed with 5% NaOH and distilled water to remove the inhibitors. Pyrrole, pure graphite (20 μm), silver nitrate ($AgNO_3$) and tri-sodium citrate were obtained from Aldrich Co. and used without further purification. Hydrochloric acid, potassium persulfate ($K_2S_2O_8$), Span60, hexadecane (HD), sodium dodecyl benzene sulfonate (SDBS), sodium bicarbonate, N-methyl pyrrolidone (NMP), tetra hydro furan(THF), hydroquinone, acetonitrile, methanol and ferric chloride ($FeCl_3$) were analytical grade chemicals (Merck) and used as received. Doubled distilled water was used for all purposes. All reactions were carried out under nitrogen atmosphere.

3.2.2 Preparation of poly (styrene-co-methylacrylate) latex (SMA)

Poly (styrene-co-methylacrylate) was prepared by emulsion polymerization technique. The recipe for the preparation of the SMA latex is given in **Table 3.1**. In a

typical synthesis, 10g of Sty, 3g of MA, 0.15g of HD and 0.02g of span 60 were mixed together. The mixture was kept in the refrigerator for 10 minutes and then sonicated for another 10 minutes to form a pre-emulsion (phase I). Another pre-emulsion (phase II) comprising of 80g of water and 0.12g of span 60 was made by stirring at room temperature for 15 minutes and then kept in the refrigerator for 10 minutes. Phase II was added to phase I drop-wise and then 0.12 g of SDBS was added to the mixture. This mixture was transferred to a four-necked round bottom flask equipped with a condenser, a mechanical stirrer, a thermometer as well as a nitrogen inlet and was heated up to 70^0 C. When temperature reached 70^0 C, $K_2S_2O_8$ (1% of the monomer) in 20 mL of water was added and degassed for 30 minutes. Polymerization was carried out at 70^0 C for 7hrs in the presence of $NaHCO_3$ buffer. Polymerization was terminated by adding 1% aqueous solution of hydroquinone. A series of SMA latex was synthesized by varying the amount of MA.

Table 3.1: The recipe for the preparation of the SMA latex

Sl. No	Ingredients (in g)	SMA I	SMA II	SMA III	SMA IV	SMA V
1	Styrene	10	10	10	10	10
2	Methylacylate	3	5	7	10	15
3	Hexadecane	0.15	0.15	0.15	0.15	0.15
4	Span 60	0.14	0.14	0.14	0.14	0.14
5	Water	110	110	110	110	110
6	SDBS	0.12	0.12	0.12	0.12	0.12
7	$NaHCO_3$	0.1	0.1	0.1	0.1	0.1
8	Hydroquinone	0.1	0.1	0.1	0.1	0.1
9	$K_2S_2O_8$	0.138	0.138	0.138	0.138	0.138

3.2.3 Synthesis of the core-shell particles with SMA core and graphite incorporated PPy as shell

A series of core-shell particles were prepared taking SMA III (**ref. Table 3.1**) as the core component. The recipe for the preparation of the core-shell particles is given in **Table 3.2**. In a typical synthesis an emulsion containing 4g of the SMA latex was added to a three necked round bottom flask equipped with a thermometer and dropping funnel and then diluted with 50 g of distilled water. The pH of the mixture was adjusted to around 1 by adding 1 g 5mol/L HCl. To this latex 0.8 g of $FeCl_3$ (in 20 g methanol), 0.67g of pyrrole and varying amount of graphite (0%, 0.25%, 0.50%, 1% w/v of pyrrole) were added in turn in a nitrogen atmosphere. The mixture was stirred for 24 h at 0^0C. The resulting black precipitates were isolated by filtration and washed several times with water and ethanol to remove unreacted monomer and unabsorbed graphite particles. The prepared composites were dried in a vacuum oven at 50^0C.

Table 3.2: Recipe of the core-shell particles with SMA core and graphite incorporated PPy as shell

Sl. No	Ingredients (in g)	CS I	CS II	CS III	CS IV
1	Core-particle	4	4	4	4
2	Water	50	50	50	50
3	5 M HCl	1	1	1	1
4	$FeCl_3$	0.8	0.8	0.8	0.8
5	Methanol	20	20	20	20
6	Pyrrole	0.67	0.67	0.67	0.67
7	Graphite	0	0.167	0.335	0.67

In another experiment a series of core-shell particles were prepared taking different core (SMA I – SMAV of **Table 3.1**) as the core component. The graphite content in the PPy shell phase was 1% in all the core-shell particles. All other ingredients were same as stated in table 3.2.

3.2.4 Solvent extraction experiments

Excess THF (20 mL) was added to ca. 100 mg of dried PPy-coated SMA powder at room temperature and this solution was left to stand overnight. The resulting black residues were filtered, washed with THF and dried overnight in a vacuum oven at 60^0C.

3.2.5 Synthesis of core-shell particles with SMA core and silver nanoparticles incorporated PPy as shell

3.2.5.1 Preparation of stable dispersion of silver nanoparticle

A stable dispersion of silver nanoparticle was synthesized by chemical (citrate) reduction method using standard procedure[54]. In a typical synthesis, 50mL 0.001M $AgNO_3$ solution was taken in a one-necked round bottom flask and stirred with constant heating up to boiling. Then 5mL of 1% tri-sodium citrate solution was added drop-wise for 10 minutes. The reaction was continued till the solution turns pale yellow. When yellow colour appears heating was ceased but continued stirring till it cools down to room temperature.

3.2.5.2 Preparation of core-shell particles with SMA latex as core and silver nanoparticle incorporated PPy as shell

Polypyrrole-silver (PPy-Ag) nanocomposite coated poly(styrene-co-methylacrylate) particles were prepared by oxidative coupling method. The recipe for the preparation of the core-shell particle is given in table 3.3. In a typical synthesis, 4g of SMA latex (SMA III of **Table 3.1**) was diluted with 30g doubled distilled. The mixture was transferred to a two necked round bottom flask and stirred vigorously at 0-5^0C. During stirring 0.67 g pyrrole monomer and 0.7g of the silver nanoparticle dispersion was added dropwise to the mixture. After 30 minute of vigorous stirring a solution of ferric chloride (0.8 g $FeCl_3$ in 20g methanol) was added drop-wise to the reaction mixture and continued stirring for 24 hours. The black precipitate was washed thoroughly with distilled water and finally dried under vacuum. A series of core-shell

particle was prepared by adding various percentage of silver nanoparticle dispersion (0%, 1%, 2%, 3%, 5%, 8% and 10%).

Another series of core-shell particles were synthesized by using different latex (SMA I - SMAV of **Table 3.1**) containing different amount of MA in the core latex. In all the experiments the percentage of silver nanoparticle dispersion was kept constant at 10%.

Table 3.3: Recipe of the core-shell particle with SMA core and silver nano particles incorporated polypyrrole as shell

Sl. No	Ingredients (in g)	SMA-PPy-Ag1%	SMA-PPy-Ag2%	SMA-PPy-Ag3%	SMA-PPy-Ag5%	SMA-PPy-Ag8%	SMA-PPy-Ag10%
1	SMA	4	4	4	4	4	4
2	Pyrrole	0.67	0.67	0.67	0.67	0.67	0.67
3	$FeCl_3$	0.8	0.8	0.8	0.8	0.8	0.8
4	Methanol	20	20	20	20	20	20
5	Dispersion of Ag nanoparticle	0.7	1.4	2.1	3.5	5.6	7.0
6	Distilled water	49.3	48.6	47.9	46.5	44.4	43.0

3.3 Characterization

3.3.1 Fourier transform infrared spectroscopy (FTIR)

The FT-IR spectra of the core-shell composite particles were recorded on a Nicolet Impact-410 IR spectrometer (USA) in KBr medium at room temperature in the region 4000–450 cm^{-1}.

3.3.2 UV-visible Spectrocsopy

The UV-visible absorption spectra of the samples in 1-Methyl-2-pyrrolidon solvent were recorded in the range 300-800nm using Shimadzu UV-2550 UV-visible spectrophotometer.

3.3.3 X-ray diffraction (XRD)

Powder XRD data were collected on a Rigaku Miniflex X-ray diffractometer (Tokyo, Japan) with Cu Kα radiation (λ= 0.15418 nm) at 30 kV and 15 mA with a scanning rate of 0.05^0/s in a 2θ range from 10^0 to 70^0

3.3.4 Scanning Electron Microscopy (SEM)

SEM micrographs of the core-shell particles were taken with a Jeol-JSM-6390L V scanning electron microscope. Latex samples were sputter coated with platinum of thickness of $200A^0$.

3.3.5 Transmission Electron Microscopy (TEM)

For the TEM analysis a Philips EM 400 at an acceleration voltage of 100 kV was used. All images were taken at a magnification of 60000 or 120000. For the TEM measurement, latexes were first sonicated, and the samples were prepared by dropping highly diluted latexes on the carbon coated copper grid and dried in a vacuum oven at room temperature.

3.3.6 Thermo Gravimetric analysis (TGA)

Thermal analysis was done in a Shimadzu TA-60 thermo gravimetric analyser. A pre weighted amount of the latex was loaded in a platinum pan and heating was done under nitrogen atmosphere at a heating rate of 10^0C/min in the range of 0-700^0 C.

3.3.7 *Electrical conductivity*

Pellets of the composite latex were made with a compression-molding machine with hydraulic pressure. High pressure was applied (1.5–2 ton) to the sample to get round shaped hard pellets (diameter =1.5 cm, breadth=2 mm); these pellets were used to measure the conductivity.

The electrical conductivity of the composite latex were measured with a four-probe technique in the temperature range 300 K ≤ T ≤433K.The current-voltage (I-V) characteristics were studied with a Keithley 2400 source meter (USA) at room temperature in the frequency range 102-106 Hz. The conductivity of the composite was calculated with following equation

$$\rho = (V/I)2\pi S \qquad (1)$$

Where ρ is the resistivity of the sample, V is the applied voltage, I is the measured current through the sample, and S is the distance between the probes.

3.3.8 Cyclic voltammetry (CV)

Electrochemical measurement was performed on a Sycopel AEW2-10 electrochemical work station (UK) with an Ag/AgCl reference electrode, a platinum wire as a counter electrode, and the latex films on indium tin oxide (ITO) coated glass as a working electrode. The electrochemical characteristics of the polymer solution in N-methylpyrrolidone (NMP) were investigated by CV scanning in 0.1M hydrogen chloride (HCl) in acetonitrile at a scan rate of 50 mV/s. A solution of 0.1M KCl prepared in 10 ml acetonitrile was used as supporting electrolyte.

3.4 Results and Discussion

3.4.1 Core-shell particles with graphite incorporated PPy shell

Copolymer particles of styrene and MA were formed by mini emulsion polymerization. These latex particles were used as template for the polymerization of pyrrole. The surface of the copolymer particles absorbs pyrrole and graphite and polymerization was performed by redox coupling reaction on the surface of the copolymer latex. The amount of pyrrole is low and forms a near uniform layer over the latex particles and results core-shell morphology. The unabsorbed graphite particles are removed by washing with water and ethanol. (**Fig 3.1**)

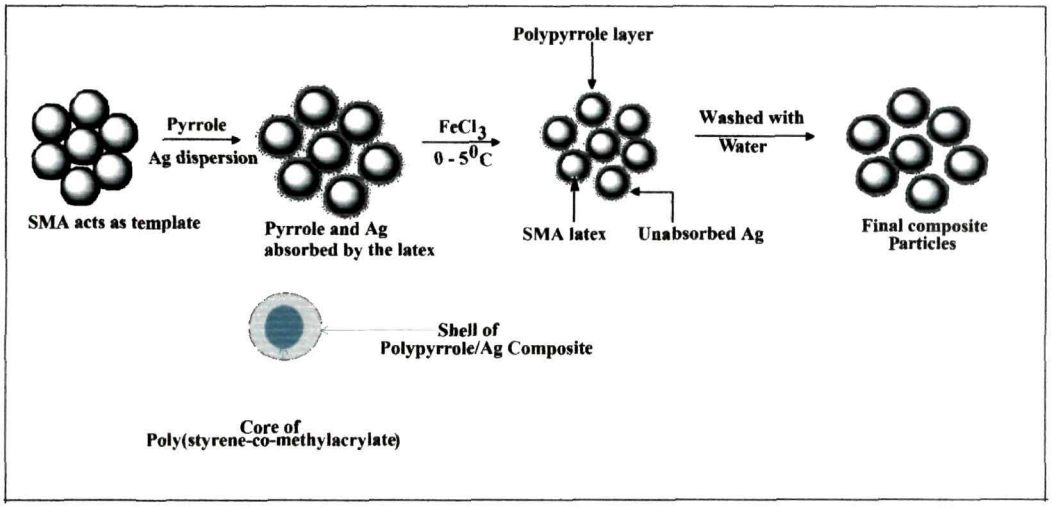

Fig 3.1: Schematic representation of the formation of the core-shell composite particles

3.4.1.1 FT-IR Spectroscopy

The FT-IR spectra of pure graphite and polypyrrole/graphite (PPy/G) are shown in **Fig 3.2**. In IR spectroscopy the broad strong bands between 3433 cm^{-1} corresponds to the absorption of N–H stretching of PPy. The frequency at 2926 cm^{-1} refers to the stretching vibration of C–H bond. The absorption at 1578 cm^{-1} was assigned to the C=C ring stretching of pyrrole. The band at 1380 cm^{-1} is due to C–H vibrations. The band at 1042 cm^{-1} is due to in plane deformation of C–H bond and N–H bond of pyrrole ring. The peak at 1727cm^{-1} and 1165cm^{-1} refer to C=O and C - O stretching of PMA. It has been observed that the peak at 1578 cm^{-1} shifts to 1638 cm^{-1} in the graphite incorporated core-shell particles. This may be attributed to the conjugation effect between the C=C of pyrrole and the graphite surface. Thus from the IR spectra it may be confirmed that the core-shell particle contains both the SMA latex as well as the graphite incorporated PPy phase.

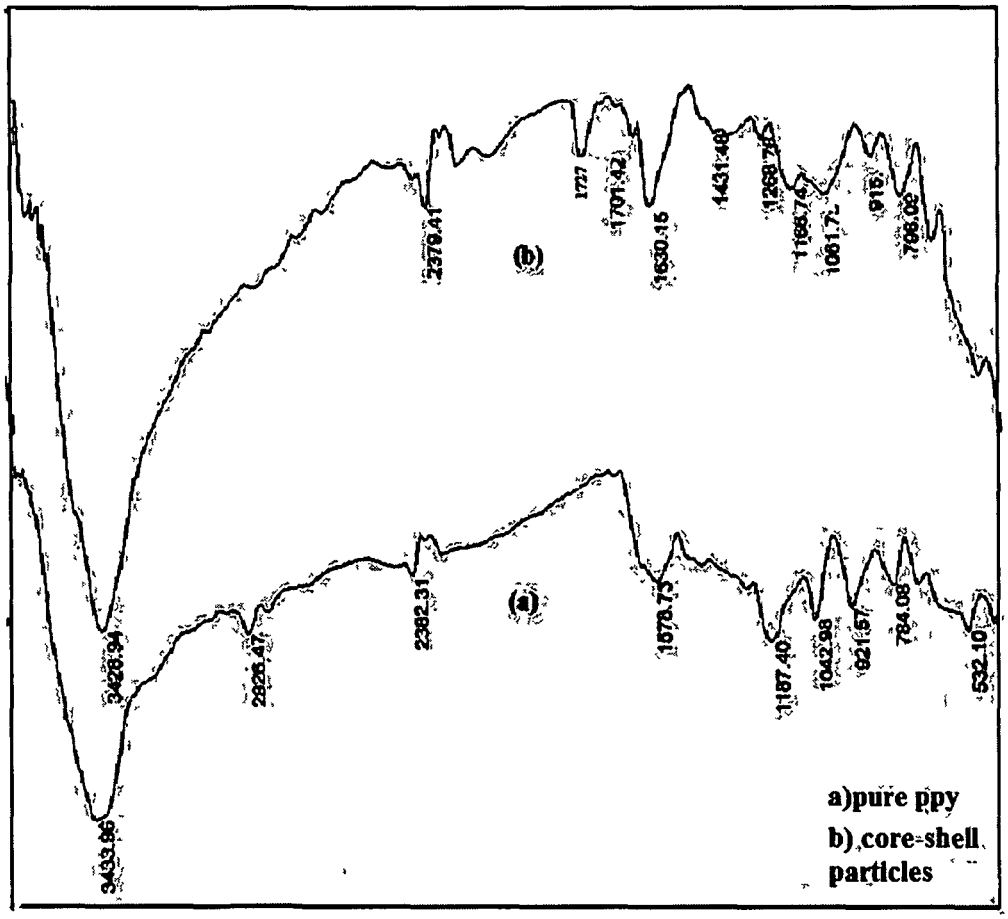

Fig 3.2: IR spectra of a) pure PPy b) core-shell particles

3.4.1.2 XRD Analysis

The XRD pattern of the core-shell composite particle is shown in **Fig 3.3**. XRD pattern of the core-shell composite particles shows the characteristic peaks at 26.35°, 44.6° and 54.65°. This matches to the (002), (101) and (004) planes of hexagonal system. This indicates the presence of graphite in the core-shell composites. The 'd' spacing for the core-shell composites are 3.34, 2.02, and 1.67 A^0 for their corresponding peaks at 26.35°, 44.60° and 54.65° respectively. This indicates the incorporation of the graphite particles on the PPy matrices.

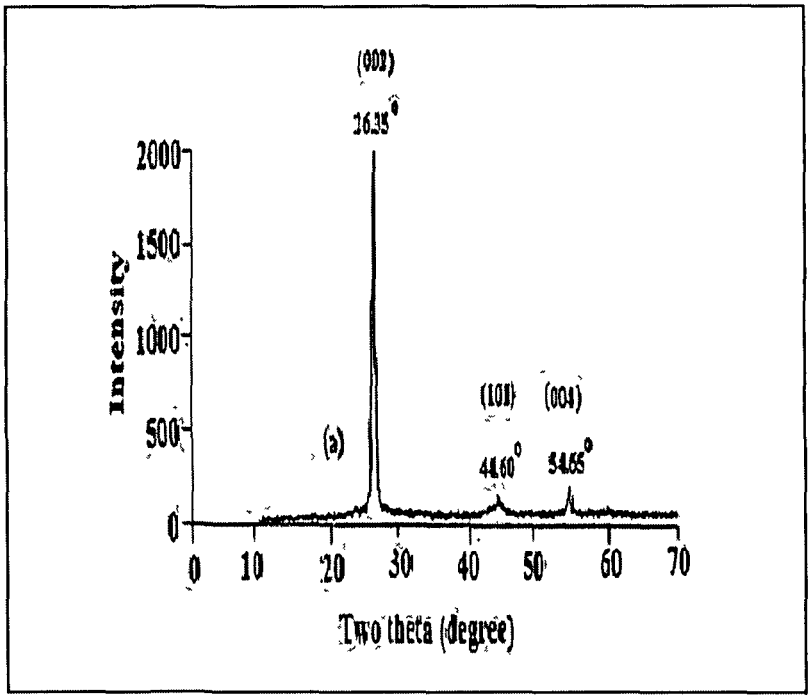

Fig 3.3: XRD analysis of the composite particles

3.4.1.3 Scanning Electron Microscopy (SEM)

Fig 3.4(a)-(b) represents the SEM images of the SMA latex and the graphite incorporated PPy coated SMA latex. **Fig 3.4**(c) represents the SEM image of the PPy coated SMA latex treated with excess of THF. When treated with THF the SMA latex in the core gets dissolved in the solvent and left a void in the interior, resulting "broken egg shell" morphology. This reveals beyond any reasonable doubt that core-shell morphology have been achieved with the SMA latex as the core and graphite incorporated PPy as the shell.

3.4.1.4 TEM Analysis

Fig 3.5 (a)-(b) represents the TEM images of the SMA latex particles and TEM image of the SMA-PPy/G composite particles. From **Fig 3.5 (a)** the spherical shape and size of about 120 nm may be confirmed. As shown in the figure, micro aggregates of SMA particles occurred when the medium water was evaporated. This is because of the fact that PMA has a relatively low Tg and hence exhibits good film formation properties at room temperature. In **Fig 3.5 (b)** it can be seen that the conducting shell is

formed as a layer on the SMA surface. The PPy over layer appears to be reasonably continuous, with little or no evidence of bare patches. This is consistent with the core-shell morphology of the resultant particles.

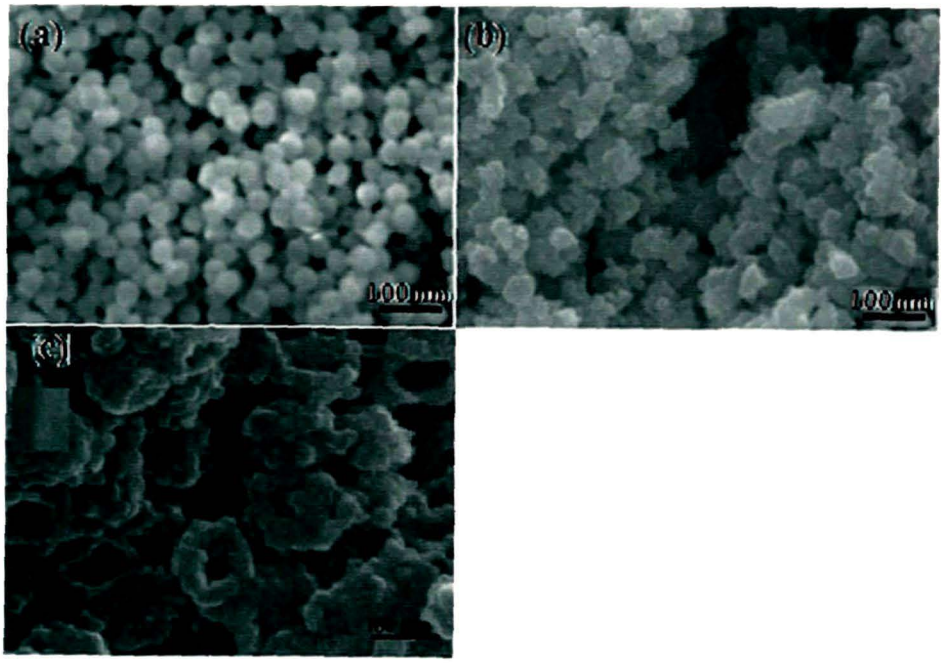

Fig 3.4: SEM images of the (a) SMA latex (b) Core-shell composite particles (c) Core-shell Composite particles after extraction with THF

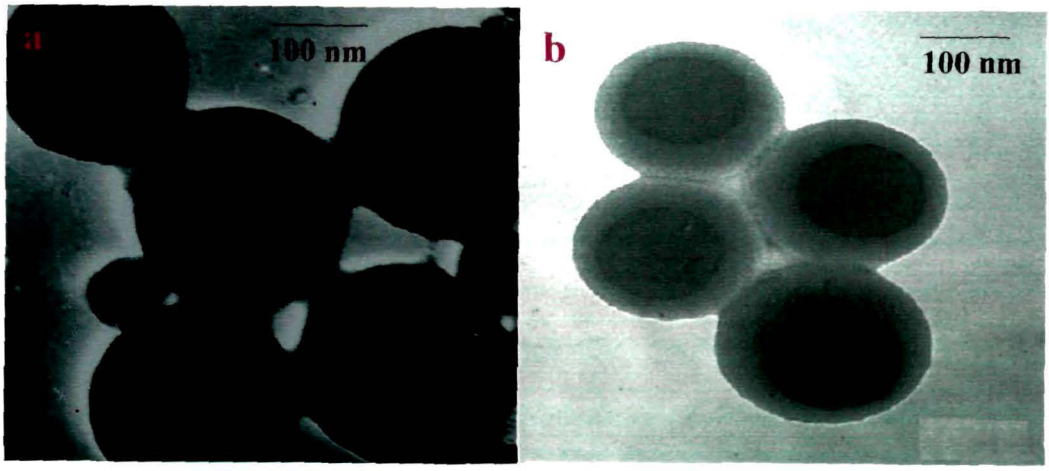

Fig 3.5: TEM images of (a) SMA latex (b) core-shell composite particles

3.4.1.5 Thermal Analysis

The thermo gravimetric profiles of PPy, pp/G and SMA-PPy/G composites are given in **Fig 3.6**. In all cases the weight loss at temperature 125 ^{0}C reveals the loss of moisture/adsorbed solvent from the polymer matrix. The major degradation occurred at 300 ^{0}C for PPy, at 400 ^{0} C for PPy/G composites and at nearly 425 ^{0} C for the core-shell composite particles. This showed that the thermal stability is improved in the core-shell composites.

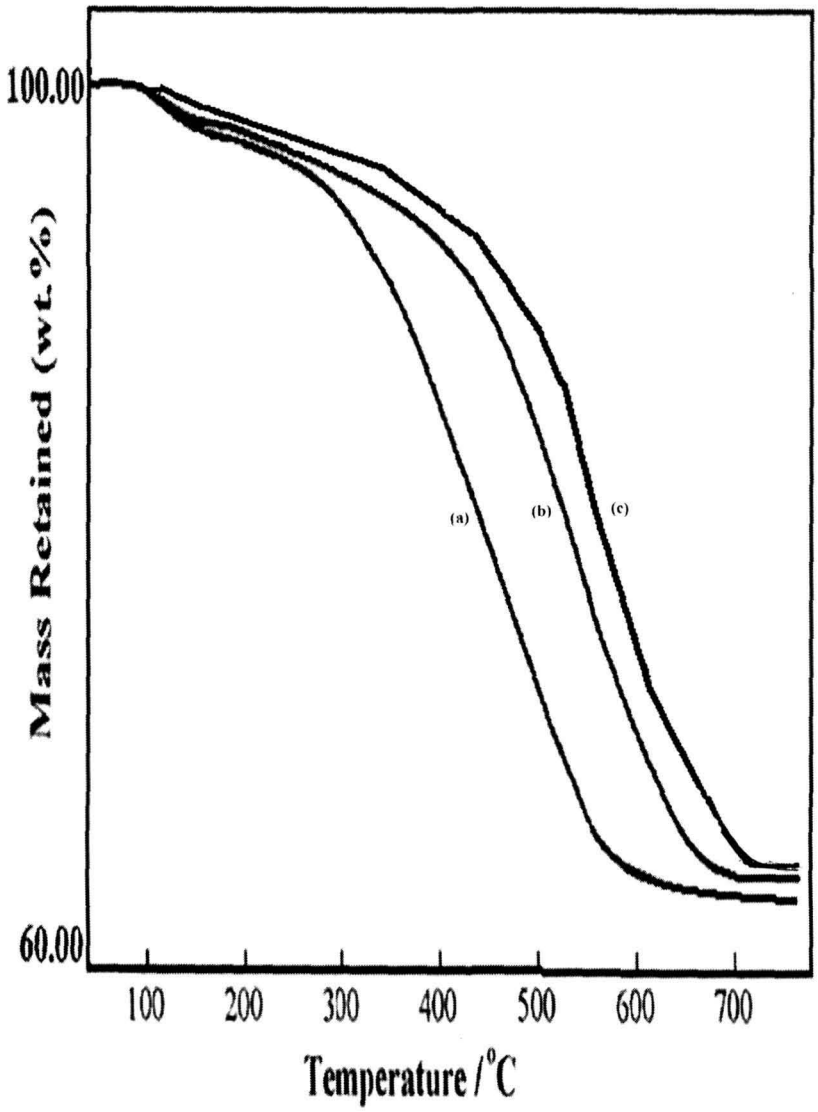

Fig 3.6: TGA of (a) PPy (b) PPy/G particles (c) Core-shell Composite particles

3.4.1.6 Electrical Behaviour

3.4.1.6.1 Current-Voltage relationship

Fig 3.7 shows the current-voltage relationship of the SMA-PPy/G composite having different graphite content. It was observed that all the synthesized core-shell composites show semi conducting behaviour. For all the samples, the potential difference (in Volt) increases linearly when the applied current (in mA) as well as the % of graphite in the PPy phase (shell) increases. This is a characteristic of semi conductor and hence it may be concluded that the core-shell composite particles are of semi conducting nature. It is also observed that the conductivity increases with increase of graphite percentage in the shell phase.

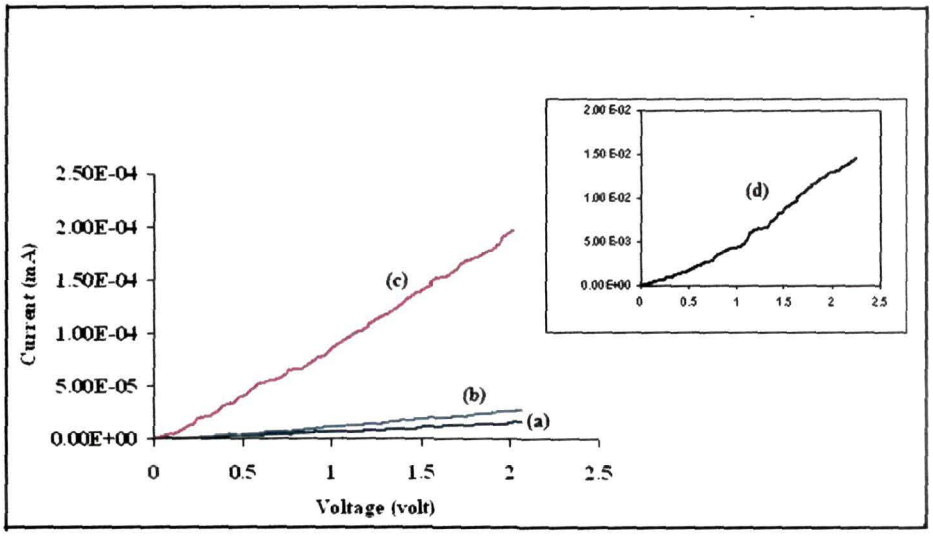

Fig 3.7: I-V plot of the core-shell particles with (a) 0% graphite (b) 0.25% graphite (c) 0.50% graphite and (d) 1% graphite

3.4.1.6.2 DC electrical conductivity

The conductivity of the SMA-PPy/G core-shell composite particles varied widely in the range of 9.3 S/cm to 26.8 S/cm depending on the graphite content in the shell phase. Thus it may be said that in the pellet of SMA-PPy/G composite particles, interfacial conductive paths consisting of the PPy/G shell were formed, and efficient

charge transport through the materials can occur without much interference from the electrically insulating SMA component.

Fig 3.8 shows the variation of the core-shell composite particles in the temperature range of 293 K< T < 413 K. It is observed that conductivity increases with increase of temperature. At high temperature inter-chain and intra-chain hoping increases and this increases the mobility of the charge carrier. This high charge carrier mobility ultimately results in increase of conductivity at high temperature[55-57]. With 1% incorporation of graphite in the PPy shell phase conductivity increases from 26.8 S/cm at 25^{0}C to 55.6 S/cm at 140 ^{0}C. This gives evidence beyond any reasonable doubt that the newly synthesized core-shell composite particles are of semi conducting nature.

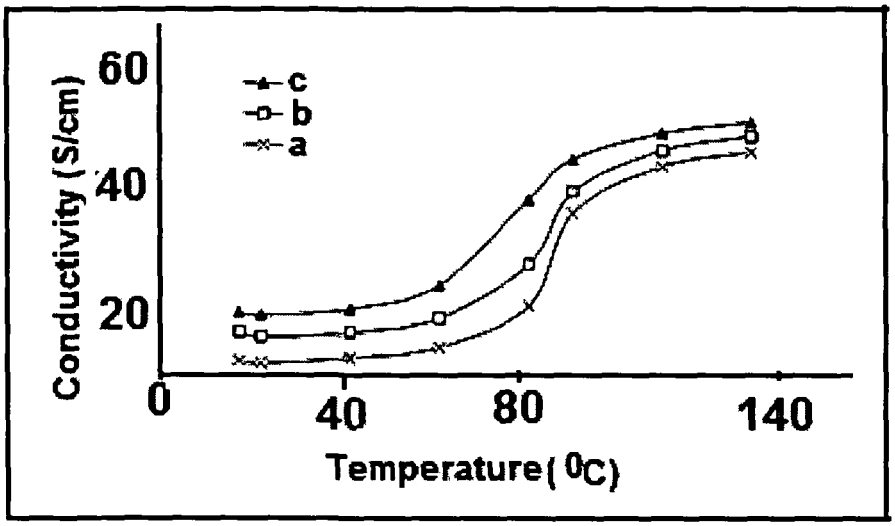

Fig 3.8: Conductivity vs temperature curve of the core-shell particles (a) 0.25% graphite (b) 0.50% graphite and (c) 1% graphite

The electrical conductivity of the core-shell composite depends not only on the concentration of graphite in the PPy shell but also on the MA content in the SMA latex. When the other conditions are the same, the electrical conductivity of the core-shell composites can be tuned to a certain extent by varying the soft monomer MA content in the SMA copolymer latex. The relationship between the conductivity and the MA content in the SMA latex of the core-shell composites having 1% graphite in the PPy phase is shown in the **Fig 3.9**. The decrease of conductivity may be presumably attributed to the increase of soft segment in the surface of the core-shell

composite particles with increase of MA content in the SMA latex. With high amount of soft content (MA) the core-shell particles can easily undergo deformation resulting poor conduction path. This creates difficulties for efficient charge transport and hence electrical conductivity decreases.

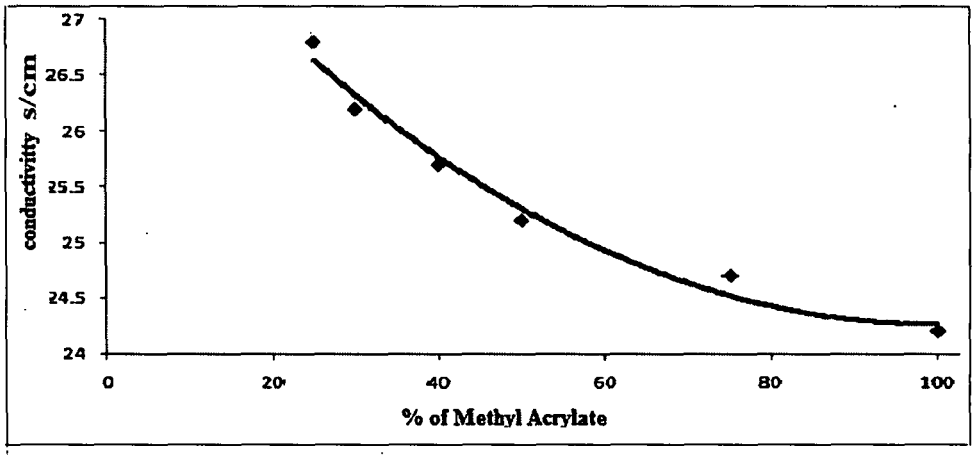

Fig 3.9: Plot of conductivity of the composite particles vs MA content in the SMA latex

3.4.1.7 Electro chemical behavior

Fig 3.10 shows the cyclic voltammogram of the core-shell composite particles having varied amount of graphite content in the shell phase. The electrochemical band gaps of the samples were calculated by using the following formulae.

$$HOMO = - [\varphi^{ox}_{onset} + 4.71] \text{ (eV)}, \quad (2)$$

$$LUMO = - [\varphi^{red}_{onset} + 4.71] \text{ (eV)}, \quad (3)$$

$$E^{g}_{ec} = (\varphi^{ox}_{onset} - \varphi^{red}_{onset}) \text{ eV}, \quad (4)$$

Where the units φ^{ox}_{onset} and φ^{red}_{onset} are V vs. Ag/AgCl. The values obtained are listed in table 3.4. The electrochemical band gap for PPy was calculated from voltammogram and found to be 2.90eV whereas in the core-shell composite particles band gaps were found to be decreasing (1.9 eV to 1.65 eV) with increasing amount of incorporated graphite in the PPy shell phase. The incorporation of graphite resulted in change in

electronic band structure manifested as new mid-gap being created and hence decreasing of band gap occurs.

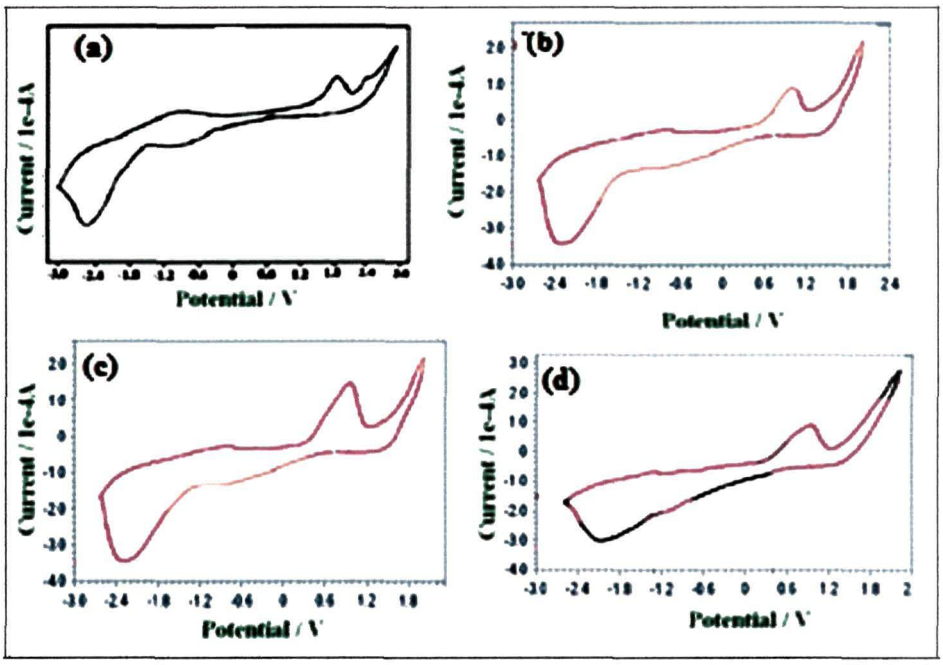

Fig 3.10: Cyclic voltamogram of the composite particles having (a) 0% graphite (b) 0.25%graphite (c) 0.50% graphite and (d) 1% graphite

Table 3.4: Electrochemical data of PPy and PPy/G composites

Sl. No	Sample (Core-shell composites)	$\varphi^{ox}_{onset}/E_{HOMO}$	$\varphi^{red}_{onset}/E_{LUMO}$	E^{g}_{ec} (eV)
1	0% (Graphite)	1.50/-6.21	-1.40/-3.31	2.90
2	0.25% (Graphite)	1.40/-6.11	-0.5/-5.21	1.9
3	0.5 (Graphite)	1.35/-6.06	-0.4/-5.11	1.75
4	1% (Graphite)	1.3/-6.01	-0.35/-4.36	1.65

3.4.1.8 Charge capacity

The electro-chemical stability of the core-shell composite particles was investigated by carrying out the cyclic voltammetry study of the core-shell composite particles (1% graphite) up to 100th cycle. (**Fig 3.11**) The study reveals that the cathodic and anodic peaks are nearly symmetrical above each other having minimum

separation. Thus it may be inferred that the core-shell composite particles are sufficiently redox stable to have manifold potential applications in the field of opto-electronics.

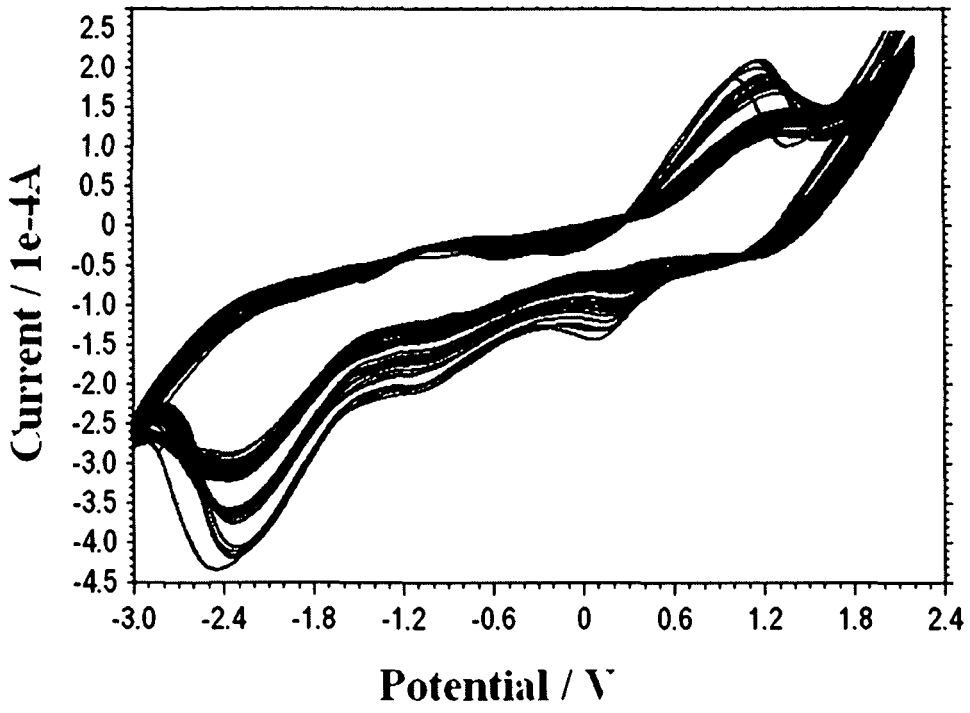

Fig 3.11: Successive electrochemical cycles of the composite particles (1% graphite) upto 100^{th} cycle.

3.4.2 Core-shell particles with Ag nanoparticles incorporated PPy shell

Silver nanoparticles were synthesized by chemical (citrate) reduction method using standard procedure. Appearance of pale yellow colour in the dispersion indicates the formation of silver nanoparticle. These dispersions are stable up to 2 months.

SMA particles were formed by miniemulsion polymerization. These latex particles were used as template for the polymerization of pyrrole. The polypyrrole coated SMA core-shell particles and polypyrrole-silver coated SMA core-shell particles were synthesized by in-situ oxidative polymerization technique. The pyrrole monomer and the Ag nanoparticles get adsorbed on the surface of the dispersed SMA particles. These adsorbed pyrroles on the surface of SMA get polymerized in presence of oxidizing agent and the Ag nanoparticles enter into the PPy matrix. Thus a layer of PPy/Ag nanocomposite is formed over the SMA latex to result core-shell morphology.

3.4.2.1 FT-IR Spectroscopy

The FT-IR spectra of the core-shell particles are given in **Fig 3.12**. FT-IR spectrum of the PPy coated SMA core-shell particle (**Fig 3.12a**) gave absorption band at 3414.19 cm^{-1}, 1163.64 cm^{-1}, 1031.16 cm^{-1} , 1721.70 cm^{-1}, 1443.94cm^{-1} and 1298.82 cm^{-1}.Here, the broad absorption band at 3414.19 cm^{-1}, 1163.64cm^{-1}, 1031.16 cm^{-1} which are due to the N-H str, N-C str and =C-H plane vibration[58]. These bands indicate the formation of PPy. Again bands at 1721.70 $cm^{-1}$and 1298.82 cm^{-1} indicate the presence of C=O and C-O group in the polymer backbone whereas band at 1443.94 cm^{-1} is due to stretching of the C=C bond of the phenyl ring[59].

On incorporation of Ag nanoparticles in the shell phase (**Fig 3.12b**) the absorption bands assigned to N-H str, N-C str and = C-H plane vibration at 3414.19 cm^{-1}, 1163.64 cm^{-1}, 1031.16 cm^{-1} shifts to 3335.88 cm^{-1}, 1164.32 cm^{-1} and 1032.61 cm^{1}. This indicates the interaction of the silver nanoparticle with the polymer backbone

Fig 3.12: FTIR spectra of the composite particle a) with 0% Ag b) with 10% Ag

3.4.2.2 UV-visible spectroscopy

Fig 3.13(a)-(b) shows the UV-visible spectra of the Ag nano particle dispersion and the core-shell particles respectively. The UV-visible spectrum of silver nanoparticle gives an absorption band with a maximum at 423nm due to surface plasmon absorption of silver nanoparticles. The surface plasmon absorption in the metal nanoparticles arises from the collective oscillations of the free conduction band electrons that are induced by the incident electromagnetic radiation. Such resonances are seen when the wavelength of the incident light far exceeds the particle diameter. Surface plasmon absorption band with a maximum of 423 nm indicates the formation of Ag nanoparticles[60].

The spectrum of the core-shell particle (**Fig 3.13b**) shows two absorption bands at 280nm and 450 nm. The absorption band at 280nm may be assigned to the excitation of C=O group in the polymethylacrylate segment (n-π^* transition)[61]. The peak at 450 nm corresponds to the plasmon resonance of the Ag nanoparticles. It is observed that the peak corresponding to the plasmon resonance of Ag nanoparticles undergoes a red shift (from 423 to 450 nm). In this work we carried out the polymerization of pyrrole in presence of the prepared Ag-dispersion. So during this process the Ag nanoparticles undergo a little bit of agglomeration and hence the particle size slightly increases. This slight increase of particle size is responsible for the observed red shift

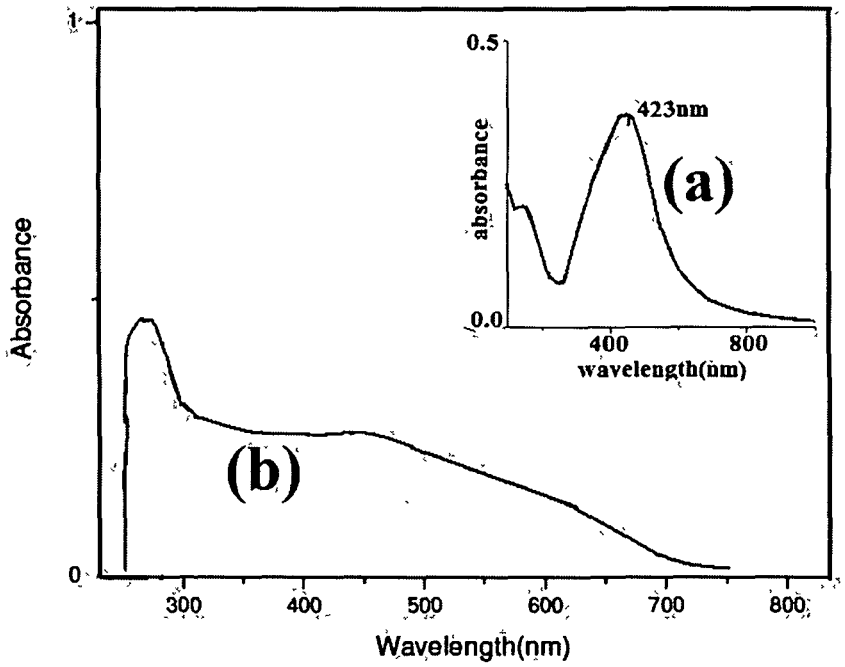

Fig 3.13: UV visible Spectra of a) Ag nanoparticle dispersion
b) SMA-PPy/Ag core-shell particles

3.4.2.3 Scanning Electron Microscopy (SEM)

Fig3.14 (a)-(b) represents the SEM images of the Ag nanoparticles and the core-shell particles respectively. The Ag nanoparticles are spherical and have particle diameter in the range of 40 to 50 nm. **Fig 3.14 (b)** shows that the conducting shell is formed as a layer on the SMA surface. The PPy layer appears to be reasonably continuous, with little or no evidence of bare patches. This is consistent with the core-shell morphology of the resultant particles. In case of the core-shell particles the particle size increases to nearly 90 nm which is consistent with the fact that a thin layer of polypyrrole is formed over the SMA layer.

3.4.2.4 EDX analysis

Fig 3.15 shows EDX spectrum of the core-shell particles. The EDX pattern shows peak of carbon, nitrogen and silver. Presence of nitrogen peak confirms beyond any reasonable doubt that PPy is successively coated over the SMA core. The presence of Ag peak strongly indicates that Ag nanoparticles are successfully incorporated within the PPy shell phase.

3.4.2.5 Transmission Electron Microscopy (TEM)

Fig 3.16 (a)-(b) represents the TEM image of the Ag nanoparticles and the core-shell particles respectively. From **Fig 3.16 (a)** it is seen that Ag particles are almost spherical and particle diameters vary in the range of 30 to 50 nm. In **Fig 3.16 (b)** it is clearly seen that a uniform layer of PPy is formed over the SMA particles. The shell layer seems to be rather continuous with little or no evidence of bare patches. This is consistent with the core-shell morphology of the particles. From the Figure it is seen that core- shell particles are spherical and have size in the range of 90 to 100 nm.

3.4.2.6 XRD analysis

Fig 3.17 shows the XRD pattern of the core-shell particles. The peak at ~26° is the characteristic peak of PPy. Diffraction peaks at 44.50 °, 52.20 ° and 76.7 ° corresponds to the (111), (200) and (220) facets of the face centred cubic crystal structure. This gives evidence of successful incorporation of the silver nanoparticles in the PPy phase. The broadening of the Bragg peaks indicates that the silver particles are in the nano range.

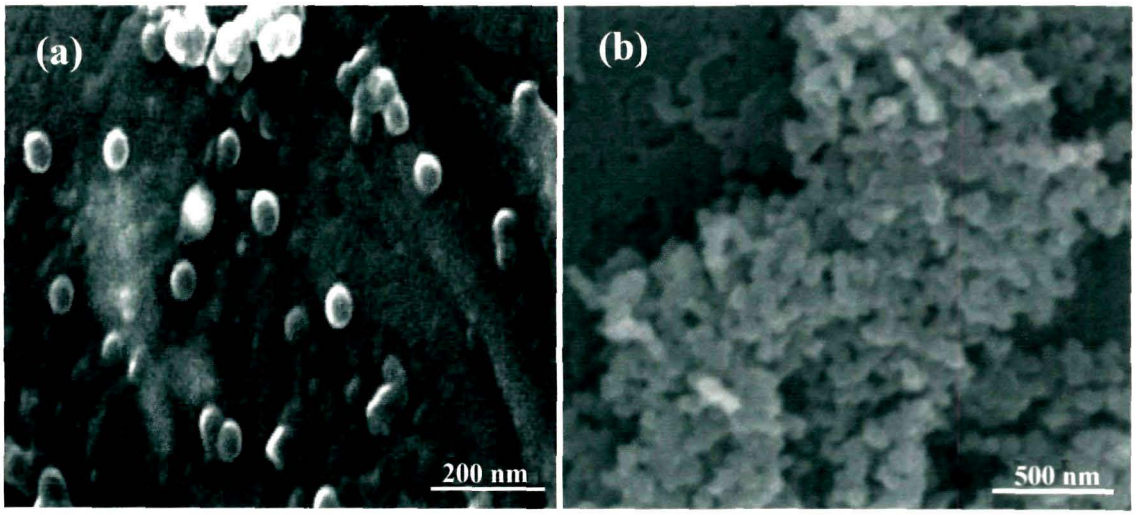

Fig 3.14: SEM micrograph of a) Ag nanoparticle dispersion
b) Final composite particle

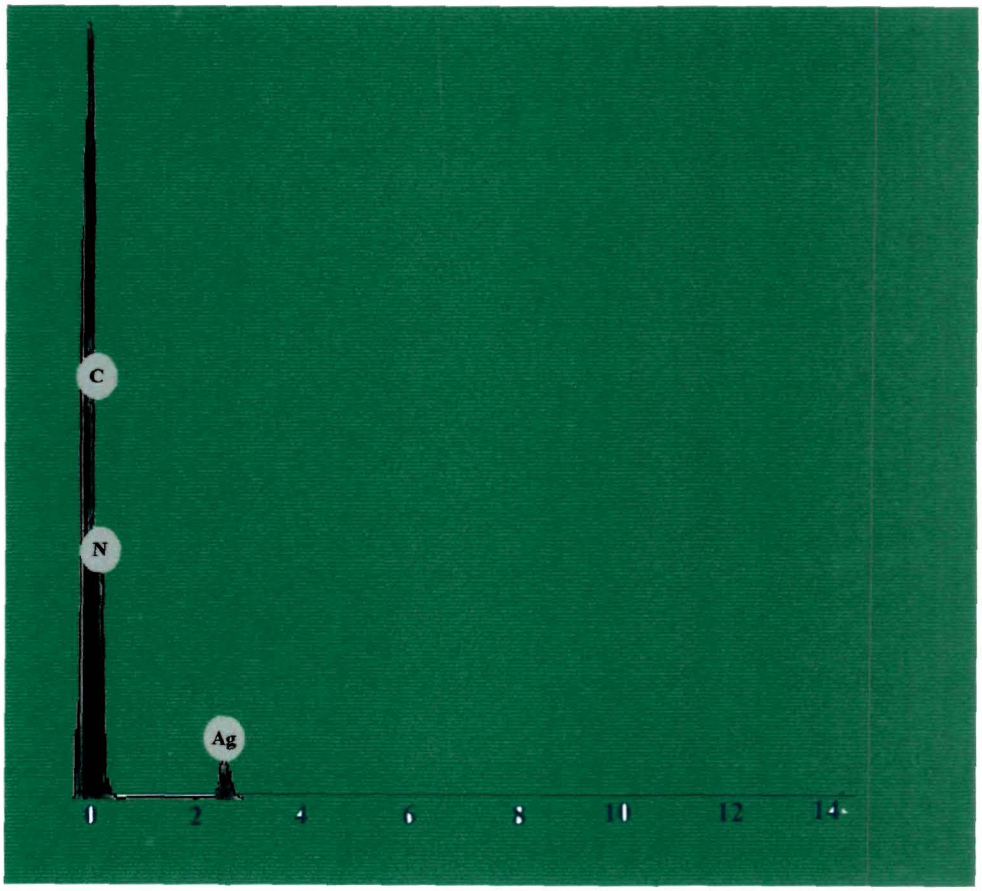

Fig 3.15: EDX pattern of the final composite particle

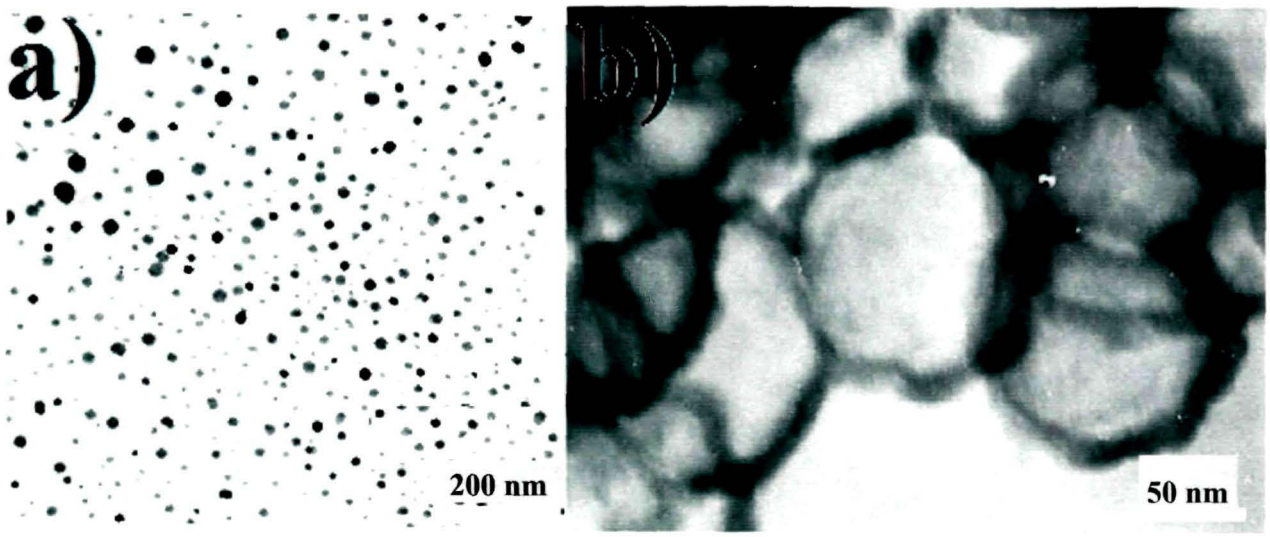

Fig 3.16: TEM micrograph of a) Ag nanoparticle dispersion
b) SMA-PPy/Ag core-shell particle

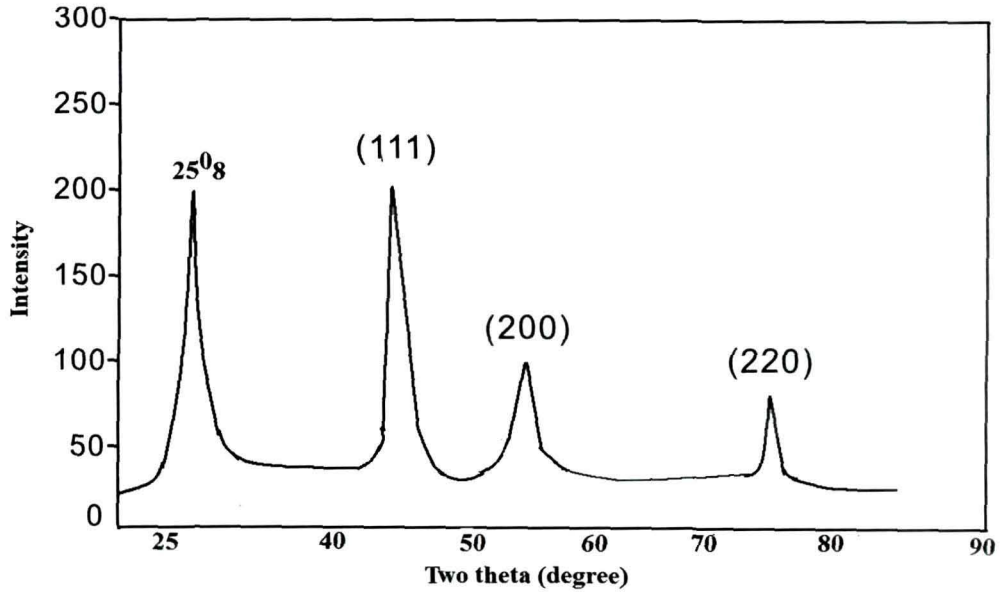

Fig 3.17: XRD pattern of the core-shell particles

3.4.2.7 Thermal Analysis

Fig 3.18 (a)-(b) represents the thermal degradation pattern of core-shell particles with 0% Ag and 3% Ag respectively. Both the core-shell particles show similar pattern, with a small variation in degradation temperature. The weight loss at about 110^0C reveals the loss of water molecules from the polymer matrix. The weight loss from 100^0C to 220^0C is due to low molecular weight oligomers. The final degradation starting from 220^0C is due to the degradation of the polymers. Fig 3.18(c) represents the degradation pattern of bare PPy/Ag composite. The degradation temperature in this case is approximately 230^0C. So it may be inferred that there is a sufficient enhancement in the thermal stability of the PPy/Ag composite when it is combined with the SMA latex. Moreover, in case of Fig 3.18(b) the final weight loss is 80% whereas in Fig 3.18(a) the final weight loss is 60%. This is strong evidence that Ag nanoparticles are successfully incorporated in the PPy shell phase.

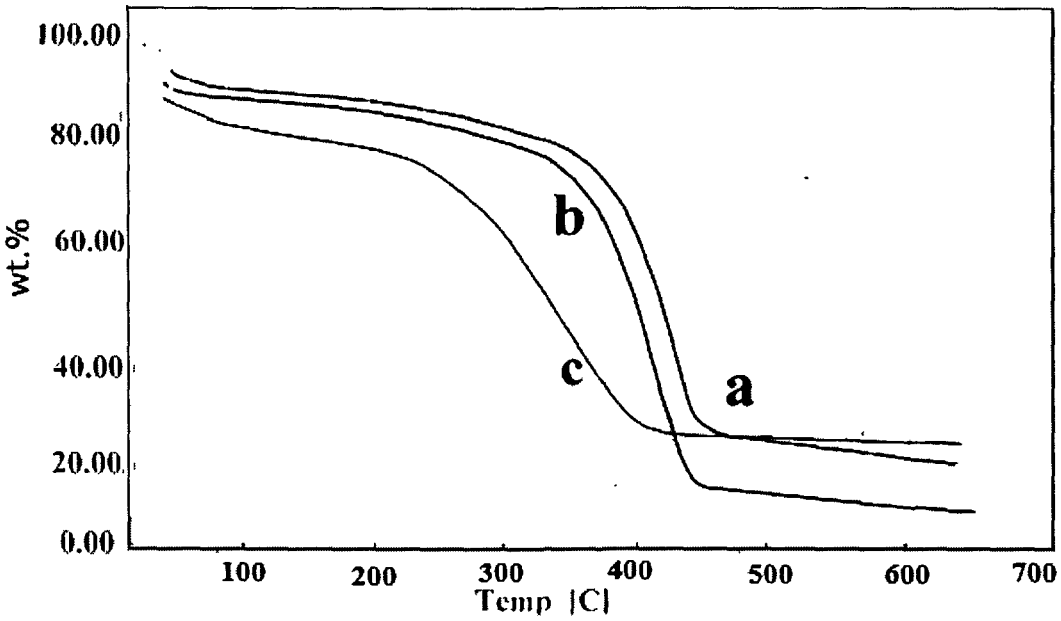

Fig 3.18: TGA of a) SMA-PPy/Ag core-shell particle
b) SMA-PPy particle c) PPy-Ag particle

3.4.2.8 Electrical Behaviour

3.4.2.8.1 Current - voltage relationship

Fig 3.19 shows the current-voltage relationship of the SMA-PPy/Ag composite having different Ag content. The current-voltage characteristic of the core-shell particles indicates that the core-shell particles behave as Schottky junction.[57] For all the samples, the potential difference (in Volt) increases when the applied current (in mA) as well as the percentage of silver in the PPy phase (shell) increases. This is a characteristic of semi conductor and hence it may be concluded that the core-shell composite particles are of semi conducting nature.

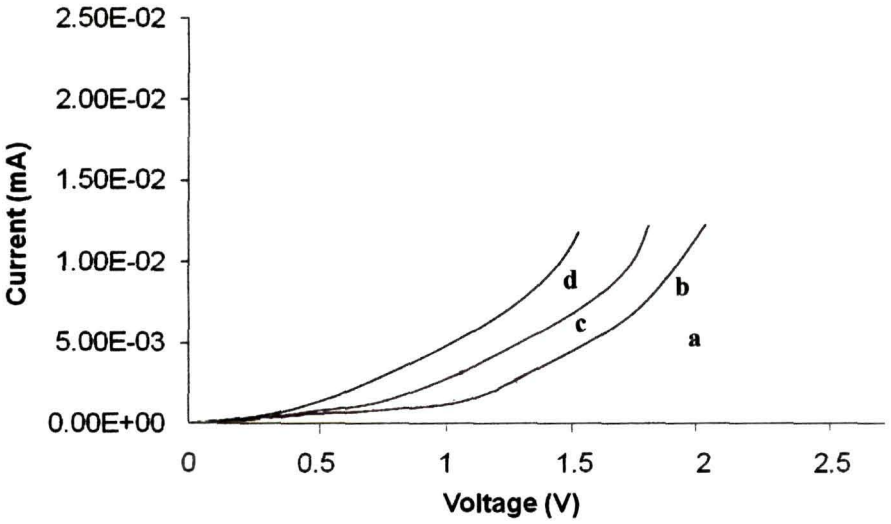

Fig 3.19: I-V Characteristics of the SMA-PPy/Ag particle with a) 0% Ag b) 3% Ag c) 5% Ag and d) 10% Ag

3.4.2.8.2 DC Conductivity

Fig 3.20 (a)-(b) show conductivity vs silver content and conductivity vs MA content curve of the core-shell particles respectively. The conductivity of the core-shells varies widely in the range of 114 $mScm^{-1}$ to 1560 $mScm^{-1}$ depending on the various concentration of the silver nanoparticle (**Table 3.5**).

Table 3.5: DC conductivity of the core-shell particles at room temperature with various concentration of silver nanoparticle

Sl. No	Core-shell particle	Concentration of silver nanoparticle (%)	Conductivity (in $mScm^{-1}$)
1	SMA-PPy-Ag 0%	0%	114.00
2	SMA-PPy-Ag 1%	1%	358.73
3	SMA-PPy-Ag 2%	2%	575.44
4	SMA-PPy-Ag 3%	3%	796.07
5	SMA-PPy-Ag 5%	5%	978.00
6	SMA-PPy-Ag 8%	8%	1080.50
7	SMA-PPy-Ag 10%	10%	1560.00

Thus it may be said that in the pellet of SMA/PPy-Ag composite particles, interfacial conductive paths consisting of the PPy-Ag shell were formed and efficient charge transport through the materials can occur without much interference from the electrically insulating SMA component. Since silver itself is conducting in nature, with increase of silver concentration in the shell phase, the inter and intra chain hopping sites increases and as a result conductivity of the core-shell particles also increases[62]. The electrical conductivity of the core-shell composite depends not only on the concentration of silver in the PPy shell but also on the MA content in the SMA latex. When the other conditions are the same, the electrical conductivity of the core-shell composites can be tuned to a certain extent by varying the soft monomer MA content in the SMA copolymer latex. The relationship between the conductivity and the MA content in the SMA latex of the core-shell composites having 1% Ag in the PPy phase is shown in the **Fig 3.20 (b)**. The decrease of conductivity may be presumably attributed to the increase of soft segment in the surface of the core-shell composite particles with increase of MA content in the SMA latex. As the amount of soft content increases it becomes difficult for efficient charge transport and hence electrical conductivity decreases. The lowest value of conductivity was observed when the MA content is 40% of the total monomer and with further increase of MA content conductivity remains almost constant(**Table 3.6**). This may be because of the fact that

the core-shell morphology becomes unstable at 40% MA content and efficient charge transport is hindered. It was observed that the conductivity of the core-shell particles suddenly increases with 6% Ag dosing .Thus it may be inferred that the core-shell particles follow percolation mechanism of conducitivity where 6% Ag is the approximate percolation threshold.

It is noteworthy that due to the poor mechanical strength PPy/Ag composites do not form stable pellets and hence their dc conductivity could not be measured. So this study reveals that this problem may be overcome by combining this composite with mechanically stable SMA latex without much lowering of inherent conductivity.

Table 3.6: DC conductivity of the core-shell particles at room temperature with various concentration of MA

Sl. No	Core-shell particle	Concentration of MA (%)	Conductivity (in $mScm^{-1}$)
1	MA 20%	20%	1560
2	MA 30%	30%	800
3	MA 40%	40%	588
4	MA 50%	50%	400
5	MA 60%	60%	390

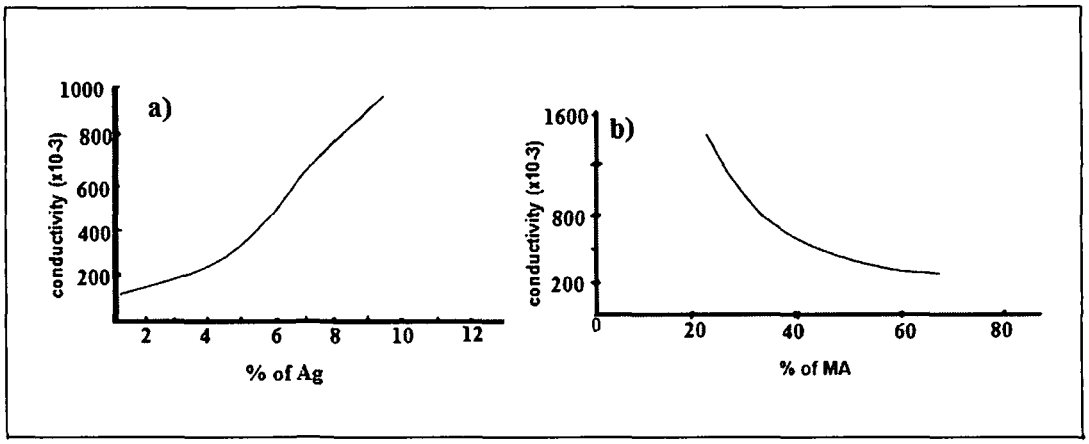

Fig 3.20: Variation of conductivity of the SMA-PPy/Ag composite particles a) % Ag in the shell phase b) % MA content in the SMA core

3.4.2.9 Electrochemical Property

Fig 3.21 shows the cyclic voltammogram of SMA/PPy-Ag core-shell particles (1%,2%,3% Ag respectively). The electrochemical band-gap of the samples was calculated by using the formulae 2, 3 and 4 stated earlier. The values obtained are listed in **Table 3.7**. The electrochemical band gap for the core-shells is found to be decreasing (from 1.6 to 1.1) with increasing amount of incorporated silver nanoparticle. The incorporation of silver nanoparticle results in change in electronic band structure manifested as new mid-gap state being created and hence decreasing of band gap occurs.

Table 3.7: Band gap of the core-shell particles

Sl. no.	Core-shell particle	Concentration of silver nanoparticle (%)	' Band gap (eV)
1	SMA-PPy-Ag 1%	1%	1.6
2	SMA-PPy-Ag 2%	2%	1.2
3	SMA-PPy-Ag 3%	3%	1.1

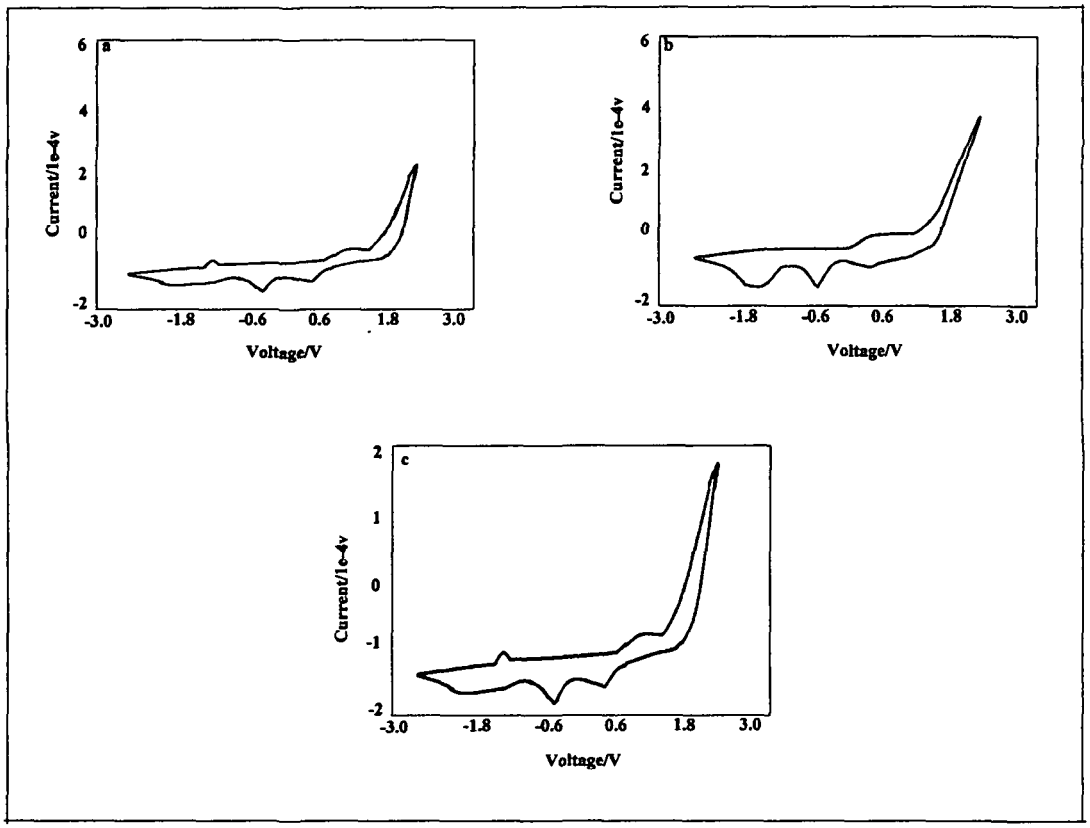

Fig 3.21: Cyclic Voltamogram of the composite particle
a) 1% Ag b) 2% Ag c) 3% Ag

3.4.2.10 Charge capacity

The area under the CV peaks could be integrated to yield charge capacity which in turn gives information of the electro activity of the core-shell particles. The cyclic voltammetry study of SMA/PPy-Ag core-shell particles (3% Ag dosing) up to 50^{th} cycle (**Fig 3.22**) reveals that cathodic and anodic peaks are nearly symmetrical above each other with minimum separation. The charge capacity of the core-shell particle does not get diminished even after the repeated cycles. This property emphasizes that SMA/PPy-Ag core-shell particles may be useful and prominent material to be used in rechargeable batteries.

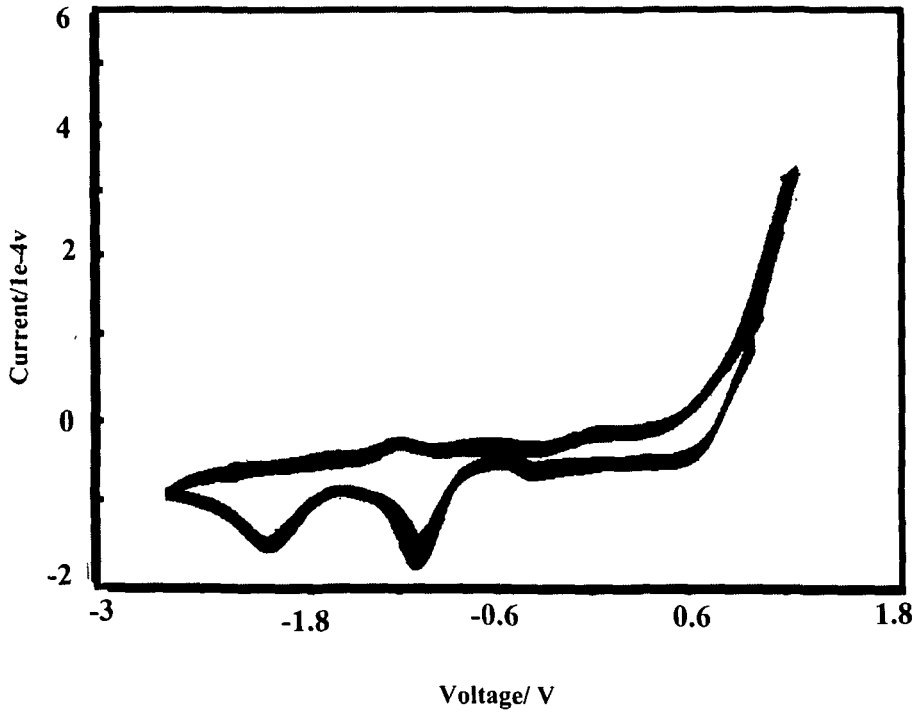

Fig 3.22: Successive electrochemical cycles of the composite particles (3% Ag dosing) upto 50th cycle

3.5 Application of core-shell particles with SMA core and graphite incorporated polypyrrole shell as Ammonia Gas Sensor

In recent years conducting polymers such as PPy, PANI and polythiophene have been studied as gas sensing materials, essentially due to their operation at room temperature and easy sensor element processing[63-66]. The principal sensing mechanism in conducting polymer is generally based on the modification of doping level due to redox interaction of the analyte molecules and thereby resulting in change in conductivity[67]. Amongst various conducting polymers, PPy has an edge due to its chemical stability against atmospheric conditions and ease of synthesis. In addition to this, the morphology of PPy can be easily tailored to nanowires, nanotubes and coral like structures by optimizing the synthesis parameters[68-69]. PPy has been reported for ammonia gas sensing applications; however the sensed concentrations are very high (>100 ppm).[70] It is known that the toxic limit of ammonia is 25 ppm in air and

therefore the PPy based sensors should sense the gas concentrations well below this limit.

Herein, we have utilised SMA/PPy-G core-shell particles as ammonia gas sensor. In order to measure the gas response, the resistances of the pellets of the core-shell particle were measured with and without exposure to gases at room temperature. Distilled water was used as diluent, for preparing various analyte concentrations. The dc electric resistance of the core-shell particles exposed to analyte vapour was measured by hanging the pellet in a closed glass container as shown in **Fig 3.23**. The distance between the sensing element and solvent surface was ~ 3 cm. Resistance measurements were performed in a simple two probe conFiguration. The contact leads were fixed 1 cm apart on one of the surface of the pellet using conducting silver paste. The resistance was measured as a function of time in a digital multimeter. The sensing measurements were carried out for different ammonia concentration such as 10, 30, 50 and 100 ppm. The resistance data were collected for 30 seconds while the pellets were exposed to ammonia vapours at ambient conditions and recovered in dry air.

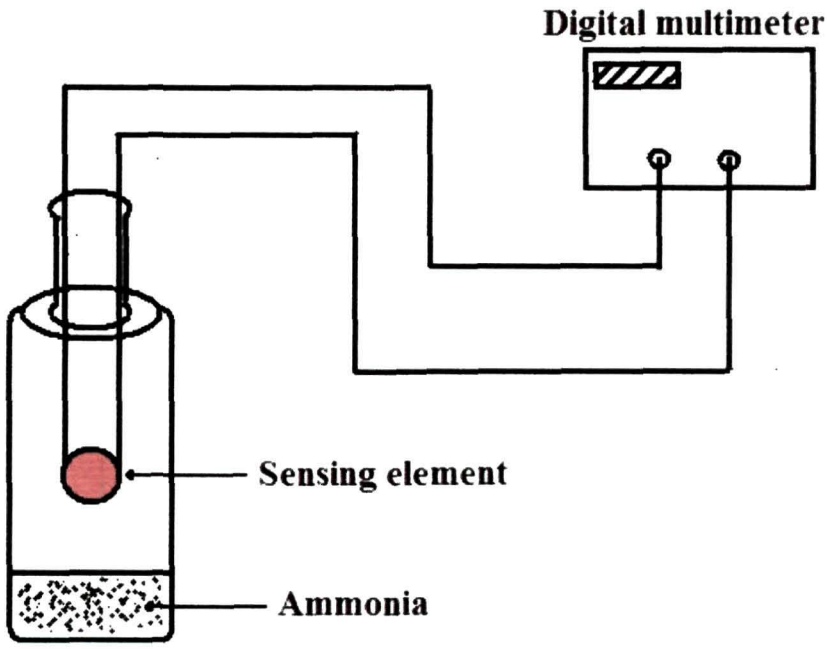

Fig 3.23: Apparatus used to study sensing performance

3.5.1 Results and Discussion

The response of the core-shell particles on exposure to various ammonia concentrations were presented as sensitivity vs. time curve (**Fig 3.24**). The sensitivity of the pellets are given by

$$\text{Sensitivity} = \blacktriangle R/R. \quad \text{---------- (5)}$$

Where ▲R is the change in the resistance of the pellets on exposure to ammonia vapour and R is the initial resistance of the sensing pellets.

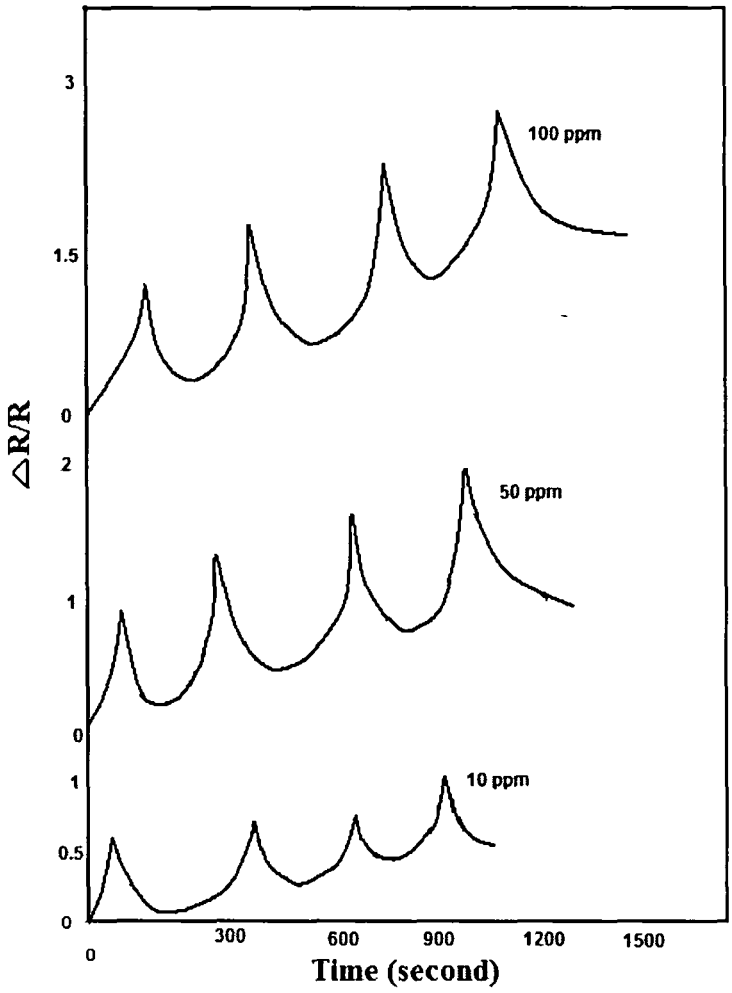

Fig 3.24: The response of core-shell particles to ammonia vapour a)10 ppm b) 30 ppm c)50 ppm d)100 ppm

From the Figure it is seen that the sensitivity of the core-shell particles increases with the increase of concentration of the ammonia vapour. However, it is observed that the sensitivity is ~0.6 for 10 ppm ammonia solution. So it may be inferred that the core-shell particles can be effectively used as an ammonia gas sensor even at very low concentration of ammonia.

We have further investigated the response of the core-shell particles to ethanol and chloroform vapour. Typical gas response curves of the core-shell pellets for 100 ppm concentrations of ammonia, ethanol and chloroform shown in **Fig 3.25**.

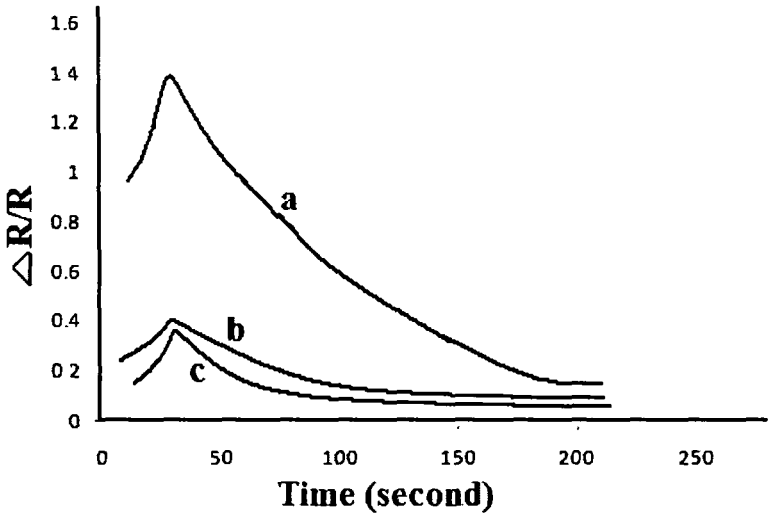

Fig 3.25: Response curve of the core-shell particles to
a) Ammonia b) Ethanol c) chloroform

It is seen that the sensitivity of ammonia (100 ppm), ethanol (100 ppm) and chloroform (100 ppm) are 1.4, 0.4 and 0.38 respectively. A high sensitivity for ammonia indicates that the core-shell particles are selective for this gas. The higher sensitivity towards ammonia than ethanol and chloroform can be explained, on the basis of different interactions between sensing film and adsorbed gas. PPy is a p-type material and when it interacts with ammonia, there is reduction in charge carrier density. This results in decreasing the conductivity of material. In comparison with this, interaction between PPy film and other gases is less than ammonia, thereby, showing less sensitivity and response.

3.6 Conclusion

- Two sets of core-shell particles with poly (styrene-co-methylacrylate) core and PPy shell were prepared by mini emulsion polymerization. In one set, graphite was used as the conducting filler while in the other set Ag nanoparticles were used as the conducting filler.
- The SEM micrographs confirm the rough surface morphology of both the core shells with almost spherical particles. The TEM micrograph gives information about the core-shell morphology. The core-shell particles have size in the range of 100-120 nm.
- XRD and EDX analysis confirms the presence of graphite and silver nanoparticle in the PPy phase of the respective core-shell.
- The thermal analysis reveals that core-shell particles possess good thermal stability.
- The electrical conductivity of the core-shell particles may be tuned within a good range by varying the conducting filler amount (graphite and Ag nanoparticles) in the PPy shell phase. Conductivity of the core-shell particles decreases with increase of the MA content in the core phase.
- The electro-chemical study reveals that the composite particles possess excellent electro-chemical reversibility having charge capacity almost unchanged up to 100^{th} cycle.
- The core-shell particles with SMA core and graphite incorporated PPy shell were applied as an ammonia gas sensing material. The sensing behaviour of the core-shell particle was studied by monitoring the increase in resistance of the core-shell particles on exposure to ammonia vapour. The core-shell particles show very good response to ammonia vapour with concentration as low as 10 ppm. Since the toxic limit of ammonia is 25 ppm in air it may be inferred that these core-shell particles can be potentially applied as an ammonia gas sensing material.

References

1. Wiersma, A.E., Vd Steeg, L.M.A., Jongeling, T.J.M. Waterborne core-shell dispersions based on intrinsically conducting polymers for coating applications. *Synth. Met.* **71**, 2269-2270 (1995)
2. Singh, A., Singh, N.P., Singh, P, Singh, R.A. Synthesis and characterization of conducting polymer composites based on polyaniline–polyethylene glycol–zinc sulfide system. *J. Polym. Res.* **18**, 67-77 (2011)
3. Skotheim, T.A., Elsenbaumer, J.R. *Reynolds (Eds.). Handbook of Conducting Polymers* (Marcel Dekker, New York, 1998)
4. Pickup, N.L., Sharpio, J.S., Wong, D.K.Y. Extraction of mercury and silver into base-acid treated polypyrrole films: A possible pollution control technology. *J Polym. Res.* **8,** 151-157 (2001)
5. Huijs, F.M., Lang, J., Kalicharan, D. Formation of transparent conducting films based on core-shell latices: Influence of the polypyrrole shell thickness. *J. Appl.Polym.Sci.***79**, 900-909 (2001)
6. Gangopadhyay, R., De, A. Conducting Polymer Nanocomposites: A Brief Overview. *Chem. Mater.* **12**, 608-622 (2000)
7. Zhang, T., He, Y., Wang, R., Geng, W. Analysis of dc and ac properties of humidity sensor based on polypyrrole materials. *Sensors and Actuators B* **131**, 687-691 (2008)
8. Majid, K., Tabassum, R., Shah, A.F., Ahmad, S., Singla, M.L. Comparative study of synthesis, characterization and electric properties of polypyrrole and polythiophene composites with tellurium oxide. *Journal of Material Science: Materials in Electronics* **20**, 958- 966 (2009)
9. Xing, S., Zhao, G. Morphology and thermostability of polypyrrole prepared from SDBS aqueous solution. *Polymer Bulletin* **57**, 933-943 (2006)
10. Kizilyar, N., Toppare, L., Önen, A., Yagci, Y., Conducting copolymers of polypyrrole/polytetrahydrofuran. *Polymer Bulletin* **40**, 639 (1998)
11. Ishiyama, K., Imamura, K., Arai, K.I. Smart actuator with magneto-elastic strain sensor. *Journal of Magnetism and Magnetic Materials* **242**, 1163-1165 (2002)

12. Smyth, C., Lau, K.T., Shepherd, R.L., Diamond, D., Wu, Y., Spinks, G.M., Wallace, G.G. Self-maintained colorimetric acid/base sensor using polypyrrole actuator. *Sensors and Actuators B* **129**, 518-524 (2008)

13. Yao, T., Wang, C., Wu, J., Lin, Q., Zhang, K. Preparation of raspberry-like polypyrrole composites with applications in catalysis. *Journal of Colloid and Interface Science* **338**, 573-577 (2009)

14. Koezuka, H., Tsumura, A. Field-effect transistor utilizing conducting polymers. *Synth. Met.* **28,** 753-760 (1989)

15. Gao, J., Heegar, H., Lee, J.Y., Kim, C.Y. Soluble polypyrrole as the transparent anode in polymer light-emitting diodes. *Synth. Met.* **82,** 221-223 (1996)

16. Landon, P.B., Gutierrez, J., Gilleland, C.L., Jordan, L. Inverse conjugated polymer opals and their luminescent spectra. *Journal of Material Science: Materials in Electronics* **18**, 235-238 (2007)

17. Partch, R., Gangolli, S.G., Matijevi, E., Cal, W., Arajs, S. Conducting polymer composites: I. Surface-induced polymerization of pyrrole on iron (III) and cerium (IV) oxide particles. *J. Colloid Interface Sci.* **144**, 27-35 (1991)

18. Chen, H., Chen, J., Liyan, K.A., Wenbo, H., Zhengping, L., Qingyue, Z. Polypyrrole-coated styrene-butyl acrylate copolymer composite particles with tunable conductivity. *Chinese Science Bulletin* **50**, 971-975 (2005)

19. Liu, Y.C., Lee, H.T., Yang, S.J. Strategy for the syntheses of isolated fine silver nanoparticles and polypyrrole/silver nanocomposites on gold substrates. *Electrochim Act.* **51**, 3441-3445 (2006)

20. Liu, C.F., Maruyama, T., Yamamoto, T. Conductive Blends of π-Conjugated Polymers and Thermoplastic Polymers in Latex Form. *Polym. J.* **25**, 363-372 (1993)

21. Guo, L., Pei, G.L., Wang, T.J., Wang, Z.W. Polystyrene coating of Fe_3O_4 particles using dispersion polymerization. *Colloids and Surfaces A: Physicochem. Eng. Aspects* **293**, 58-62 (2007)

22. Liu, Y.D., Fang, F.F., Choi, H.J. Core–Shell Structured Semiconducting PMMA/Polyaniline Snowman-like Anisotropic Microparticles and Their Electrorheology. *Langmuir* **26**, 12849–12854 (2010)

23. Lee, J.M., Lee, D.G., Lee, S.J., Kim, J.H. One-Step Synthetic Route for Conducting Core–Shell Poly (styrene/pyrrole) Nanoparticles. *Macromolecules* **42**, 4511–4519 (2009)

24. Lee, D.G., Lee, J.M., Jo, Y.H., Lee, S.J. Kim, J.H. Cheong, I.W. Self-doped conducting core-shell poly (styrene/pyrrole) nanoparticles via two-stage shot-growth. *J. Nanosci. Nanotechnol.* **10**, 6912-6915 (2010)

25. Xuan, S., Fang, Q., Hao, L., Jiang, W., Gong, X., Hu, Y., Chen, Z. Fabrication of spindle Fe2O3@polypyrrole core/shell particles by surface-modified hematite templating and conversion to spindle polypyrrole capsules and carbon capsules. *Journal of Colloid and Interface Science* **314,** 502–509 (2007)

26. Kohut-Svelko, N., Reynaud, S., Dedryvère, R., Martinez, H., Gonbeau, D., François, J. Study of a nanocomposite based on a conducting polymer: polyaniline. *Langmuir* **21**, 1575-1583 (2005)

27. Jang, B.J., Oh, J.H. Fabrication of a highly transparent conductive thin film from polypyrrole/poly (methyl methacrylate) core/shell nanospheres. *Adv. Funct. Meter.* **15**, 494-502 (2005)

28. Pickup, N.L., Shapiro, J. S., Wong, D. K. Y. Extraction of mercury and silver into base-acid treated polypyrrole films: A possible pollution control technology. *J. Poly. Res.* **8,** 151-157 (2001)

29. Fitch, R.M. *Polymer Colloids, A comprehensive introduction* (Academic Press, San Diego, USA, 1997)

30. Roncali, J., Garreau, R., Yassar A., Marque, P., Garnier, F., Lemaire M. Effects of steric factors on the electrosynthesis and properties of conducting poly (3-alkylthiophenes) *J. Phys. Chem.* **91**, 6706–6714 (1987)

31. Yuan, W.L., O'Rear, E.A., Grady, B.P., Glatzhofer, D.T. Nanometer-thick poly (pyrrole) films formed by admicellar polymerization under conditions of depleting adsolubilization. *Langmuir* **18,** 3343- 3351 (2000)

32. Hong, X.Y., Tyson, J.C. Controlling the macromolecular architecture of poly (3-alkylthiophene)s by alternating alkyl and fluoroalkyl substituents. *Macromolecules* **33**, 3502- 3504 (2000)

33. Hoffmann, K.J., Samuelsen, E.J., Carlsen, P.H.J. Broken conjugated thiophenesystems: 1. Synthesis and polymerization of 2, 2-di (alkylthienyl) methanes. *Synth. Met.* **113,** 161- 166 (2000)

34. Hua, M.Y. Hwang, G.W. Chuang, Y.H. Chen, S.A. Soluble n-doped polyaniline:synthesis and characterization. *Macromolecules* **33**, 6235-6238 (2000)

35. Wang, J. Construction of Redispersible Polypyrrole Core–Shell Nanoparticles for Application in Polymer Electronics. *Adv. Mater.* **21**, 1137-1141 (2009)

36. Armes, S.P., Gottesfeld, S., Beery, J.G., Garzon, F., Agnew, S.F. Conducting polymer-colloidal silica composites. *Polymer* **32**, 2325- 2330 (1991)

37. Wu, T.M., Chang, H.L. Preparation and characterization of conductive carbon nanotube–polystyrene nanocomposites using latex technology. *Composites Science and Technology* **68**, 2254-2259 (2008)

38. Khan, M.A., Armes, S.P. Conducting Polymer-Coated Latex Particles. *Adv. Mater.* **12,** 671-674 (2000)

39. Huijs, F.M., Vercauteren, F.F., Kalicharan, D., Hadziioannou, G. Shell morphology of core-shell latexes based on conductive polymers. *Synth. Met.* **102**, 1151-1152 (1999)

40. Lascelles, S.F., Armes, S.P. Synthesis and characterization of micrometersized polypyrrole-coated polystyrene latexes. *Adv. Mater.* 7, 864-866 (1995)

41. Aoki, K., Chen, J., Ke, Q. Redox Reactions of Polyaniline-Coated Latex Suspensions. *Langmuir* **19**, 5511-5516 (2003)

42. Khan, M.A., Armes, S.P. Synthesis and Characterization of Micrometer-Sized Poly (3, 4-ethylenedioxythiophene)-Coated Polystyrene Latexes. *Langmuir* **15**, 3469-3475 (1999)

43. Huijs, F.M., Lang, J. Morphology and film formation of poly (butyl methacrylate)–polypyrrole core–shell latex particles. *Colloid. Polym. Sci.* **278**, 746-756 (2000)

44. Wang, J., Sun, L., Mpoukouvalas, K., Lienkamp, K., Lieberwirth, I. Construction of Redispersible Polypyrrole Core–Shell Nanoparticles for Application in Polymer Electronics. *Adv Mater.* **21,** 1137-1141 (2009)

45. Huijs, F.M., Vercauteren, F.F., Hadziioannou, G. Resistance of transparent latex films based on acrylic latexes encapsulated with a polypyrrole shell. *Synth. Met.* **125**, 395-400 (2002)

46. Han, M., Zhao, K., Zhang, Y., Chen, Z., Chu, Y. Dielectric properties of polystyrene-polypyrrole core-shell conducting spheres suspended in aqueous solution. *Colloids and Surfaces A: Physicochemical and Engineering Aspects* **302,** 174-180 (2007)

47. Xie, H.Q., Ma, Y.M., Guo, J.S. Conductive polyaniline-SBS composites from in situ emulsion polymerization. *Polymer* **40**, 261-265 (1999)

48. Ruckenstein, E., Yang, S. J. An emulsion pathway to electrically conductive polyaniline-polystyrene composites. *Synth. Met.* **53**, 283-292 (1993)

49. Liyan, H., Wenbo, H., Zhengping, L., Qingyue, Z. Polypyrrole-coated styrene-butyl acrylate copolymer composite particles with tunable conductivity. *Chinese Science Bulletin* **50**, 971-975 (2005)

50. Wang, Y., Shi, Y., Xu, X., Liu, F., Yao, H., Zhai, G. Preparation of PANI-coated poly (styrene-co-styrene sulfonate) nanoparticles in microemulsion media. *Colloids and Surfaces A: Physicochem. Eng. Aspects* **345**, 71-74 (2009)

51. Jang, J., Oh, J.H., Stucky, G.D. Fabrication of Ultrafine Conducting Polymer and Graphite Nanoparticles. *Angew. Chem. Int. Ed.* **41**, 4016-4019 (2002)

52. Jang, B.J., Oh, J.H. Fabrication of a Highly Transparent Conductive Thin Film from Polypyrrole/Poly(methyl methacrylate) Core/Shell Nanospheres. *Adv. Funct. Meter.* **15**, 494-502 (2005)

53. Rivas, L., Cortes, S.S., Ramos, J.V.G., Morcillo, G. Growth of Silver Colloidal Particles Obtained by Citrate Reduction To Increase the Raman Enhancement Factor. *Langmuir* **17,** 574-577 (2001)

54. Konwer, S., Pokhrel, B., Dolui, S.K. Synthesis and characterization of polyaniline/graphite composites and study of their electrical and electrochemical properties. *J. Appl. Polym. Sci.* **116**, 1138-1145 (2010)

55. Liu, J., Wan, M. Synthesis, characterization and electrical properties of microtubules of polypyrrole synthesized by a template-free method. *J. Mater. Chem.* **11**, 404 -408 (2001)

56. Leeuw, D.M., Simenon, M.J., Brown, A.R., Einerhand, R.E.F. Stability of n-type doped conducting polymers and consequences for polymeric microelectronic devices. *Synth. Met.* **87**, 53-59 (1997)

57. Bhadra, S., Singha, N.K., Khastgir, D. Electrochemical synthesis of polyaniline and its comparison with chemically synthesized polyaniline. *J Appl. Polym. Sci.* **104**, 1900-1904 (2007)

58. Vishnuvardhan, T.K., Kulkarni, V.R., Basavaraja, C., Raghavendra, S.C. Synthesis, characterization and a.c. conductivity of polypyrrole/Y_2O_3 composites. *Bull. Mater. Sci.* **29**, 77-85 (2006)

59. Calixto, C.M.F., Mendes, R.K., Oliveira, A.C., Ramos, L.A., Cervini, P. Cavalheiro, E.T.G. Development of graphite-polymer composites as electrode materials. *Materials Research* **10**, 109-114 (2007)

60. Dey, A., De, S. Characterization and dielectric properties of polyaniline–TiO_2 nanocomposites. *Nanotechnology* **15**, 1277 (2004)

61. Pavia, D.L., Lampman, G.M., Kriz, G.S. *Introduction to spectroscopy* (Thomson Brooks/Cole, 2000)

62. Chandrasekhar, P. *Conducting Polymers, Fundamentals and Applications: A Practical Approach* (Kulwer Academic Publishers, London, 1999)

63. Ameer, Q., Adeloju, S.B. Polypyrrole-based electronic noses for environmental and industrial analysis. *Sens. & Actu. B.* **106,** 541-552 (2005)

64. Ramanathan, K. *etal.* Bioaffinity Sensing Using Biologically Functionalized Conducting-Polymer Nanowire. *J. Am. Chem. Soc.* **127,** 496-497 (2005)

65. Yan, H., Zhang, L., Shen, J., Chen, Z., Shi G., Zhang, B. Synthesis, property and field-emission behaviour of amorphous polypyrrole nanowires. *Nanotechnology* **17,** 3446-3450 (2006)

66. Penza, M., Milella, E., Alba, M.B., Quirini, A., Vasanelli, L. Selective NH_3 gas sensor based on Langmuir-Blodgett polypyrrole film. *Sens. & Actu. B.* **40**, 205-209 (1997)

67. Sharma, S., Nirkhe, C., Pethkar, S., Athawale, A.A. Chloroform vapour sensor based on copper/polyaniline nanocomposite. *Sensors and Actuators B: Chemical* **85**, 131-136 (2002)

68. Jun, H.K., Hoh, Y.S., Lee, B.S., Lee, S.T., Lim, J., Lee, D.D., Huh, J.S. Electrical properties of polypyrrole gas sensors fabricated under various pretreatment conditions. *Sens.& Actu. B* **96**, 576-581 (2003)

69. Arora, K. *etal.* Application of electrochemically prepared polypyrrole–polyvinyl sulphonate films to DNA biosensor . *Biosens. Bioelectro.* **21**, 1777-1783 (2006)

70. Tai, H., Jiang, Y., Xie G., Yu, J., Zhao, M. Self-assembly of TiO_2/polypyrrole nanocomposite ultrathin films and application for an NH_3 gas sensor. *Int. J. Environ. Anal. Chem.* **87,** 539-551 (2007)

CHAPTER 4

Development of core-shell nano composite of poly (styrene-co-methyl acrylate) and bentonite clay by ultra sonic assisted miniemulsion polymerization

Chapter 4

4.1 Introduction

Polymers in their pristine form do not have good mechanical strength, thermal strength, load bearing capacity, gas barrier property etc. So they are often mixed with some fillers such as clay, metal particles etc. to improve the above mentioned properties. The resulting materials are called composite materials[1-5]. In recent time scientists have given importance in developing polymer nanocomposites which consist of a polymeric material (e.g. thermoplastics, thermosets or elastomers) and a reinforcing material (nanoparticle). The nanoparticles have at least one dimension in nanometer scale. Polymer nanocomposites show major improvements in mechanical properties, gas barrier properties, thermal stability, fire retardancy and other areas[6-12]. Amongst various nanocomposites, polymer/clay nanocomposites are of great interest during a last decade due to the enhancement of mechanical and thermal properties as compared to the homopolymer or other fillers[13-17]. The nano clays are made up of two-dimensional nano scale layers of an alumina octahedral sheet, sandwiched between two silica tetrahedron sheets. They are held together by van der Waals and weak ionic forces and are capable of being partially or completely intercalated and exfoliated[18]. The nanoclays exhibit large aspect ratio and hence can be potentially applied in barrier coatings, in food packaging, in agricultural and pharmaceutical industries etc[19-21]. Various techniques are employed for the preparation of polymer/clay nanocomposites. Vaia et al.[22,23] prepared PS/clay nanocomposite by melt method to intercalate polymer in layered silicates. Doh, Lous, Fu etc. [24-28] reported the synthesis of polymer clay nanocomposites by bulk polymerization technique.

A part of this chapter is published in

* **L.J.Borthakur**, D.Das, S.K.Dolui. *Materials Chemistry and Physics*, **124** , 1182–1187 (2010)

Bottcher et al.[29] reported the use of solution polymerization technique for this purpose. Many researchers employed emulsion,[30-35] suspension,[36] and living free radical[29] polymerization techniques for development of polymer/clay nanocomposites. Mahdavian et al.[6] reported core-shell nanocomposite of poly(styrene-co-butyl acrylate)/Cloisite 30B and poly(styrene-methyl methacrylate)/Al_2O_3 by miniemulsion polymerization technique.

Miniemulsion polymerization, a branch of conventional emulsion uses a material called costabilizer (water-insoluble, monomer soluble) which provides the conditions needed for the encapsulation of a layered clay[37]. This is performed by reducing the diffusional degradation (Ostwald ripening) of a monomer/water emulsion as well as diminishing the monomer droplet size to within a range of 50-500 nm via applying high shear and the monomer droplets become the primary loci for particle nucleation. The polymerization of such miniemulsions extends the possibilities of widely applied emulsion polymerization and provides advantages with respect to incorporation of hydrophobic compounds and composition of the oil phase[38]. Another advantage of this technique is that it uses no volatile organic solvents and hence is environmentally benign.

On the other hand, ultrasonic cavitations can generate local high temperature and high pressure and a very rigorous environment for chemical reaction[39]. Under these rigorous conditions, radicals can be generated due to the decomposition of water, monomer, surfactant or rupture of polymer chains to initiate the polymerization of monomer. It is obvious that clay and nanoclay exfoliation lies in the synergistic effect of chemical and mechanical interactions. Under strong mechanical force of ultrasonication, the polymer particles tend to stick to the organoclay surface, forming clay polymer microaggregates that could be stabilized by adding surfactant or dispersing agents. By further applying mechanical force to the system, although it is in a water dispersion form, the polymer molecules could be enforced to diffuse into the basal spacing of the nanoclay and thus resulting in an exfoliated nanocomposite suspension

Although many literature are found on the polymer/clay nanocomposites only a few deals with the development of core-shell morphology[6-8]. To date and to the best of our knowledge, no report exists that describes the encapsulation and

thereafter, exfoliation of bentonite inside copolymer particles to give core-shell nanocomposites . In this chapter we report the synthesis of core-shell nanocomposite particles of SMA as the shell and organically modified bentonite as the core by miniemulsion polymerization under ultrasonic irradiation. The affecting factors were also examined in detail by using Infra red spectroscopy (FT-IR), X-ray diffraction (XRD), Scanning electron microscopy (SEM), Transmission electron microscopy (TEM) etc. Thermo gravimetric analysis (TGA) reveals that there is a significant enhancement of thermal stability of the newly synthesised nanocomposite particles as compared to the pristine copolymer. These nanocomposites may find potential applications such as barrier coatings in areas like food packaging, agricultural, pharmaceutical industries etc.

4.2 Experimental

4.2.1 Materials

The monomers styrene (Sty) and methyl acrylate (MA) were received from Aldrich and washed with 5% NaOH and then with distilled water to remove the inhibitors. The organoclay bentonite is a commercially available natural montmorillonite modified with an organic modifier named octadecyl amine. It was purchased from Aldrich and was used as received. The surfactant Sodium dodecyl benzene sulphonate (SDBS), Span 60 and the co-surfactant hexadecane (HD) were received from Merck chemicals and were used with no further purification. The initiator $K_2S_2O_8$ was of analytical grade and recrystallized before use. For all purposes doubled distilled water was used. All the reactions were carried out under nitrogen atmosphere.

4.2.2 Effect of surfactant on the exfoliation of bentonite

Bentonite is a natural montmorillonite modified with octadecyl amine (d_{00}=2.01 nm). To get good dispersion in the organic phase[39] a series of experiment (S-20, S-40, S-60, S-80) were performed using a series of Span surfactant (20, 40, 60, 80). In all the experiments a phase containing bentonite (0.5g), water (50 g), Span (0.15g) and SDBS (0.1g) was sonicated for 2 h and then magnetically stirred for 24 h. Then the mixture

was dried in vacuum oven at 60^0 C for 24 h. Then the samples were grinned to powder and XRD analysis was performed.

4.2.3 Miniemulsion polymerization of poly (styrene-co-methyl acrylate)

10 g Styrene (sty), 5 g methyl acrylate (MA), 75 g water, 0.15 g Span 60, 0.15 g SDBS and 0.15 g hexadecane were taken in a 100 mL beaker and stirred magnetically for 1h at room temperature. It was cooled to 0°C and then subjected to ultrasonic agitation for 30 min. The miniemulsion thus obtained had solid contents of 15% and was used for further polymerization using $K_2S_2O_8$ (0.14 g) initiator at 70°C for 7 h. Polymerization was carried out in a four necked round bottom glass reactor equipped with a condenser, a mechanical stirrer, a thermometer and a nitrogen inlet.

4.2.4 Miniemulsion polymerization of poly (styrene-co-methyl acrylate) in presence of bentonite

A typical recipe for the formation of miniemulsion is given in **Table 4.1**. Bentonite, styrene (Sty) and methyl acrylate (MA) were taken in a 100 mL beaker and stirred magnetically for 1h at room temperature. It was cooled to 0°C and then sonicated for 30 min. (Phase I). Meanwhile, the aqueous phase (II) was prepared by mixing 75 g water, 0.15 g span 60, 0.15 g SDBS and 0.15 g hexadecane under simple stirring at room temperature for 30 min.

Phase I and Phase II were mixed under vigorous magnetic stirring for 30 min. Then the mixture was homogenized by sonicating for 15 min. This miniemulsion was used for subsequent polymerization.

Table 4.1 Typical recipe for the miniemulsion polymerization of poly (styrene-co-methyl acrylate)-bentonite nanocomposite latex particles

Ingredients (in g)	Sample				
	Blank	NC(0.2)	NC(0.5)	NC(1)	NC(2)
Styrene	10	10	10	10	10
Methyl acrylate	5	5	5	5	5
Bentonite	0	0.03	0.075	0.15	0.3
Water	75	75	75	75	75
Span-60	0.15	0.15	0.15	0.15	0.15
SDBS	0.15	0.15	0.15	0.15	0.15
Hexadecane	0.15	0.15	0.15	0.15	0.15
$K_2S_2O_8$	0.14	0.14	0.14	0.14	0.14

4.2.5 Polymerization

Polymerization was carried out in a four necked round bottom glass reactor equipped with a condenser, a mechanical stirrer, a thermometer and a nitrogen inlet. The formerly prepared miniemulsion was transferred to this reactor and subsequently degassed by N_2 at room temperature for 30 min. When temperature of the system reaches 70^0 C, 0.14g of $K_2S_2O_8$ (1% of the monomer) was added to initiate polymerization. The polymerization was conducted at this temperature for 7 h under continuous mechanical stirring. The reaction was terminated by adding 1 mL of 1% hydroquinone solution into the latex sample. When the reactor reaches room temperature the concentrated milky miniemulsion latex was collected and filtered to remove any coagulum present. A series of nanocomposite particles were prepared by incorporating different percentage (with respect to the total monomer content) of clay in the miniemulsion.

4.3 Characterization

4.3.1 Fourier transform infrared spectroscopy (FT-IR)

The FT-IR spectra of the nanocomposite particles were recorded on a Nicolet Impact-410 IR spectrometer (USA) in KBr medium at room temperature in the region 4000-450 cm^{-1}. For preparing nanocomposite spectra the latex was coagulated with methanol. Then, the coagulum was separated from the aqueous phase and washed with distilled water in order to separate the non-encapsulated clay or adsorbed ones. The coagulated polymer was dried at 60°C in an oven overnight for taking FT-IR spectrum

4.3.2 X-ray diffraction (XRD)

Powder XRD data were collected on a Rigaku Miniflex X-ray diffractometer (Tokyo, Japan) with Cu Kα radiation (λ= 0.15418 nm) at 30 kV and 15 mA with a scanning rate of 0.05^0/s in a 2θ range from 2^0 to 12^0. For XRD analysis the latex was coagulated with methanol. Then, the coagulum was separated from the aqueous phase and washed with distilled water in order to separate the non-encapsulated clay or adsorbed ones. The coagulated polymer was dried at 60°C in a vacuum oven overnight.

4.3.3 Scanning Electron Microscopy (SEM)

The scanning electron microscope (SEM) is a type of electron microscope that images the sample surface by scanning it with a high energy beam of electrons in a raster scan pattern. The electrons interact with the atoms that make up the sample producing signals that contain information about the sample's surface topography, composition and other properties such as electrical conductivity.

The surface topography of the particles was studied with a Jeol-JSM-6390L V Scanning Electron Microscope. For the analysis latex samples were sputter coated with platinum of thickness of $200A^0$.

4. 3.4 Transmission Electron Microscopy (TEM)

For the TEM analysis a Philips EM 400 at an acceleration voltage of 100 kV was used. All images were taken at a magnification of 60000 or 120000. Latex samples were cleaned by using a filtration unit (Advantec MFS Inc. type UPH-76) to remove all water soluble oligomers from the emulsion. All latex samples were diluted to 3% solids and washed with distilled water in the filtration cell using a polycarbonate nuclepore membrane with a pore size of 0.1 micron.

The diluted latex was treated with 2wt% aqueous solution of uranyl acetate (UAc). One drop of diluted sample was placed onto copper (Cu) grid and allowed to dry. For potential staining of the shell phase by RuO_4, the sample was then exposed to RuO_4 vapour. The RuO_4 vapour was generated by the reaction of Ruthenium (III) chloride hydrate and sodium hyperchloride solution. All the samples were dried at 30^0 C for 24 h before TEM measurements.

4.3.5 Thermo Gravimetric Analysis (TGA)

Thermal analysis was done in a Shimadzu TA-60 thermo gravimetric analyser. A pre weighted amount of the latex was loaded in a platinum pan and heating was done under nitrogen atmosphere at a heating rate of 10^0C/min in the range of 30^0 C - 700^0 C.

4.4 Results and Discussion

4.4.1 Effect of surfactant

The exfoliation of clay is normally performed in a non-ionic-ionic surfactant mixture[40]. A mixture of SDBS and span 60 were used to investigate the extent of exfoliation of the bentonite clay. The bentonite nanoclay has d-spacing of 2.01 nm. the d-spacing of the nanoclay decreases to 1.72 nm with span 80. The results are given in **Table 4.2**. The decrease in d-spacing may be attributed to the fact that SDBS have the ability to extract the organic modifier from the clay surface in presence of water and Span surfactant due to its cation exchange ability. From the result it was seen that the decrease in d-spacing of bentonite is almost similar in presence of all the surfactants (span 20, span 40 and span 60) except span 80 (**Table**

4.2). On the basis of this result we chose span-60 for the synthesis of the nanocomposite.

Table 4.2: Calculated d-spacing of the samples measured by XRD in the presence of span series

Sl. No.	Sample	Surfactant	d-spacing (nm)
1	S-0	No Surfactant	2.01
2	S-20	Span 20	1.79
3	S-40	Span 40	1.78
4	S-60	Span 60	1.77
5	S-80	Span 80	1.72

4.4.2 Polymerization

A schematic representation of the overall polymerization is given in **Fig 4.1**. While preparing phase I bentonite was dispersed within the monomer mixture with the aid of sonication. The monomers are absorbed by the pore/layers of bentonite and the monomers form a layer over the clay. Subsequently the monomer covered clay particles were dispersed in water in presence of span 60 and SDBS. The dispersion is stabilized by the non-ionic- ionic (span 60-SDBS) surfactant mixture. This dispersion was subjected to sonication to initiate polymerization. Ultrasonic irradiation generates high temperature and pressure within the cavity and under this rigorous condition polymerization is initiated. In the meantime, presence of the surfactant mixture causes the exfoliation of the clay layers. Polymerization was carried out in presence of $K_2S_2O_8$ initiator at 70°C. The polymer phase forms a nearly uniform layer over the exfoliated layers of the bentonite particles. The newly synthesised nanocomposite particles are spindle shaped where as the pristine polymer particles have uniform spherical structure which is completely distorted in case of the nanocomposite particles. Since the nanoclay has a sheet like structure, its presence in the core phase distorts the spherical structure of the nanocomposite particles. This confirms the formation of nanocomposite particles with core-shell morphology.

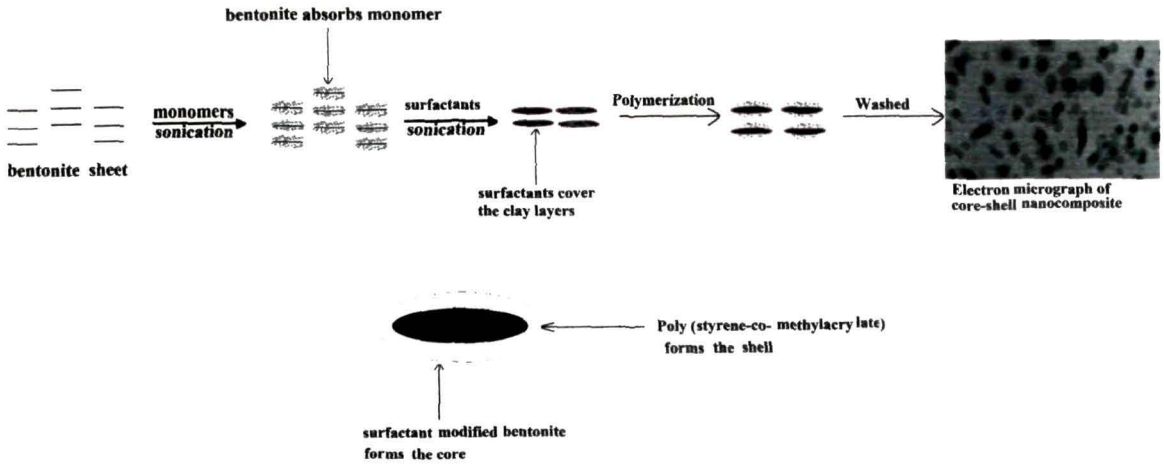

Fig 4.1: Schematic representation of the polymerization

4.4.3 FT-IR Spectroscopy

The poly (styrene-co-methyl acrylate)-bentonite nanocomposite particles prepared via miniemulsion polymerization were characterized by FT-IR analysis primarily. **Fig 4.2** shows the FT-IR spectra of the pristine polymer (**Fig 4.2 a**), poly (styrene-co-methyl acrylate)–bentonite nanocomposite (**Fig 4.2 b**) and bentonite (Fig 1c) respectively. In **Fig. 4.2 c**, the peak at 3,438 cm^{-1} corresponds to -OH stretching of silicate layers. The sharp peak centred at 1,045 cm^{-1} is related to the Si–O stretching vibration of silicate layer too. The peaks at 525 and 461 cm^{-1} are due to the stretching of Al–O and bending of Si–O, respectively. Fig 4.2b clearly demonstrates the existence of bentonite major absorbance peaks in poly (styrene-co-methyl acrylate) spectrum which proves the existence of clay inside the dried latex particles and indicative of encapsulation of bentonite inside the final nanocomposite particles. However, the peak at 3,438 cm^{-1} shifts to 3520 cm^{-1} in the nanocomposite. The shifting of the bentonite peak may be attributed to the interaction of the silicate layer of bentonite with the polymer surface. Thus from IR study we may infer that bentonite is successfully incorporated in the polymer matrix.

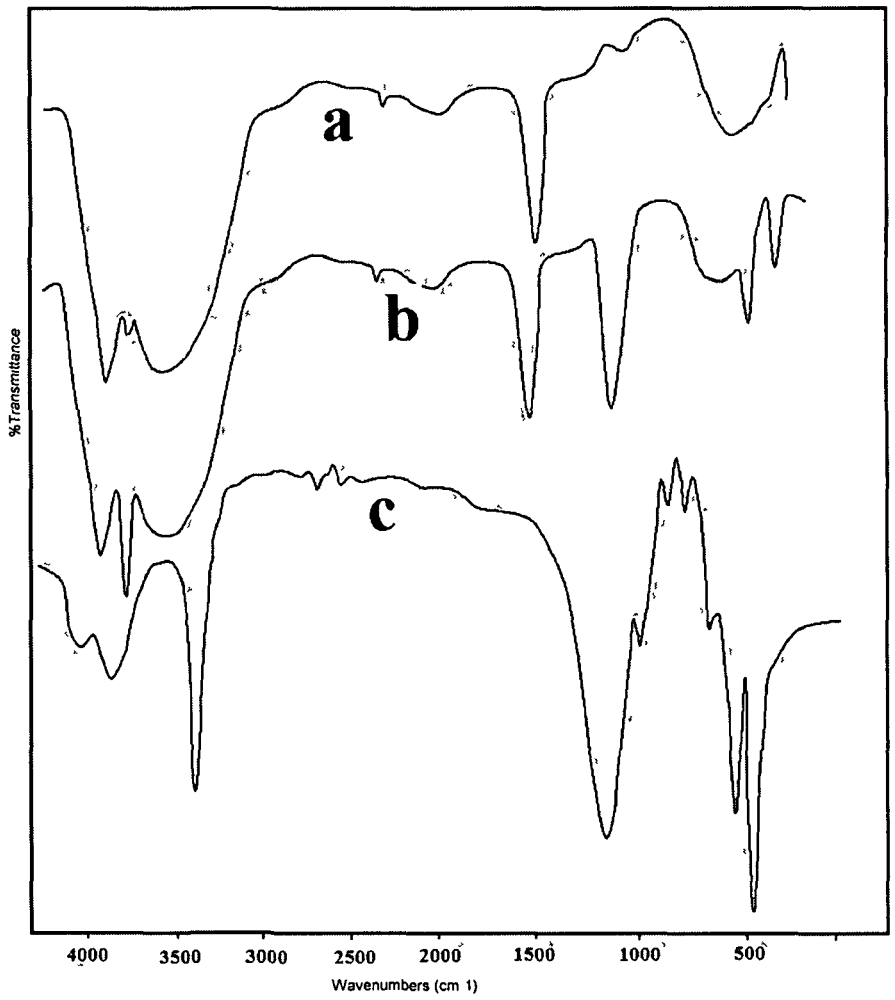

Fig 4.2 IR spectra of a)Polymer b) Nanocomposite c) Bentonite

4.4.4 XRD analysis

The exfoliated nature of the nanocomposite particles was investigated by XRD analysis. **Fig 4.3** shows the XRD pattern of pristine bentonite and the final poly (styrene-co-methyl acrylate)-bentonite nanocomposite particles. Bentonite has an interlayer spacing of 2.01 nm at 2θ ca. 4.4° calculated from Bragg equation (d_{001} is the interplanar distance of (001) reflection plane). In the nanocomposite with 1% and 2% clay dosing (**Fig 4.3 d-e**) the peak at 4.4° shifts to 2.2° which is an indication of partial exfoliation. For the nanocomposite with 0.5% clay dosing this peak almost disappears implying almost 100% exfoliation. This implies that lower percentage of clay in the polymer matrix results exfoliated nanocomposite. SDBS has high anionic charge density and hence the ability to enter into the basal surfaces of bentonite by

formation of ionic networks with the modifier segment. It will increase the hydrophobicity of intergalleries due to the presence of long alkyl chain in SDBS. This is the key factor for intercalation of clay, which helps in the exfoliation process through insertion of monomer molecules and subsequent polymerization. Moreover SDBS absorbs the -OH group on the edges of the clay platelets which decreases the hydrophobicity of the clay particles. These results enhance colloidal stability as well as increase the exfoliation of the clay platelets. The high shear through ultrasonic irradiation also helps in exfoliation. Thus SDBS helps in entering the co-monomers within the layer and they widen up the gap between the layers. The polar carboxyl groups of the methyl acrylate interact with the polar groups in the intergalleries. This interaction further helps in the continuous entry of the bulky styrene monomers in the intergalleries and compels the clay layers to undergo exfoliation.

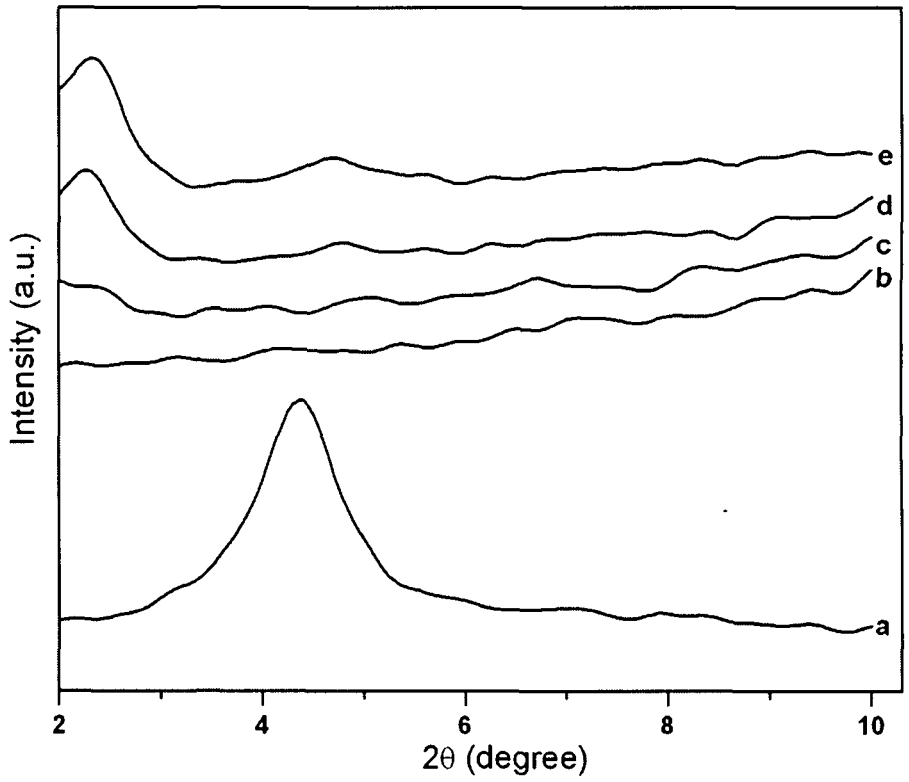

Fig 4.3: XRD analysis of a) Bentonite b) poly (styrene-co- methyl acrylate) c) nanocomposite with 0.5% nanoclay d) nanocomposite 1% nanoclay e) nanocomposite with 2% nanoclay

4.4.5 Scanning Electron Microscopy (SEM)

The SEM micrographs of the composite particles are given in the **Fig 4.4** and **Fig 4.5**. From the Figure it can be seen that the particles are nearly mono dispersed and have smooth surface without any attached or adsorbed clay on the particles' surface. The polymer particles have average diameter of about 200 nm and the composite particles are of about 500 nm in size. The observed increase in particle diameter of the nanocomposite particles could be a further evidence of an effective encapsulation of clay through polymerization reaction.

4.4.6 Transmission Electron Microscopy (TEM)

For further investigation of morphology of the obtained nanocomposite particles and verifying exfoliation of bentonite, TEM micrographs were taken by dropping diluted latex on TEM copper grids. **Fig 4.6** represents the TEM image of the poly (styrene-co-methyl acrylate) particles and **Fig 4.7** represents the TEM images of the nanocomposite particles. The polymer particles have diameter in the range of 200 nm and the composite particles have diameter in the range of 450 nm. From the micrographs it may be seen that the spherical nature of the polymer particles is lost in the composites structure. In the composites polymer phase forms a layer over the bentonite particles. Bentonite has a sheet like structure and its presence in the core distorts the spherical nature of the particles. Moreover, these micrographs are indicative of exfoliation (stretched and separated lines) of bentonite platelets, which were uniformly dispersed inside the final synthesized latex particles via miniemulsion polymerization. No clay armoured latex particle was observed.

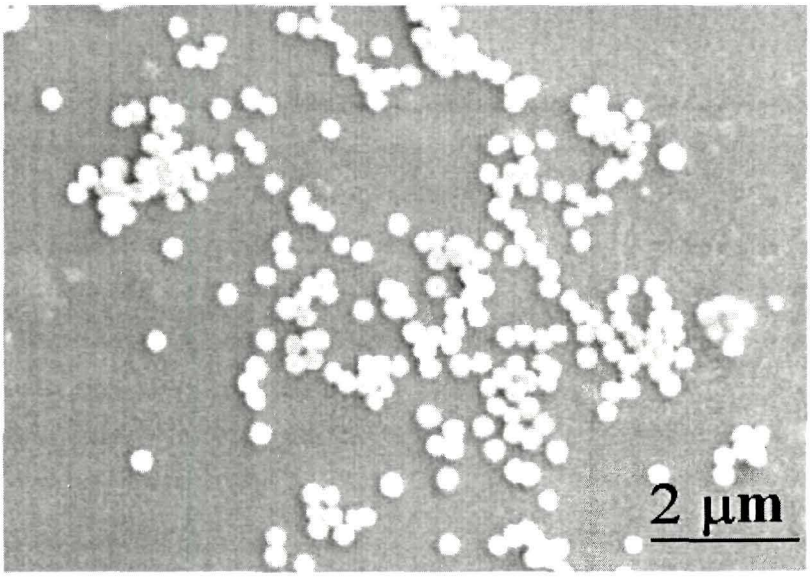

Fig 4.4: SEM micrograph of a) poly (styrene-co-methyl acrylate)

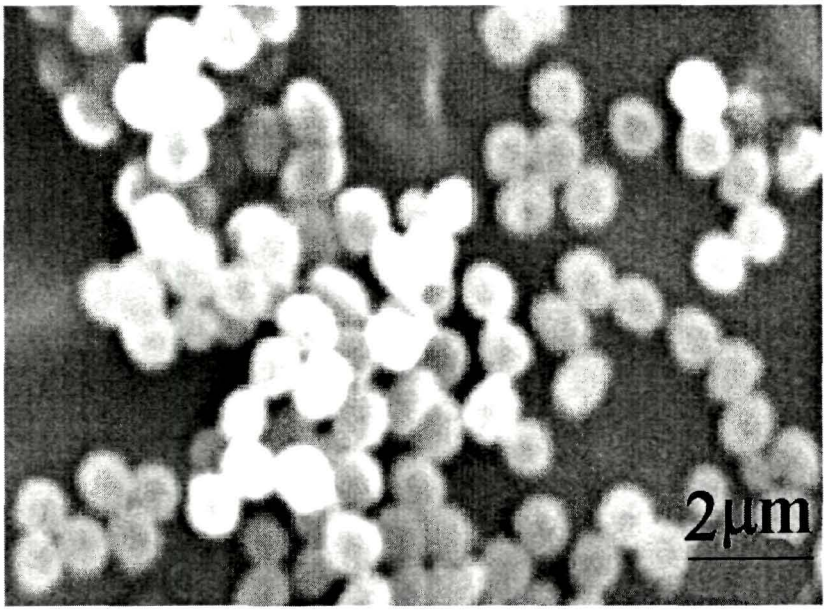

Fig 4.5: SEM micrograph of poly (styrene-co-methyl acrylate)–bentonite nanocomposite

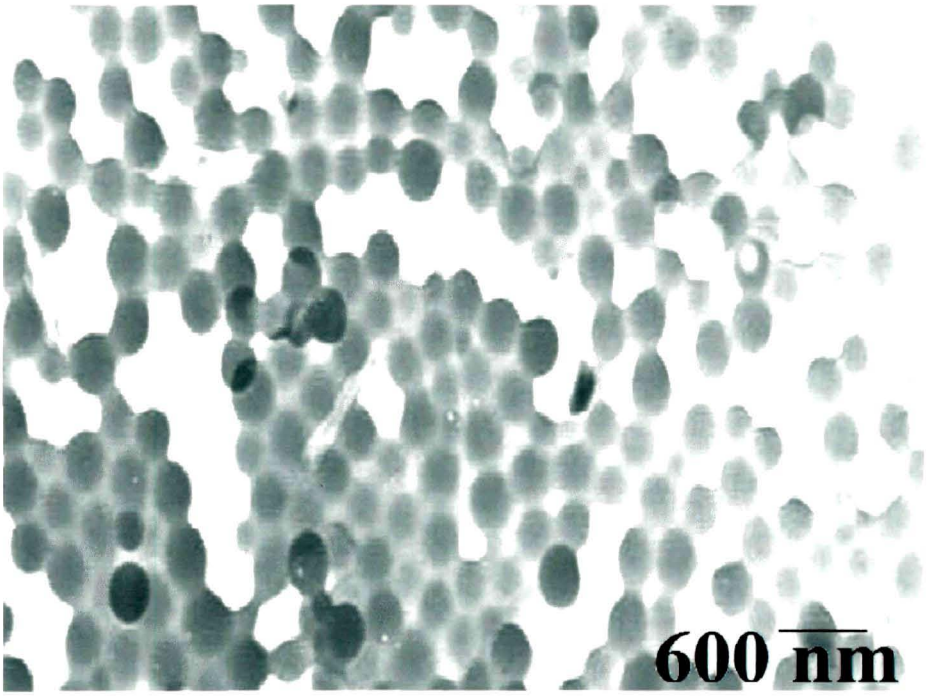

Fig 4.6: TEM micrograph of poly (styrene-co-methyl acrylate)

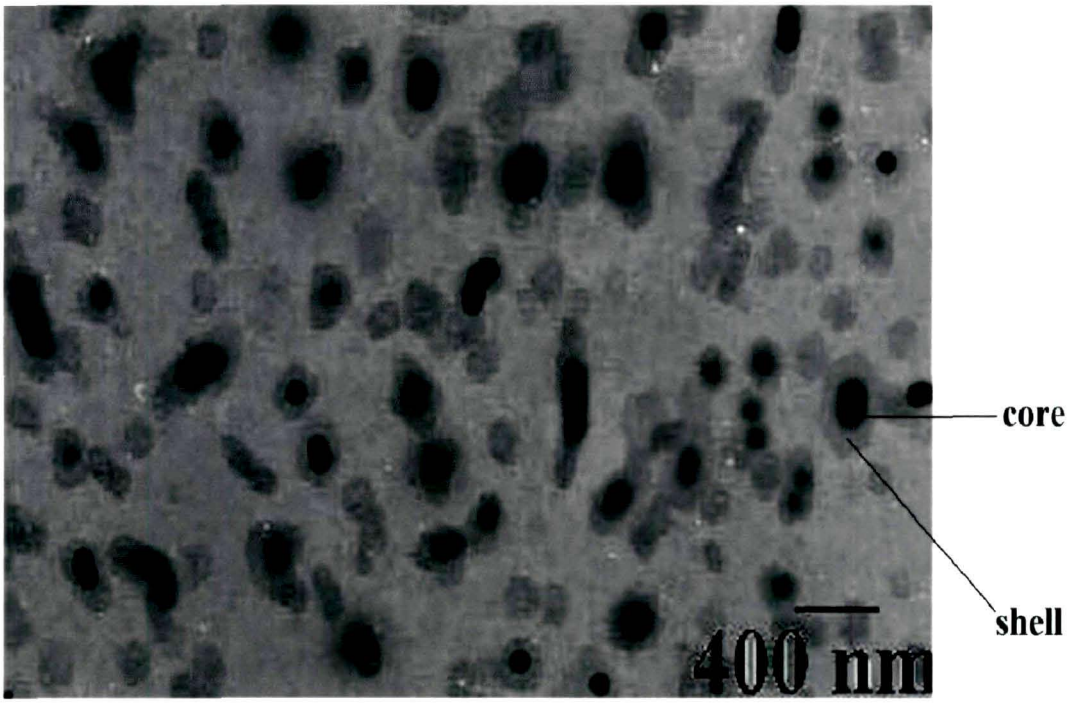

Fig 4.7: TEM micrograph poly (styrene-co-methyl acrylate) – bentonite nanocomposite

4.4.7 Thermo Gravimetric Analysis (TGA)

The TGA curves of the nanocomposite particles are shown in the **Fig 4.8**. The onset of decomposition of the polymer is nearly 340^0 C (point (i) **of Fig 4.8**) in the which increases up to nearly 380^0 C (point (ii) of **Fig 4.8**) for the nanocomposite particles with 2% dosing of clay (**Fig 4.8 d**). That is with 2% clay dosing there is approximately a 40^0 C rise of onset temperature. Thus it may be inferred that the nanocomposite particles exhibit better thermal stability than the pristine polymer. The increase in thermal stability may be due to the dispersal of the layer structure (bentonite) in the polymer chain. The layered structure of the clay can stop heat transfer between areas and also strengthen the polymer chain to avoid heat degradation.

4.4.8 Determination of Bentonite Content

TGA thermograms were used to determine the amount of bentonite encapsulated in the copolymer. For providing samples latex were coagulated with methanol, filtered off and washed with plenty of distilled water to remove the adsorbed surfactant and methanol. Then the samples were vacuum dried at 60^0C for an overnight. This procedure has the advantage of separation of freely dispersed bentonite in the latex from the encapsulated ones. So, the residual weight percent after disappearance of the organic polymer at 650^0C could be considered as the encapsulated bentonite nanoparticles. The results are given in **Table 4.3**. It may be observed that the percentage of encapsulation of clay in the polymer phase is satisfactory in all the cases. (90% to 95%)

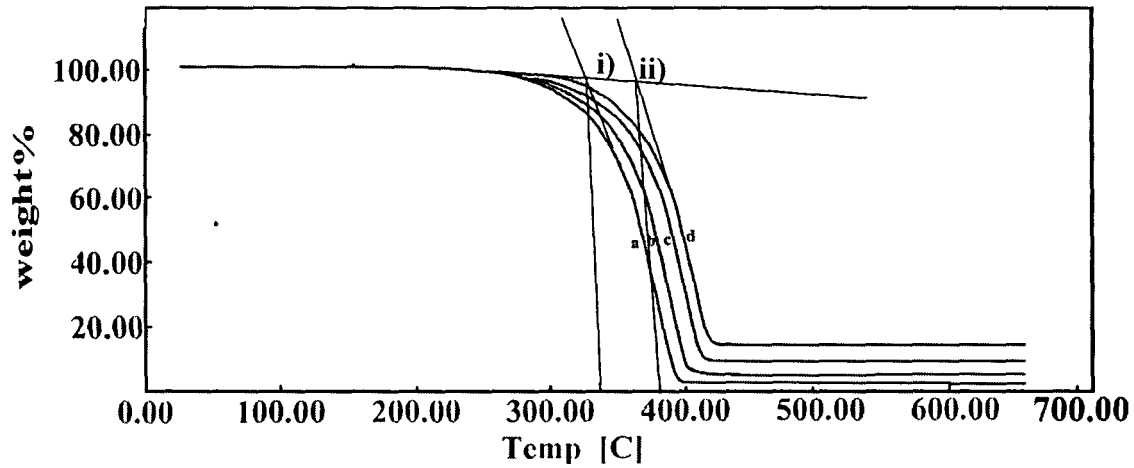

Fig 4.8: TGA curves of a) poly(styrene-co-methyl acrylate) b) nanocomposite with 0.5% clay c) nanocomposite with 1% clay d) nanocomposite with 2% clay

Table 4.3: Thermal Analysis for determination of encapsulated nanoclay

Sl. No	Sample	Added Nanoclay (wt%[a])	Residue(wt%[b])	Obtained Nanoclay (wt%[c])	Encapsulation Efficiency	Decomposition temperature(^{0}C)
1	Blank	0	4	0	0	340
2	NC(0.2)	0.2	4.19	0.19	95	352
3	NC(0.5)	0.5	4.47	0.47	94	358
4	NC(1)	1	4.92	0.92	92	362
5	NC(2)	2	5.8	1.8	90	380

Note: NC(x)-nanocomposite with different % of clay dosing, e.g. NC(0.2)-nanocomposite with 0.2% clay dosing.

[a] Weight percent relative to the total amount of monomers.

[b] Weight percent obtained at 650 °C from TGA.

[c] Relative to the added nanoclay

4.4.9 Stability of the nanocomposites emulsion

The emulsions of the nanocomposites are quite stable. **Fig 4.9** shows the stability of the nanocomposite emulsion. The emulsions of the nanocomposite particles were kept in air tight bottles and the stability of the emulsions were monitored from time to time. It was found that the nanocomposite emulsions are quite stable up to 90 days. The high environmental stability implies that the nanocomposites may find many suitable end on applications.

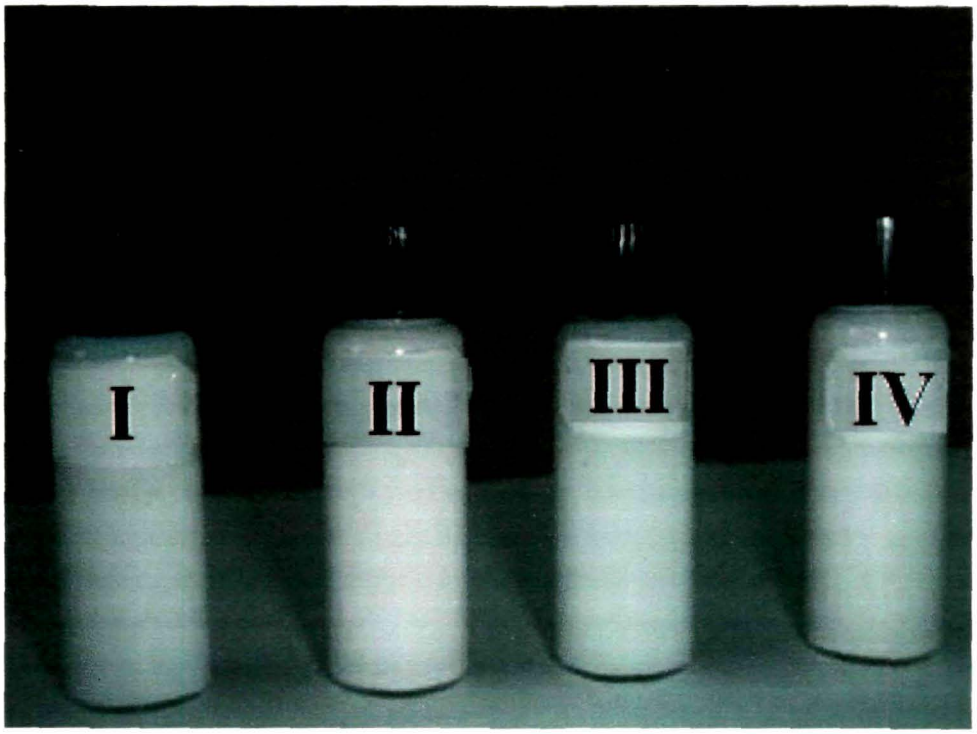

Fig 4.9: Stability of the nanocomposite 15 days (NCI), 30 days (NCII), 60 days (NCIII), 90 days (NCIV)

4.4.10 Transparency of the film

Retention of transparency is a characteristic of nanocomposite particles. To check the transparency of the synthesised nanocomposite films of the polymer and the nanocompsoite were drawn. Letters (A for nanocomposite and B for polymer) were written on both side of the films.(**Fig 4.10**) From the Figure it may be seen that the transparency of the polymer retains in the nanocomposite too. Retention of transparency implies exfoliation of clay inside the polymer phase and that there is no pristine or aggregate of the clay in the corresponding film.

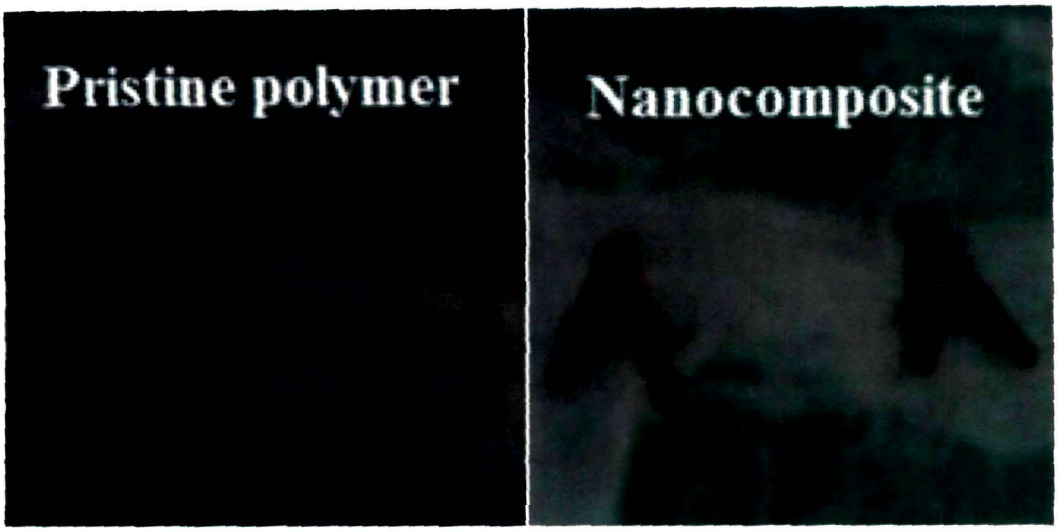

Figure 4.10: Films of poly (styrene-co-methyl acrylate) and nanocomposite with 2% clay dosing showing retention of transparency

4.5 Conclusion

- Nanocomposite particles of poly (styrene-co-methyl acrylate)-bentonite (organo clay) were prepared by miniemulsion polymerization process. Ultrasonic irradiation generates high temperature and pressure within the cavity and under this rigorous condition polymerization is initiated.
- SDBS interacts with the cationic modifier of the clay and enter into the intergalleries of the clay. This makes these spaces more organophilic and helps the entry of the comonomers within the galleries for exfoliation and results in further expansion of the clay galleries to accommodate the polymer chains. SDBS can strongly adsorb onto the OH groups on the edges of clay platelets, which influence not only the colloidal stability but also exfoliation of the platelets by decreasing clay hydrophilicity.
- The nanocomposite particles are spherical in shape and have the average diameter of 450 nm. TEM analysis shows that the clay particles undergo full exfoliation within the polymer matrix.
- Thermal analysis confirms that the newly prepared nanocomposite particles are sufficiently thermal stable than the pristine polymer. So, these newly prepared nanocomposite particles can have improved potential application such as barrier properties etc.

References

1. Zhang, K., Park, B.J., Fang, F.F., Choi, H. J. Sonochemical Preparation of Polymer Nanocomposites. *Molecules* **14,** 2095-2110 (2009)
2. Tong, Z., Deng, Y. Synthesis of polystyrene encapsulated nanosaponite composite latex via miniemulsion polymerization. *Polymer* **48**, 4337-4343 (2007)
3. Utracki, L.A., Sepehr, M., Boccaleri, E. Synthetic, layered nanoparticles for polymeric nanocomposites (PNCs). *Polym. Adv. Technol.* **18,** 1-37 (2007)
4. Lyons, J.G., Holehonnur, H. The incorporation of an organically modified layered silicate in monolithic polymeric matrices produced using hot melt extrusion. *Materials Chemistry and Physics* **103**, 419-426 (2007)
5. Diaconu, G., Asua, J.M., Paulis, M., Leiza, J.R. High solids content waterborne polymer-clay nanocomposites. *Macromol. Symp.* **259,** 305-317 (2007)
6. Mahdavian, A.R., Sehri, Y., Mobarakeh, H.S. Nanocomposite Particles with Core- Shell Morphology. I. An Investigation into the Affecting Parameters on Preparation of Fe_3O_4- Poly (butylacrylate- styrene) Particles via Miniemulsion Polymerization. *European Polymer Journal* **44,** 2482-2488 (2008)
7. Mirzataheri, M., Mahdavian, A.R., Atai, M. Nanocomposite particles with core-shell morphology IV: an efficient approach to the encapsulation of Cloisite 30B by poly (styrene-*co*-butyl acrylate) and preparation of its nanocomposite latex via miniemulsion polymerization. *Colloid Polym. Sci.* **287,** 725-732 (2009)
8. Mahdavian, R., Sarrafi, Y., Shabankareh, M. Nanocomposite particles with core–shell morphology III: preparation and characterization of nano Al_2O_3–poly (styrene–methyl methacrylate) particles via miniemulsion polymerization. *Polym. Bull.* **63,** 329-340 (2009)
9. Yao, X.F., Zhou, D., Yeh, H.Y. Macro/microscopic fracture characterizations of SiO_2/epoxy nanocomposites. *Aerospace Science and Technology* **12**, 223-230 (2008)

10. Hu, J., Chen, M., Wu, L. Organic-inorganic nanocomposites synthesized *via* miniemulsion polymerization. *Polym. Chem.* **2,** 760-772 (2011)
11. Jung, H. M. Preparation of poly (vinyl acetate)/clay and poly (vinyl acetate)/poly (vinyl alcohol)/clay microspheres. *Fibers and Polymers* **7,** 229-234 (2006) .
12. Gupta, R.K., Bhattacharya, S.N. Polymer-clay Nanocomposites: Current Status and Challenges. *Indian Chemical Engineer* **50**, 242-267 (2008)
13. Landfester, K., Bechthold, N., Tiarks, F., Antonietti, M. Formulation and Stability Mechanisms of Polymerizable Miniemulsions. *Macromolecules* **32**, 5222-5228 (1999)
14. Li, C.Y., Chen, C.H., Yeh, A.I., Lai, V.M.F. Preliminary study on the degradation kinetics of agarose and carrageenans by ultrasound. *Food Hydrocolloids* **13**, 477-481 (1999)
15. Jeon, H.S., Rameshwaram, J.K., Kim, G. Structure-property relationships in exfoliated polyisoprene/clay nanocomposites. *J. Polym. Sci. Part B: Polym Phys.* **42**, 1000-1009 (2004)
16. Lee, J.Y., Lee, H.K. Characterization of organobentonite used for polymer nanocomposites. *Materials Chemistry and Physics* **85,** 410-415 (2004)
17. Okamoto, M., Nam, P. H., Maiti, P., Kotoka, T., Hasegawa, N., Usuki, A. A Hope of Cards in Polypropylene/Clay Nanocomposites under Elongation flow. *Nano Letters* **1**, 295-298 (2001)
18. Orolinova, Z., Mockovciakova, A. Structural study of bentonite/iron oxide composites. *Materials Chemistry and Physics* **114,** 956-961 (2009)
19. Pinnavaia, T.J., Beall, G.W. *Polymer-clay nanocomposites* (Wiley, New York, 2001)
20. Gopakumar, T.G., Page, D.J.Y.S. Compounding of nanocomposites by thermokinetic mixing. *J Appl. Polym. Sci.* **96**, 1557-1563 (2005)
21. Vaia, R.A., Ishii, H., Giannelis, E.P. Synthesis and properties of two-dimensional nanostructures by direct intercalation of polymer melts in layered silicates. *Chem. Mater.* **5,** 1694-1696 (1993)

22. Vaia, R.A., Jandt, K.D., Kramer, E.J., Giannelis, E.P. Microstructural Evolution of Melt Intercalated Polymer–Organically Modified Layered Silicates Nanocomposites. *Chem. Mater.* **8,** 2628 -2635 (1996)
23. Doh, J.G., Cho, I. Synthesis and properties of polystyrene-organoammonium montmorillonite hybrid. *Polym. Bull.* **41,** 511-518 (1998)
24. Laus, M., Camerani, M., Lelli, M., Sparnacci, K., Sandrolini, F. Hybrid nanocomposites based on polystyrene and a reactive organophilic clay. *J. Mater. Sci.* **33,** 2883-2888 (1998)
25. Okamoto, M., Morita, S., Taguchi, H., Kim, Y.H., Kotaka, T., Tateyama, H. Synthesis and structure of smectic clay/poly (methyl methacrylate) and clay/polystyrene nanocomposites via in situ intercalative polymerization. *Polymer* **41,** 3887-3890 (2000)
26. Fu, X., Qutubuddin, S. Synthesis of polystyrene–clay nanocomposites. *Mater. Lett.* **42,** 12-15 (2000)
27. Fu, X., Qutubuddin, S. Polymer–clay nanocomposites: exfoliation of organophilic montmorillonite nanolayers in polystyrene. *Polymer* **42,** 807 - 813 (2001)
28. Zeng, C., Lee, L.J. Poly(methyl methacrylate) and Polystyrene/Clay Nanocomposites Prepared by in-Situ Polymerization. *Macromolecule,* **34,** 4098-4103 (2001)
29. Bottcher, H., Hallensleben, M.L. Organic/inorganic hybrids by 'living'/controlled ATRP grafting from layered silicates. *J. Mater. Chem.* **12,** 1351-1354 (2002)
30. Noh, M.W. Lee, D.C. Synthesis and characterization of PS-clay nanocomposite by emulsion polymerization. *Polym. Bull.* **42,** 619-626 (1999)
31. Chen, G., Liu, S., Zhang, S., Qi, Z. Self-assembly in a polystyrene/montmorillonite nanocomposite. *Macromol. Rapid Commun.* **21,** 746-749 (2000)
32. Chen, G., Qi, Z. Shear-induced ordered structure in polystyrene/clay nanocomposite. *J. Mater. Res.* **15,** 351-356 (2000)

33. Chen, G., Ma, Y. Qi, Z. Preparation and morphological study of an exfoliated polystyrene/montmorillonite nanocomposite. *Scripta Mater.* **44** 125-128 (2001)

34. Voulgrais, D., Petridis, D. Emulsifying effect of dimethyldioctadecyl ammonium-hectorite in polystyrene/poly (ethyl methacrylate) blends. *Polymer* **43**, 2213-2218 (2002)

35. Qutubuddin, S., Fu, X.A., Tajuddin, Y. Synthesis of polystyrene-clay nanocomposites via emulsion polymerization using a reactive surfactant. *Polym. Bull.* **48,** 143-149 (2002)

36. Xie, W., Hwu, J.M., Jiang, G. J., Buthelezi, T.M., Pan, W.P. A study of the effect of surfactants on the properties of polystyrene-montmorillonite nanocomposites. *Polym. Eng. Sci.* **43**, 214 -222 (2003)

37. Moraes, R.P *etal.* Poly (styrene-co-butyl acrylate)-Brazilian Montmorillonite Nanocomposites, Synthesis of Hybrid Latexes via Miniemulsion Polymerization. *Macromol. Symp.* **245,** 106-115 (2006)

38. Ishida, H., Campbell, S., Blackwell, J. General Approach to Nanocomposites Preparation. *Chem. Mater.* **12,** 1260-1267 (2000)

39. Weiner, M.W., Chen, H., Giannelis, E.P., Sogah, D.Y. Direct Synthesis of Dispersed Nanocomposites by in situ Living Free Radical Polymerization Using Silicate –Anchored Initiator. *J. AM. Chem. Soc* **121**, 1615-1616 (1999)

40. Vaia, R.A., Giannelis, E.P. Polymer Melt Intercalation in Organically -Modified Layered Silicates; Model Predictions and Experiments. *Macromolecules* **30,** 8000-8009 (1997)

CHAPTER 5

Conclusion and future scope

Chapter 5

Conclusion and future scope

5.1: Conclusion

Core-shell particles are structured composite particles comprising of at least two phases: one forms the core and other forms the shell. These particles have the uniqueness in the sense that they show properties both of the core as well as shell phase. Due to this uniqueness, core-shell particles find application in various fields ranging from coatings, adhesives, optoelectronics, actuators, column chromatography, paper industries, catalysis etc. Due to their versatility in applications these particles have gained immense importance among the material researchers in recent time.

The purpose of this thesis is to provide an insight into the synthesis, characterization and property evaluation of some polymeric core-shell particles and to find some potential application of these particles.

The major finding of the thesis are described below

I. Preparation of core-shell latex particles by emulsion co- polymerization of styrene and butyl acrylate and evaluation of their pigment properties in emulsion paints

a) A series of core-shell particles prepared by seeded emulsion polymerization. The core contains poly (n-butylacrylate- co- methacrylic acid-co-ethyleneglycol dimethylacrylate) and the shell contains poly (styrene-co-methylmethacrylate).

b) SEM and TEM analysis confirms the core-shell morphology. The core-shell particles have diameter ~ 0.75 μm.

c) Core-shell particles were applied as pigment in emulsion satin paints and the properties of the paint viz. opacity, gloss, rock hardness are evaluated.

d) The opacity of the paint do not change up to 17 wt% replacement of TiO_2 in the pigment volume by the core-shell particles.

II. Preparation of conducting composite particles of poly (styrene-co-methyl acrylate) as the core and polypyrrole as the shell by mini emulsion polymerization

a) Two sets of core-shell particles with poly (styrene-co-methylacrylate) core and polypyrrole shell were prepared by mini emulsion polymerization.

b) In one set, graphite was used as filler while in the other set Ag nanoparticles were used as filler.

c) The core-shell particles show excellent pellet forming ability without much reduction of conductivity.

d) SEM micrographs confirm the rough surface morphology of both the core-shells with almost spherical particles; TEM micrograph confirms the formation of the core-shell morphology.

e) XRD and EDX analysis confirms the presence of graphite and silver nanoparticle in the polypyrrole phase of the respective core-shell.

f) Thermal analysis reveals the superior thermal stability of the core-shell particles.

g) Electrical study reveals the semi conducting nature of the core-shell particles.

h) Electrical conductivity increases with increase of concentration of the conducting filler and decreases with the increase of the poly (methylacrylate) content in the core phase.

i) Electrochemical study reveals that both the core-shell particles are quite stable electrochemically to find potential application in various optoelectronic field.

j) Core-shell particles with graphite incorporated polypyrrole shell were applied as an ammonia gas sensor.

k) They show good sensitivity towards ammonia up to concentration as low as 10 ppm.

l) Since the toxic limit of ammonia in the atmosphere is 25 ppm these particles may be potentially applied as an ammonia gas sensor.

III. Development of core-shell nanocomposite of poly(styrene-co-methyl acrylate) and bentonite clay by ultra sonic assisted miniemulsion polymerization

a) Nanocomposite particles of poly (styrene-co-methylacrylate)-bentonite (organoclay) were prepared by ultra sonic assisted miniemulsion polymerization process.

b) TEM analysis confirms the core-shell morphology of the nanocomposite.

c) XRD analysis gives evidence about the exfoliated nature of the nanocomposite.

d) Thermal analysis shows that the nanocomposite particles exhibit superior thermal stability over the pristine polymer.

5.2 Future Scope of the present investigation

1) To improve efficiency of the core-shell particles as opaque pigment in emulsion paints.

2) Development of conducting core-shell particles in the nanoscale and their potential application.

3) Variation of the thickness of the conducting shell layer and its impact on electro and electro-chemical behavior.

4) Application of core-shell nanocomposite particles as gas barrier material.

List of publications

Journal Publications

1. A. Gogoi,, **L. J Borthakur**, A. Choudhury, G.A Stanciu and G. A Ahmed "Detector array incorporated optical scattering instrument for nephelometric measurements on small particles" *Meas. Sci. Technol.* **20,** 901-911(2009)
2. I. R. kamrupi, **L. J. Borthakur**, S.K. Dolui "Emulsion Polymerization of Styrene in Supercritical Carbon dioxide (sc-CO2) Stabilized with (Trifluoromethyl) Undecafluorocyclohexane(C7F14)" *J. Polym. Mater.*, **27,** 113-123 (2010)
3. **L. J. Borthakur**, T. Jana, S.K. Dolui "Preparation of core–shell latex particles by emulsion co-polymerization of styrene and butylacrylate, and evaluation of their pigment properties in emulsion paints" *J. Coat. Technol. Res.*, **7,** 765–772 (2010)
4. **L.J.Borthakur**, D. Das, S.K. Dolui "Development of core–shell nano composite of poly (styrene-co-methyl acrylate) and bentonite clay by ultra sonic assisted mini-emulsion polymerization" *Materials Chemistry and Physics* **124,**1182–1187 (2010)
5. **L.J.Borthakur**, S. Sharma, S.K. Dolui "Studies on Ag/Polypyrrole composite deposited on the surface of styrene-methyl acrylate copolymer microparticles and their electrical and electrochemicalproperties" *J Mater Sci: Mater Electron* (article in press)
6. **L. J. Borthakur** , S. Konwer , R. Das , S. K. Dolui "Preparation of conducting composite particles of styrene–methyl acrylate copolymer as the core and graphite-incorporated polypyrrole as the shell by surfactant-free mini emulsion polymerization" *J. Polym Res* (article in press)
7. S. Konwer, **L. J. Borthakur**, S.K. Dolui "Synthesis of graphite incorporated core-shell composite of styrene-methylacrylate/ polyaniline by surfactant free mini-emulsion polymerization and evaluation of their electrical property," *J Mater Sci: Mater Electron* (Revision Submitted)

8. **L.J. Borthakur**, S.K. Dolui "Studies on the ammonia gas sensing behaviour of SMA/PPy/G core-shell particles." (Under communication)
9. **L.J. Borthakur**, B.B. Gogoi, F. Yesmin, S.K. Dolui "Synthesis of polypyrrole/Ag nanocomposites and evaluation of their anti-algal activities." (Under communication)

Conference Publications

1. **L.J. Borthakur**, S.K. Dolui "Development of core-shell latex particles of polystyrene PMMA by emulsion polymerization." Inetrnational Seminar on Frontier in Polymer Science and Technology (POLY-2007) Guwahati, Assam, India, November 1-3, 2007.(Awarded best paper)

2. **L.J. Borthakur**, S.K. Dolui "Development of core-shell particles of Polystyrene in Super Critical CO2 medium." National Seminar on Green Chemistry for Sustainable Future of Humanity A.D.P. College, Nagaon, Assam, Oct.19-20,2008

3. S. Borkataki, **L.J. Borthakur**, S.K. Borthakur "Ethnobotanical study on non-timber forest products used by tea tribes of Nagaon District." National Seminar on Bioresources of North-East India: Industrial potential and Intellectual property rights issues. Nowgong College, Nagaon, India. Jan. 2-3, 2009

4. M. Boruah, **L.J. Borthakur**, B. Pokhrel, P. Gogoi, S.K. Dolui "Development of Jatropha Curcas oil based alkyd resin suitable for surface coating" National Seminar on Conservation and Utilization of Resources In North-East india. Nowgong College, Nagaon, India. Jan. 10-11, 2011